Hydrological Modeling of the Upper South Saskatchewan River Basin: Multi-basin Calibration and Gauge De-clustering Analysis

by

Cameron Dunning

A thesis

presented to the University of Waterloo

in fulfillment of the

thesis requirement for the degree of

Master of Applied Science

in

Civil Engineering

Waterloo, Ontario, Canada, 2009

I hereby declare that I am the sole author of this thesis. This is a true copy of the thesis, including any required final revisions, as accepted by my examiners.

I understand that my thesis may be made electronically available to the public.

Abstract

This thesis presents a method for calibrating regional scale hydrologic models using the upper South Saskatchewan River watershed as a case study. Regional scale hydrologic models can be very difficult to calibrate due to the spatial diversity of their land types. To deal with this diversity, both a manual calibration method and a multi-basin automated calibration method were applied to a WATFLOOD hydrologic model of the watershed.

Manual calibration was used to determine the effect of each model parameter on modeling results. A parameter set that heavily influenced modeling results was selected. Each influential parameter was also assigned an initial value and a parameter range to be used during automated calibration. This manual calibration approach was found to be very effective for improving modeling results over the entire watershed.

Automated calibration was performed using a weighted multi-basin objective function based on the average streamflow from six sub-basins. The initial parameter set and ranges found during manual calibration were subjected to the optimization search algorithm DDS to automatically calibrate the model. Sub-basin results not involved in the objective function were considered for validation purposes. Automatic calibration was deemed successful in providing watershed-wide modeling improvements.

The calibrated model was then used as a basis for determining the effect of altering rain gauge density on model outputs for both a local (sub-basin) and global (watershed) scale. Four de-clustered precipitation data sets were used as input to the model and automated calibration was performed using the multi-basin objective function. It was found that more accurate results were obtained from models with higher rain gauge density. Adding a rain gauge did not necessarily improve modeled results over the entire watershed, but typically improved predictions in the sub-basin in which the gauge was located.

Acknowledgements

I am very grateful to my supervisors, professors Ric Soulis and James Craig. Each gave me a different perspective on the problems I faced throughout the completion of this research. Their diverse problem solving styles has been a great benefit towards my understanding of hydrologic modeling.

I would also like to thank Dr. Frank Seglenieks for his time during my completion of this work. His assistance with the WATFLOOD modeling software was a key towards my progress in completing this project.

I would like to thank my thesis committee members, Dr. Bryan Tolson, and Dr. Jeff West for their time and helpful comments during the review process.

Finally, thank you to the GEOIDE Network for providing funding for the completion of this project.

Table of Contents

List of Tables vii

List of Figures viii

1 Introduction 1

1.1 Problem Description ... 1
1.2 Objectives ... 2
1.3 Site Description ... 3
1.4 Outline of Contents ... 4

2 Background 6

2.1 Literature Review ... 6
2.1.1 Hydrologic Modeling ... 6
2.1.2 Calibration of Hydrologic Models ... 8
2.1.3 Temporal and Spatial Data Interpolation Methods ... 13
2.1.4 De-Clustering ... 15
2.2 Watflood ... 18
2.2.1 Model Requirements ... 19
2.2.2 Model Parameters ... 19

3 Model Development & Calibration 22

3.1 Upper South Saskatchewan River Model Development ... 23
3.1.1 Study Area & Model Discretization ... 23
3.1.2 Gauge Locations & Available Data Sets ... 28
3.2 Manual Calibration ... 30
3.2.1 Objective Function ... 31
3.2.2 Sub-basins Selected for Calibration ... 32
3.2.3 Calibrated Parameters ... 36
3.2.4 Manual Calibration Steps ... 38
3.2.5 Calibration Results ... 42
3.3 Automated Calibration ... 44

3.3.1 Optimization Algorithm (DDS) 44
3.3.2 Parameter Selection & Parameter Ranges 44
3.3.3 Objective Function Weighting Method 46
3.3.4 Sub-basin Selection 47
3.3.5 Automated Calibration Results 48
3.4 Summary 51

4 Impacts of Precipitation De-clustering 55
4.1 De-clustering Method 56
4.1.1 Rain Gauge Removal Order 56
4.1.2 De-clustering Trials 57
4.2 Calibration Results 60
4.3 Discussion 68

5 Summary 72

References 74

APPENDICES 79
A Gridded Model Set-up Data 80
B "MultiNash" Script 95

List of Tables

2.1 De-clustering example station locations 16
2.2 Example CI calculation ……..17
3.1 Land use for sub-basins in the Upper South Saskatchewan River watershed …28
3.2 Available historic streamflow data for the Upper South Saskatchewan River watershed ……29
3.3 Sub-basins selected for manual calibration ……35
3.4 River class parameter initial sensitivity and hydrograph impacts for sub-basin nine …….37
3.5 Land class parameter initial sensitivity and hydrograph impacts for sub-basin nine …….....38
3.6 River class parameter values obtained through manual calibration ……...42
3.7 Land class parameter values obtained through manual calibration ……42
3.8 Pre-calibrated and manually calibrated Nash-Sutcliffe coefficients……...43
3.9 Automated calibration parameters selected by hydrologic process……....45
3.10 Sub-basins used for automated calibration …….47
3.11 River class parameter values obtained through automated calibration……...49
3.12 Land class parameter values obtained through automated calibration ……...49
3.13 Nash-Sutcliffe coefficients from manual and automated calibrations……50
3.14 Nash-Sutcliffe coefficients from pre-calibrated and automatically calibrated model ……..51
4.1 Rain gauge removal order……...57
4.2 Rain gauges removed for each de-clustering trial ……..58
4.3 Initial daily Nash-Sutcliffe coefficients for de-clustering models……..60
4.4 Initial monthly Nash-Sutcliffe coefficients for de-clustering models…….61
4.5 Initial and calibrated weighted daily Nash-Sutcliffe coefficients for de-clustering trials ……..64
4.6 Calibrated daily Nash-Sutcliffe coefficients for each de-clustering trial……64
4.7 Calibrated monthly Nash-Sutcliffe coefficients for each de-clustering trial …..65

List of Figures

1.1 Satellite image of study area with gridded overlay of watershed boundaries 4
2.1 Example study area for de-clustering method ……17
2.2 Group response unit and runoff routing concept ……18
3.1 Upper South Saskatchewan River basin ……24
3.2 Gridded form of Upper South Saskatchewan River watershed used in WATFLOOD ……..24
3.3 River class assignment for Upper South Saskatchewan River used in WATFLOOD ……..25
3.4 Land usage for the Upper South Saskatchewan River watershed ……..26
3.5 Sub-basins and stream gauge locations on the WATFLOOD model grid for the Upper South Saskatchewan River……...27
3.6 Weather station locations in the Upper South Saskatchewan River watershed..30
3.7 Sub-basins selected for manual calibration ……35
3.8 Measured streamflows vs. modeled streamflows from pre-calibrated model of Red Deer River below Burnt Timber Creek (sub-basin 9) ……39
3.9 Measured streamflows vs. modeled streamflows from manual calibration of Red Deer River below Burnt Timber Creek (sub-basin 9)…….....41
3.10 Automated calibration parameter adjustment flow chart……....46
3.11 Sub-basins used for automated calibration ……48
3.12 Measured streamflows vs. modeled streamflows from pre-calibrated model of Red Deer River below Burnt Timber Creek (sub-basin 9) ……52
3.13 Measured streamflows vs. modeled streamflows from manually calibrated model of Red Deer River below Burnt Timber Creek (sub-basin 9)……..52
3.14 Measured streamflows vs. modeled streamflows from automated calibration of Red Deer River below Burnt Timber Creek (sub-basin 9) ……53
4.1 Rain gauges used for de-clustering trials …….....59
4.2 River class parameter variation resulting from de-clustering trials …….....62
4.3 Land class parameter variation resulting from de-clustering trials…….63

4.4 Daily Nash-Sutcliffe values from de-clustering trials ……66
4.5 Monthly Nash-Sutcliffe values from de-clustering trials ……...66
4.6 Sub-basin 16-25 shown with full precipitation set locations……..67
4.7 Sub-basin 26-29 shown with full precipitation set locations……..67
A.1 Grid cell numbers……80
A.2 Grid cell areas ……81
A.3 Flow direction for each grid cell……82
A.4 Grid cell elevations ……83
A.5 Grid cell contours ……...84
A.6 Number of channels in each grid cell ……85
A.7 Land class 1 (dense forest) allocation for each grid cell……86
A.8 Land class 2 (light forest) allocation for each grid cell ……..87
A.9 Land class 3 (mixed forest) allocation for each grid cell……88
A.10 Land class 4 (open) allocation for each grid cell ……89
A.11 Land class 5 (wetland) allocation for each grid cell ……...90
A.12 Land class 6 (agricultural) allocation for each grid cell ……91
A.13 Land class 7 (glacier) allocation for each grid cell……92
A.14 Land class 8 (water) allocation for each grid cell……...93
A.15 Land class 9 (impervious) allocation for each grid cell……..94

Chapter 1

Introduction

1.1 Problem Description

Hydrologic simulation models have been used since 1966 to help hydrologists better understand different hydrologic processes, describe the hydrology of a specific region, and to predict the potential hydrologic impact that future development may cause. While hydrologic models are often useful, accurate model predictions can be difficult to achieve. Hydrologic modeling software typically requires large quantities of input data that may necessitate extensive pre-processing before a model can be properly run. Additionally, the number of unknown parameters in hydrologic models is often large, and a significant degree of calibration may be required to ensure the model is able to represent historical and future trends.

For regional scale hydrologic models, data management and calibration can be a very complex task. The modeled region of interest can contain diverse land types, which can be difficult to classify and parameterize. Regional scale models can also have inconsistent and poorly distributed input data (i.e., precipitation, temperature, wind speed, and humidity). The availability and relative density of weather stations strongly influences the accuracy estimated rainfall, temperature, etc., between stations. Since these inputs drive the model, poor data density or interpolation can lead to flawed results.

This thesis presents two contributions to the scientific literature on regional-scale hydrologic modeling. First, a general approach used for calibration of regional scale hydrologic models, with application to a WATFLOOD model of the Red Deer River, the Bow River, and the Old Man River watersheds in Alberta, is presented. In this method, a structured approach towards manual calibration is initially used to determine parameters that have a significant influence on model output. This parameter set is then subjected to automated calibration to optimize parameter values. The objective function used for the automated calibration is calculated based on the model results from multiple sub-basins.

The second component of this study is an investigation into the impacts of de-clustered precipitation data upon hydrologic model calibration. The goal of this portion of the study is to determine a relationship between gauge density and a hydrologic model's potential to be accurately calibrated.

1.2 Objectives

There are two objectives of this study. The first is to calibrate a regional scale hydrologic model using both manual calibration and automatic calibration methods. The steps taken to meet this objective include:

1. **Model development and assessing project limitations:** The study area and the pre-calibrated model are assessed with the purpose of determining major study limitations. Three types of limitations are encountered. The first is caused by missing historic data. Data sets used to fuel the model (historic precipitation), and data sets used to evaluate the model (historic streamflows) both have missing data for portions of the study period. The second limitation is the unknown behavior of certain man-made hydrologic features within the study area such as dams, irrigation canals, and reservoirs, and incorporating these features into a continuous model is outside the scope of this project. The final limitation comes from WATFLOOD itself. While WATFLOOD is designed to handle many hydrologic features, not all processes can be modeled and this puts restrictions on the ability to accurately model portions of the watershed.

2. **Manual calibration:** This involves trial and error variation of each of the unknown model parameters with the purpose of determining how each parameter influences modeling results, and to improve the modeling results. Each parameter is also given a range based on model sensitivity that is used during automated calibration. Both subjective visual inspection and a formal objective function are used for model comparison in this step.

3. **Automated calibration:** The objective function used in this step is designed to consider the results of multiple sub-basins in the model. Using the parameter set and ranges obtained through manual calibration, a search algorithm is used to optimize the objective function and the find calibrated values for each parameter. The calibration is performed based on the objective function alone and the model is validated using the results from sub-basins not used in the objective function calculation.

The second objective of this study is to assess the relationship between rain gauge density and calibration accuracy. Four models are set up, each with a reduced rain gauge density. Each model is calibrated using the calibration method used in the first portion of the study, and impacts of the de-clustered input data sets are discussed and interpreted.

1.3 Site Description

Located mostly in southern Alberta, Canada, the watershed used for this study is the upper South Saskatchewan River, which consists of the Red Deer River, the Bow River, and the Old Man River. With a contributing area of over 120,000 km^2, these three basins flow through diverse land types including mountains, foothills, and prairies. The study area drains from west to east between the Rocky Mountains at the western border of Alberta (continental divide) and the prairies of western Saskatchewan. Figure 1.1 shows a satellite image of the study area with an overlay of the boundaries of the watersheds.

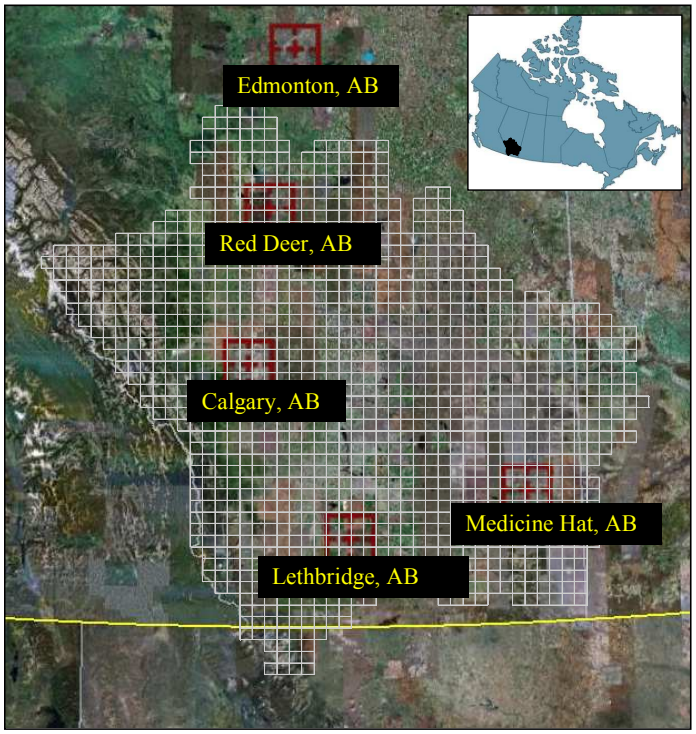

Figure 1.1: Satellite image of study area with gridded overlay of watershed boundaries

1.4 Outline of Contents

Chapter 2 (Background) provides a background of techniques and tools used to complete this study. The first of the two main sections provides a background on: hydrologic modeling, calibration of hydrologic models, data interpolation, and de-clustering. The second section provides a brief outline of the WATFLOOD modeling software including: model description, input requirements, and parameter types.

Chapter 3 (Model Development & Calibration Methodology) describes the steps taken in calibrating the WATFLOOD model from a pre-calibrated to a fully calibrated model. The chapter is divided into three main sections. The first section provides information on the model including: model discretization, gauge locations, available data sets, and limitations of the study. The second section describes the steps taken during manual calibration. These include: description of objective function, sub-basin selection,

a description of calibrated parameters, parameter sensitivity, and calibration results. The final section of this chapter outlines how the automated calibration process was completed. This section includes: parameter selection, parameter ranges, basin selection for the multiple basin automated trails, and calibration results.

Chapter 4 (Impacts of Precipitation De-clustering) contains information on the de-clustering experiment. The first of the two main sections describes the method used for de-clustering the rain gauge data and the interpolation used to create the new data sets. The second section presents the automated calibration results for each de-clustering trial, and an assessment of the impacts of data density upon model calibration and performance.

Chapter 5 (Summary & Discussion) provides a summary of the results obtained in this thesis and contains a brief discussion of the significance of this work, future considerations, and recommendations.

Chapter 2

Background

This study uses a multiple basin calibration approach to calibrate a regional scale model comprised of multiple sub-basins and multiple stream gauges. This multiple basin calibration method has the benefit that it allows a hydrologic model to be efficiently calibrated when testing the model against rain gauge density alterations and de-clustering.

This chapter is dedicated to providing a background on both the techniques and tools used to complete this study. The literature review (section 2.1) provides a background on hydrologic modeling, calibration of hydrologic models, and methods for interpolating and de-clustering rain gauge data. This chapter also provides a brief summary of the WATFLOOD hydrologic modeling software (section 2.2).

2.1 Literature Review

2.1.1 Hydrologic Modeling

Hydrologic modeling is an attempt to represent different aspects of the hydrologic cycle through statistical and/or mathematical simulation. It is a powerful tool that can be used for both research purposes and for planning and development (Seth, 2004). Software codes capable of simulating several parts of the hydrologic cycle are sometimes used to represent an entire hydrologic system. Although the understanding of the hydrologic cycle continues to improve, there is still much to be learned on how hydrologic systems function, and how they can be better modeled to meet the needs of today's researchers and practitioners.

Computer-based hydrologic modeling started during the 1960's when large computer models were used to attempt to match historical hydrologic data. The ability to

perform many calculations using the computer was helpful for answering complicated hydrologic questions.

The first computational hydrologic model was created at Stanford University and was called the Stanford Watershed Model (Crawford & Linsley, 1966). It was able to effectively simulate precipitation, evaporation, evapotranspiration, infiltration, surface runoff, ground water flow, and streamflow (Bedient & Huber, 2002). The goal of these earlier programs was to continuously simulate hydrologic processes and to include all of the interacting processes in the same model structure (Crawford & Burges, 2004).

Since the development of these early computer-based hydrologic models, there have been several types of software of varying complexity developed to assist hydrologists in understanding complex hydrologic processes. As a result of continued advancement, hydrologic modeling remains a key component of the advancement of hydrologic study. Often, the development and calibration of hydrologic models gives insight into the limitations of modeling specific hydrologic processes and leads to improvements in modeling software. Additionally, increased computing power has created a demand for more field data, which in turn allows for further hydrologic study. If applied correctly, hydrologic models are currently the best way to estimate and understand complex hydrologic systems (Bedient & Huber, 2002). There are many types of hydrologic models, but the three most used types are: conceptual, stochastic, and physically-based models.

Conceptual hydrologic models use very little information about the watershed, and provide efficient estimates of how a watershed will respond to precipitation (Fenicia et al., 2007). Some examples of conceptual hydrologic models are linear models, Nash instantaneous unit hydrograph, the rational method, and kinematic or dynamic wave methods for overland flow (Bedient & Huber, 2002).

Stochastic hydrologic models use mathematics and statistics to produce an output based on a set of input data. A typical example of this would be producing synthetic streamflows based on a set of input precipitation data based on historical statistics from the specific watershed (Bedient & Huber, 2002).

Physically-based hydrologic models attempt to simulate the hydrologic processes as they occur in the real world and are based on our understanding of the physics of individual hydrologic processes, e.g., infiltration, snowmelt, etc. (Seth, 2004). Physically-based distributed models can be applied to many types of hydrologic problems (Seth, 2004). Some common inputs for a physically based hydrologic model include precipitation, temperature, wind speed, humidity, and initial snow depth. These are used as input parameters to mass transfer and energy budget equations that can be used to model snow melt, evaporation, and infiltration (Bedient & Huber, 2002).

Physically-based hydrologic models are typically set up to be single event models or continuous models. Single event models are primarily used for the design of hydraulic systems to handle large floods based on a single extreme precipitation event. They are convenient in that it is easy to set up the antecedent conditions in the system, and because they have very short run times. Continuous models are long term simulations that usually simulate several historic precipitation events. These can range from a single season to many years. Like single event models, continuous models can also be used in the design of hydraulic systems, but may also include simulation goals related to base flow depletion/recharge, evaporation, or snow melt as these hydrologic processes take much longer than would be simulated by a single event model.

2.1.2 Calibration of Hydrologic Models

Most hydrologic models contain general equations that are intended to be useful over a large variety of geographic areas. These equations include parameters that can be varied to account for the hydrology of a specific study area. Without calibration, such "general-purpose" models will not likely produce accurate, acceptable results (Debo & Reese, 2002). This is partly because the equations intended to represent natural hydrologic processes contain parameters and coefficients that are difficult if not impossible to estimate from field data. Once a hydrologic model has been set up to represent the diversity of the specified, model calibration can begin.

Calibration of a hydrologic model is the process by which parameters that heavily influence model output are modified in an attempt to replicate the model outputs with historic data from the watershed (Debo & Reese, 2002). For example, it is often desirable for the model to be able to simulate historic streamflow data given historic precipitation data. Depending on the purpose of the model, the requirements for calibration may vary: one model may be intended to best meet peak flows, another may be focused on simulating low or mid flows. The goals of calibration are typically expressed in terms of a calibration objective function defined such that the optimal solution is that with the smallest (or largest) objective function.

There are several objective functions that can be used to assess the accuracy of a hydrologic model. The objective function selected may depend on the specific goals of the study. The most common objective function used for calibration of hydrologic models is the Nash-Sutcliffe model efficiency coefficient (Nash & Sutcliffe, 1970) defined as:

$$E = 1 - \frac{\sum_{t=1}^{T} (Q_O^t - Q_m^t)^2}{\sum_{t=1}^{T} (Q_O^t - \overline{Q}_O)^2} \tag{2.1}$$

where Q_o is observed discharge and Q_m is modeled discharge. The coefficient is a measure of the model's predictive ability. The Nash-Sutcliffe model efficiency coefficient has a range of $-\infty$ to 1.0. The maximum value of 1.0 indicates a perfect match between the model and the observed data. A value of 0.0 indicates that the model is as good of a predictor as the mean of the observed flows. A value greater than 0.0 means that the model is a more accurate predictor than the mean of the observed data, while a value less than 0.0 results when the model is a less accurate prediction than the mean of the observed data.

While the Nash-Sutcliffe model efficiency coefficient is one of the most common methods for evaluating the accuracy of a hydrograph, it has been shown that very poor models can possess relatively high Nash-Sutcliffe coefficients, and low Nash-Sutcliffe

coefficients can result from a good model. Because of this, it is beneficial not to conclude on the performance of a model based on the Nash-Sutcliffe coefficient alone (Jain & Sudheer, 2008).

Once an objective function is selected, the calibration process can be executed using either manual calibration or automated calibration. Manual calibration is a method in which parameters are manually varied one at a time in an attempt to improve the model results and gain an understanding of how certain parameters influence model outputs. Automated calibration is a method where parameters are simultaneously varied using a search algorithm to find the parameter set that produces the most accurate model results.

Manual calibration is the most widely used method to calibrate hydrologic models (Boyle et al., 2000). Usually used in the early stages of the calibration of a hydrologic model (prior to automated calibration), it is a method that essentially uses trial-and-error parameter adjustment to improve the model and determine a good parameter set (Madsen, 2000).

Often, the comparison between the observed hydrograph and the simulated hydrograph is made purely from visual inspection. Experienced modelers can obtain very accurate models through manual calibration, but without an objective function, it is difficult to quantify its quality in comparison to equally plausible models (Madsen, 2000). If automated calibration is to take place following manual calibration, it can be a good idea to monitor the selected objective function during manual calibration so that a better understanding can be gained of how that objective function is reacting to visual improvements in the model.

Manual calibration provides modelers with some advantages over automated calibration. Because parameters are varied one at a time, modelers see each varied parameter changes model outputs. This allows a modeler to determine the set of dominant parameters that strongly influence the specific watershed. Through this process, a modeler is also able to understand the sensitivity of each parameter and determine reasonable starting points and ranges for the parameter set to be used during automated calibration; this will reduce the number of iterations required during

automated calibration. Modelers that manually calibrate their models gain a better understanding about how different hydrologic processes impact the output hydrographs. Additionally, these modelers are better prepared to identify problems that may be encountered during automated calibration (Madsen, 2000).

Though popular and useful, manual calibration has drawbacks. Each model run requires visual hydrograph analysis (and possibly objective function calculation) and parameter adjustment by the modeler, and makes manual calibration a labor intensive process. The method can be complicated, and expertise from one modeler is difficult to pass on to another modeler as the best method for improving one's manual calibration skill is through hands on experience and training (Boyle et al., 2000).

An increasingly popular method of improving the quality of hydrologic models is automated calibration; however, because automated calibration approaches often require a mathematical background and use more complicated computational tools than manual calibration, it still remains unused by many modelers (Boyle et al., 2000). Each parameter varied in automated calibration must be given a range defined by maximum and minimum values. The set of specified parameter ranges is called the parameter space. Automated calibration uses optimization algorithms to search the parameter space to find the parameter set that will result in the best value of the objective function. The technique is not labor intensive, nor is it biased by the modeler's expert knowledge or opinions (Madsen, 2003), except in the selection of the objective function and parameter ranges.

Three things are necessary to complete an automated calibration: an objective function, a parameter set with an initial parameter space, and an optimization algorithm. As previously discussed, there are different objective functions to choose from. Properly selecting an objective function that meets the needs of the specific study is critical for developing a model that meets the needs of the modeler. It has been found that performing a single criteria approach to automated calibration can lead to good curve fitting, but can lead to a parameter set that is hydrologically unrealistic (Boyle et al., 2000). A method that can help to avoid this situation is to complete in-depth manual

calibration prior to automated calibration to see that there are hydrologically realistic parameter values.

The final component of an automated calibration is an optimization algorithm. For this, there are many to choose from, which can be categorized as either local or global search methods. Both local and global search methods are used for computationally complex problems in which no specific algorithm can be used to solve the problem in its entirety (MacFarlane & Tuson, 2008). While both methods may start searching from the same point in the parameter space, local search methods will improve the result of the objective function towards a local maximum (or local minimum) value. Global search methods are designed to solve optimization problems that may have multiple optima (Zabinsky, 1998).

Because rainfall runoff models can have numerous locally optimal solutions within the parameter space (Duan et al., 1993), local search methods will often not produce a global optimum because the results will depends on the search starting point. Because of this, global search methods should be employed to solve hydrologic calibration problems (Madsen, 2000). Some of the most popular methods for automated calibration are evolution-based searches such as the shuffled complex evolution (Duan et al., 1993) and genetic algorithms (Wang, 1991). Several studies (Duan et al., 1993; Gan & Biftu, 1996; Cooper et al., 1997; Kuczera et al., 1997; Franchini et al., 1998; Thyer et al., 1999) have compared genetic algorithms and shuffled complex evolution (SCE), and find that the SCE algorithm is more effective and efficient. It has been widely used in conceptual rainfall runoff models (Madsen, 2000).

The optimization algorithm chosen for this study is a dynamically dimensioned search (DDS) (Tolson & Shoemaker, 2007). The DDS algorithm is novel and simple stochastic single-solution based heuristic global search algorithm (Tolson & Shoemaker, 2007). With a purpose of finding good global solutions instead of globally optimal solutions, the algorithm is designed to scale the search to the user-specified number of function evaluations (Tolson & Shoemaker, 2007). Initially, the algorithm searches globally, and as the number of specified objective function evaluations approaches, the

search becomes more localized (Tolson & Shoemaker, 2007). To interact with a hydrologic model DDS requires a parameter set with pre-determined user-assigned ranges for each parameter.

DDS has been compared to the SCE method, and has been shown to require only 15-20% of the model evaluations used by the SCE method to obtain equally good values of the objective function (Tolson & Shoemaker, 2007).

2.1.3 Temporal and Spatial Data Interpolation Methods

The most important input to a hydrologic model is the temporal and spatial distribution of rainfall (Lynch & Schulze, 1995; Yoo, 2002). The output of a regional scale model with sparse rainfall data can be strongly influenced by the interpolation routine that generates rainfall values for unmeasured areas of the watershed, and having an accurate areal precipitation representation is crucial in hydrologic modeling (Dorninger et al., 2008). Selecting a method to estimate rainfall distribution from rain gauges can often be a time consuming but important problem (Lynch & Schulze, 1995).

In regional scale models with complex terrain, properly using the available data is an important aspect of developing an accurate model (Dorninger et al., 2008). Rainfall interpolations for regional scale models are effected by the distribution and density of rain-gauges as this can significantly contribute to the sampling error in the estimation of the total volume of rainfall over a given area (Yoo, 2002). Beven and Hornberger (1982) found that, for predicting streamflow hydrographs, the correct assessment of rainfall input volume is more important that the spatial rainfall pattern.

While a majority of this study is dedicated to the calibration of a regional scale model, once complete, the calibration method is tested using several rain-gauge input data sets. Input data sets are generated by interpolating precipitation input sets that decrease in density with each subsequent trial. Though the method of interpolation is not

varied to generate these data sets, it is a key aspect of this study and as such must be selected carefully.

Many techniques exist that modelers use to estimate rainfall between rain gauge point measurements. Common techniques include: inverse distance interpolation, Shepard's weighted interpolation, Schafer interpolation, SACLANT interpolation, and Kriging (Lynch & Schulze, 1995).

Inverse distance weighting (IDW) is determined according to the following equations (Shepard, 1968):

$$F(x,y) = \sum_{i=1}^{n} w_i f_i \tag{2.2}$$

$$w_i = \frac{d_i^{-2}}{\sum_{j=1}^{n} d_j^{-2}} \tag{2.3}$$

where d is the distance between the location (x,y) where rainfall is unknown and the given weather station (i), and F is the value of rainfall at the given weather station. Shepard's method employs the same weighting function, but only within a certain radius; otherwise the weighting function is equal to zero. The radius should be selected based on the geographic density of the data points (gauge density), and should be chosen so that each sample radius includes at least five sample points (Yoeli, 1975).

Schafer interpolation makes use of the assumption that daily rainfall distribution similarly resembles median monthly rainfall distribution (Lynch & Schulze, 1995). The daily rainfall measurements from each rain gauge station are transformed into a percentage of the median monthly rainfall at that station for that specific data (Schafer, 1991). Those values are interpolated using a two dimensional interpolation technique onto a rectangular grid (SACLANT, 1979). The interpolated values are then multiplied by the gridded median monthly rainfall values to result in daily rainfall estimates (Dent, Lynch and Schulze, 1988).

SACLANT interpolation is another two dimensional interpolation used for a rectangular-gridded shaped study area, such as that used in the WATFLOOD software. Values are initially assigned to each unknown point in the rectangular grid and then an iterative process is performed where the unknown values are altered (improved) until the surface of the precipitation values has obtained a targeted value of smoothness through the known data points (SACLANT, 1979).

The Kriging method of interpolation uses a semi-variogram model to interpolate a set of points (ArcInfo, 1991). The semi-variogram is a function that represents the expected difference in value between sample points based on a given radius and orientation (Clark, 1979). This model can be altered to be spherical, circular, exponential, Gaussian, linear, universal linear or universal quadratic. A study investigating the influence of different semi-variogram models (Lynch & Schulze, 1995) found the universal linear model to produce the lowest root mean square errors when attempting to interpolate known rainfall data. Statistical methods like Kriging can be optimal in a statistical sense but are not applicable to some studies (Ahrens, 2005).

It has been found that for a regional scale models with a strong climactic gradient and a sparse data set that IDW and Kriging are the most efficient towards generating a model that can produce accurate hydrographs when calibrated (Ruelland et al., 2008). The IDW method was found to be a significantly less time consuming process relative to Schafer, SACLANT, and Kriging (Lynch & Schulze, 1995), and is the method selected for this study.

2.1.4 De-Clustering

While it has been found that varied rain-gauge density can have very little effect on modeling results in regions with relatively high rain-gauge densities (Allen & DeGaetano, 2005), this study focuses on a region with a sparse, poorly distributed data set. For this study, rain-gauge density will be decreased using the de-clustering method

described in this section, and the impacts on hydrologic model calibration will be assessed.

De-clustering is a term used to describe a method in which data points are removed to reduce the known, unknown, or estimated negative effects of clustered data to obtain a data set that is more representative of underlying data (Smith, Goodchild, Longley, 2006). While several methods for de-clustering data exist, the technique has not been extensively studied in the context of hydrologic modeling. Ahrens (Ahrens, 2005) found a slight improvement using de-clustering for one of four rain gauge densities evaluated. The method used by Ahrens (Ahrens, 2005) selected the closest pair of rain gauges and eliminated the gauge which had the next closest rain gauge to it. For this study, de-clustering will be performed using a search that will calculate a "clustering index" for each rain gauge as follows:

$$CI = \sum_{i=1}^{N} d_i^2 \tag{2.4}$$

where d_i is the distance between the selected rain gauge and the closest neighboring rain gauge and N is the number of neighboring rain gauges used to calculate CI. For each rain gauge, d_i is calculated for the closest four neighboring rain gauges and the gauge with lowest CI is removed and the process is repeated. An example study area is shown below in figure 2.1. In this example, the x-y locations of the rain gauges, labeled X_i, are shown in table 2.1.

Table 2.1 – De-clustering example station locations

	X Coordinate	Y Coordinate
X1	0	0
X2	2	0
X3	4	0
X4	1	1
X5	3	1
X6	4	2
X7	1	3

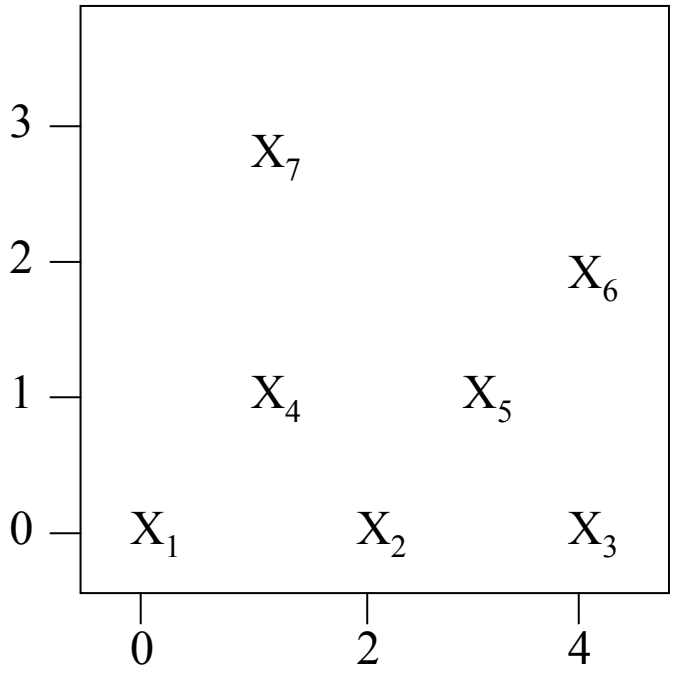

Figure 2.1 – Example study area for de-clustering method

The corresponding *CI* values are calculated (equation 2.4) for each rain gauge and the results are displayed in table 2.2.

Table 2.2 – Example CI calculation

	X1	X2	X3	X4	X5	X6	X7	Min 1	Min 2	Min 3	Min 4	Sum (CI)
X1	-	16	256	4	100	400	100	4	16	100	100	220
X2	16	-	16	4	4	64	100	4	4	16	16	40
X3	256	16	-	100	4	16	324	4	16	16	100	136
X4	4	4	100	-	16	100	16	4	4	16	16	40
X5	100	4	4	16	-	4	64	4	4	4	16	28
X6	400	64	16	100	4	-	100	4	16	64	100	184
X7	100	100	324	16	64	100	-	16	64	100	100	280

Table 2.2 shows the *CI* calculated using the lowest four distance squared values for each rain gauge. The gauge selected through this method was gauge X_5 with a *CI* of 28. That gauge would be removed from the interpolation, and if further de-clustering was desired, the process would be repeated, but starting with the updated gauge distribution.

2.2 Watflood

The hydrologic model used for the study is WATFLOOD. It is a physically-based routing model combined with a conceptual hydrologic simulation model (Kouwen, 2007). In WATFLOOD, a watershed is divided into a Cartesian grid, and each grid square is subdivided into one or more land use types based on satellite imagery. The behavior of each assigned land class is then governed by the equations of conceptual hydrologic models and the land class parameters of WATFLOOD (section 2.2.2). An example of how a specific grid square is handled is shown in figure 2.2.

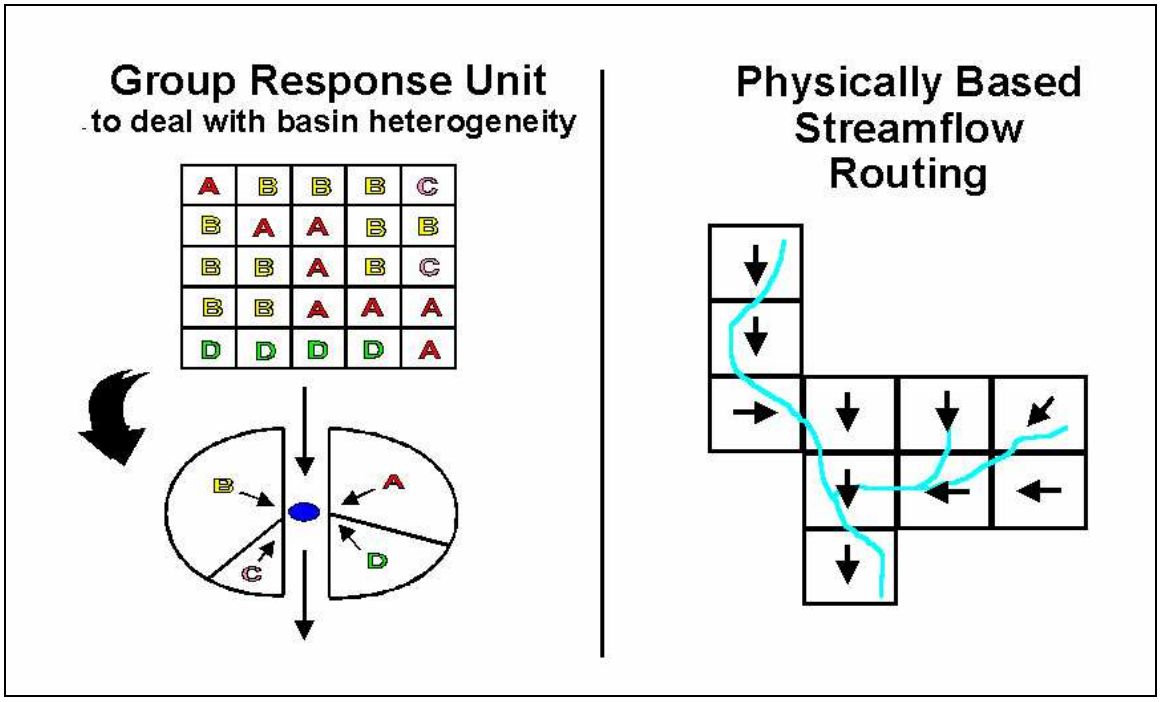

Figure 2.2 – Group response unit and runoff routing concept (Donald, 1992; Kouwen, 2007)

In figure 2.2, the grid square is allocated in to land types (*A, B, C, D*) based on the satellite image, and each land type is handled in the model as a separate watershed. The runoff from each of the individual land class models is added to the physically based streamflow routing model (Kouwen, 2007).

WATFLOOD simulates only a subset of the physical processes occurring in nature, but includes: infiltration, evaporation, snow accumulation, interflow, base flow, and overland channel routing (Kouwen, 2007).

2.2.1 Model Requirements

The WATFLOOD model used for this calibration is essentially fuelled by just two hydroclimatic inputs: temperature and rainfall. Each of these inputs is taken from historic data sets, and unknown data points (grid cells) are interpolated. Additionally, each grid cell requires information to describe the specific land it represents including (Kouwen, 2007):

N – Grid cell number

NEXTI – Receiving cell number. This tells WATFLOOD which grid cell the streamflow will be sent to.

XX, YY – Grid cell location from bottom left corner of grid.

DA– Drainage area in km^2.

IBN – River class

1,2,…N – Fractions in each land cover type.

The model requires parameter assignment for both the land type and river class parameters (described in section 2.2.2) as well as values for the initial conditions of both snow depth and streamflow, all of which can be modified in the WATFLOOD input files.

2.2.2 Model Parameters

While directly measured meteorological data is used to fuel the model, model behavior heavily relies on the values of many adjustable system parameters. The primary parameters driving the model results may be divided into land class parameters, which

are dictated by land use and soil type, and river class parameters, which are dictated by drainage area, geographic location, and sub-basin boundaries. The default values listed with each parameter shown are not considered WATFLOOD specific defaults, but are simply the defaults arrived at in this study.

There are five river class parameters. The first two are related to how WATFLOOD handles base flow:

LZF – Lower zone function (default = 0.200×10^{-5})

PWR – Exponent on lower zone function (default = 0.200×10^{1})

Both *LZF* and *PWR* effect base flow the depletion function *(QLZ)* according to the following equation:

$$QLZ = LZF * LZS^{PWR} \tag{2.5}$$

where *LZS* is the lower zone storage in each grid cell and *QLZ* is the lower zone flow (base flow). All land classes present in each grid (except impervious) contribute to the lower zone storage.

There are two river roughness parameters:

R1 – Flood plain roughness coefficient (default = 0.200×10^{1})

R2 – River channel roughness coefficient (default = 0.100×10^{1})

Both *R1* and *R2* are transformed to values of Manning's n and then subject to Manning's equation to determine the average channel velocity:

$$V = \frac{k}{n} R_h^{\frac{2}{3}} S^{\frac{1}{2}} \tag{2.6}$$

where k is a conversional constant, n is the Gaucklet-Manning coefficient, R_h is the hydraulic radius, and S is the slope of the water surface.

MNDR – Meander factor (default = 0.100 x 10^1)

The meander factor is a ratio of how long each channel in the grid is relative to the length of the grid.

The parameters related to land use are as follows:

- ***DS*** – Depression storage (mm) (default = 0.200 x 10^2)
- ***DSFS*** – Depression storage for snow (mm) (default = 0.200 x 10^2)
- ***RE*** – Interflow depletion coefficient (default = 0.302 x 10)
- ***AK*** – Soil permeability for bare ground (default = 0.904 x 10^1)
- ***AKFS*** – Soil permeability under snow (default = 0.140 x 10^2)
- ***RETN*** – Upper zone specific retention (default = 0.750 x 10^2)
- ***AK2*** – Upper zone resistance factor for bare ground (default = 0.125 x 10)
- ***AK2FS*** – Upper zone resistance factor under snow (default = 0.984 x 10)
- ***R3*** – Overland roughness for bare ground (default = 0.101 x 10^2)
- ***R3FS*** – Overland roughness under snow (default = 0.394 x 10^2)
- ***R4*** – Impervious area roughness (default = 0.100 x 10^2)
- ***CH*** – Channel efficiency factor (default = 0.900 x 10)
- ***MF*** – Melt factor (mm/°C/hr) (default = 0.139 x 10)
- ***BASE*** – Base melt temperature (°C) (default = -0.115 x 10^1)
- ***RHO*** – Snow density (relative to rho H_20) (default = 0.333 x 10)
- ***FTAL*** – Forest vegetation coefficient (default = 0.850 x 10)

Not all parameters described above will have a significant effect on modeling results. Depending on the specific model, certain parameters can strongly influence different portions of the model. The entire parameter set will be analyzed for significance during manual calibration; however, not all parameters will be adjusted during automated calibration.

Chapter 3

Model Development & Calibration

Properly calibrating a hydrologic model is an essential step towards using that model as a basis for experimentation and understanding. While many methods of calibration can be used to improve the accuracy a model's outputs, no method can guarantee the most accurate model possible; in fact, it is likely that no 'best' solution exists and that several equally accurate models can be produced with very different parameter sets (Beven, 2000).

Parameters that affect the behavior of the entire model are sometimes determined through the calibration of only one sub-basin. For local scale models, this can be very effective since many parameters are not likely to vary significantly through the basin. However, due to variation of land types of a regional scale model, calibrating parameters one sub-basin at a time is less likely to produce a parameter set that represents the behavior of the entire watershed; therefore, multi-basin calibration approaches are needed. The calibration method described this chapter is performed on a regional scale model. It promotes parameter determination through an objective function that is calculated from the results in multiple sub-basins.

The following sections review the development of the hydrologic model for the Upper South Saskatchewan River case study, as well as model calibration as it applies to WATFLOOD hydrologic models. Section 3.1 outlines the model development and data analysis that was performed prior to calibration. This includes the model discretization, gauge locations, available data sets, and study limitations. Section 3.2 provides a description of the manual calibration process. This section includes a description of the objective functions used, sub-basin selection methods, a description of the parameters used for calibration and how they affect model outputs, an example manual calibration for a single sub-basin, and a summary of the calibration results. Section 3.3 outlines the steps taken during automated calibration. These include a brief overview of the

optimization algorithm, a summary of the parameters selected and their optimization ranges, a description of the objective function weighting method, an overview of the sub-basins used for the automated process, and a summary of the automated calibration results.

3.1 Upper South Saskatchewan River Model Development

Before model calibration can begin, the study area and the available historic data must be understood. This section provides an overview how the study area has been represented using a WATFLOOD hydrologic model, a summary of the data sets available for the study, and a review of some limitations that were encountered during model development.

3.1.1 Study Area & Model Discretization

The watershed used for this study is the Upper South Saskatchewan River. Located in southern Alberta, Canada, this watershed is made up of three major rivers: the Red Deer River, the Bow River, and the Old Man River. The watershed has a contributing area of over 120,000 km^2 and flows east from the continental divide. For the purpose of developing a regional scale hydrologic model of the watershed, the study area has been divided up into 1341 grid cells, each with an area of approximately 100 km^2 (10 km x 10 km). Figure 3.1 shows a map of the study area, while Figure 3.2 shows the gridded form of the study area.

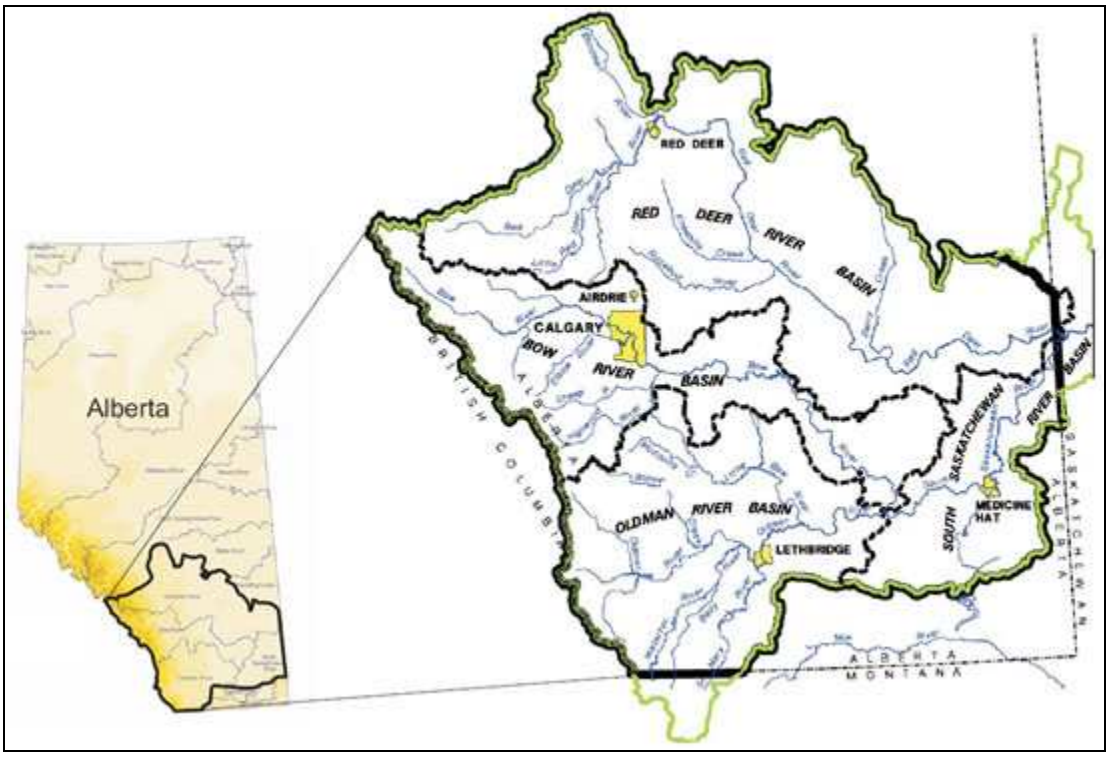

Figure 3.1: Upper South Saskatchewan River Basin (Alberta Environment, 2009)

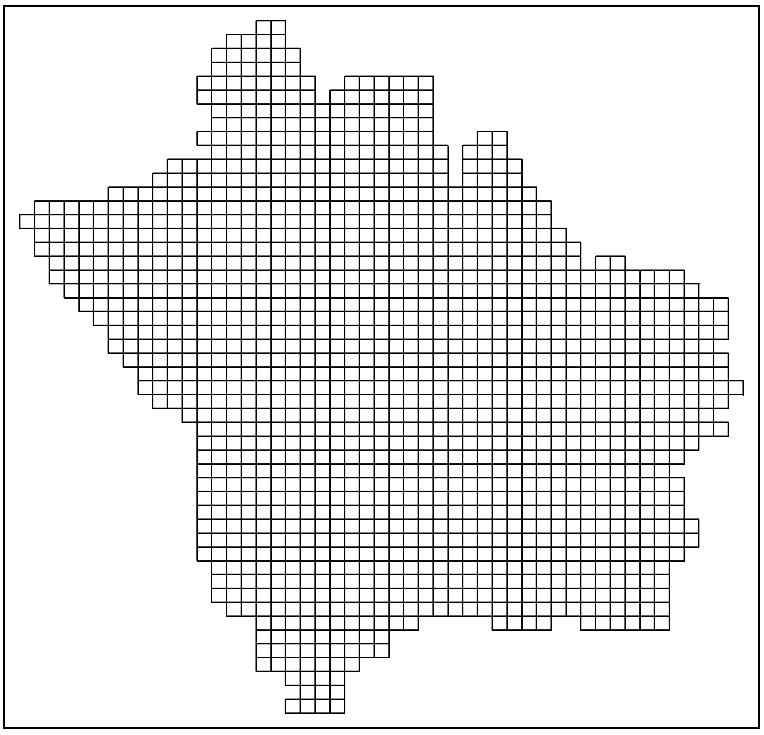

Figure 3.2: Gridded form of Upper South Saskatchewan River watershed used in WATFLOOD

Each grid cell must have a designated river class, and must be assigned one or more land uses. Using a combination of satellite imagery, sub-basin boundaries, and contributing area, three river classes were designated. The three river classes are:

Class 1 – Mountain/Foothills stream (contributing area < 1000 km^2 and visually identifiable as a region with high vegetation from satellite imagery)

Class 2 – Prairie stream (contributing area < 1000 km^2 and visually identifiable as a region with low vegetation from satellite imagery)

Class 3 – Major River (contributing area > 1000 km^2)

Figure 3.3 shows the assigned river classes for each grid cell.

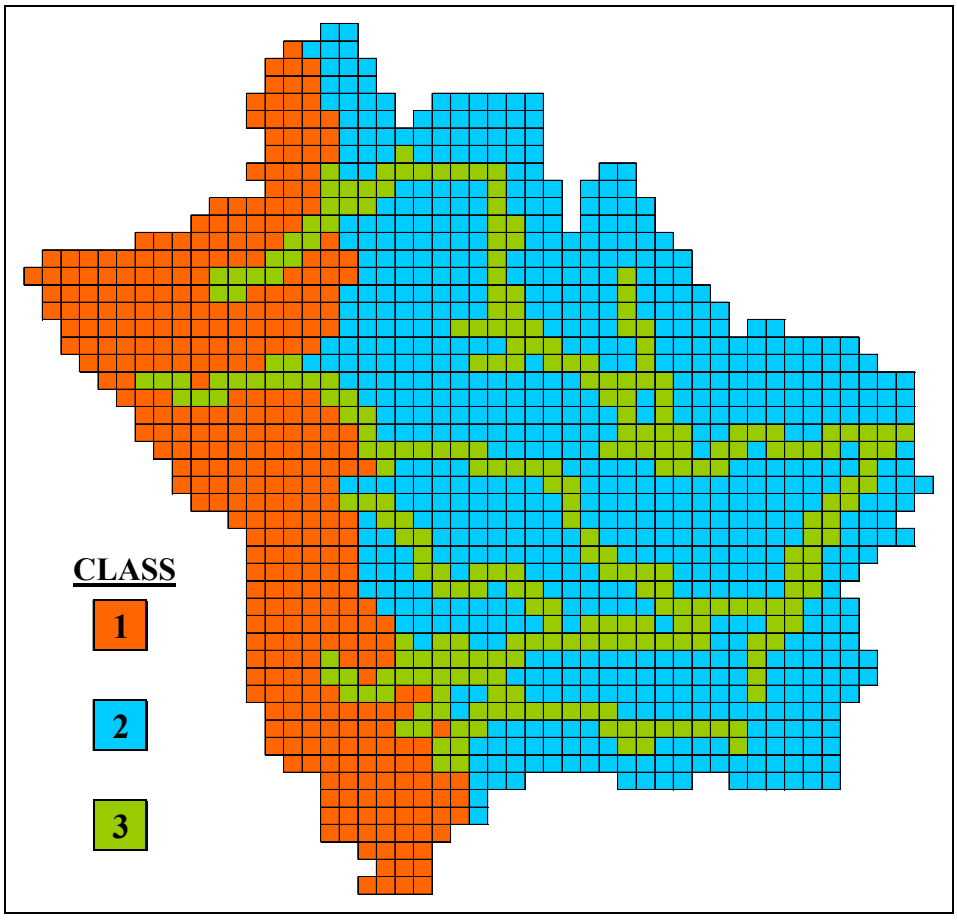

Figure 3.3: River class assignment for Upper South Saskatchewan River used in WATFLOOD

For this study, land use was divided into nine land classes: dense forests, light forests, mixed forests, open, wetlands, agriculture, glacier, water, and impervious. Each land class was assigned using remotely sensed land cover data (Kouwen, 2007). Figure 3.4 shows the distribution of each land class in the watershed.

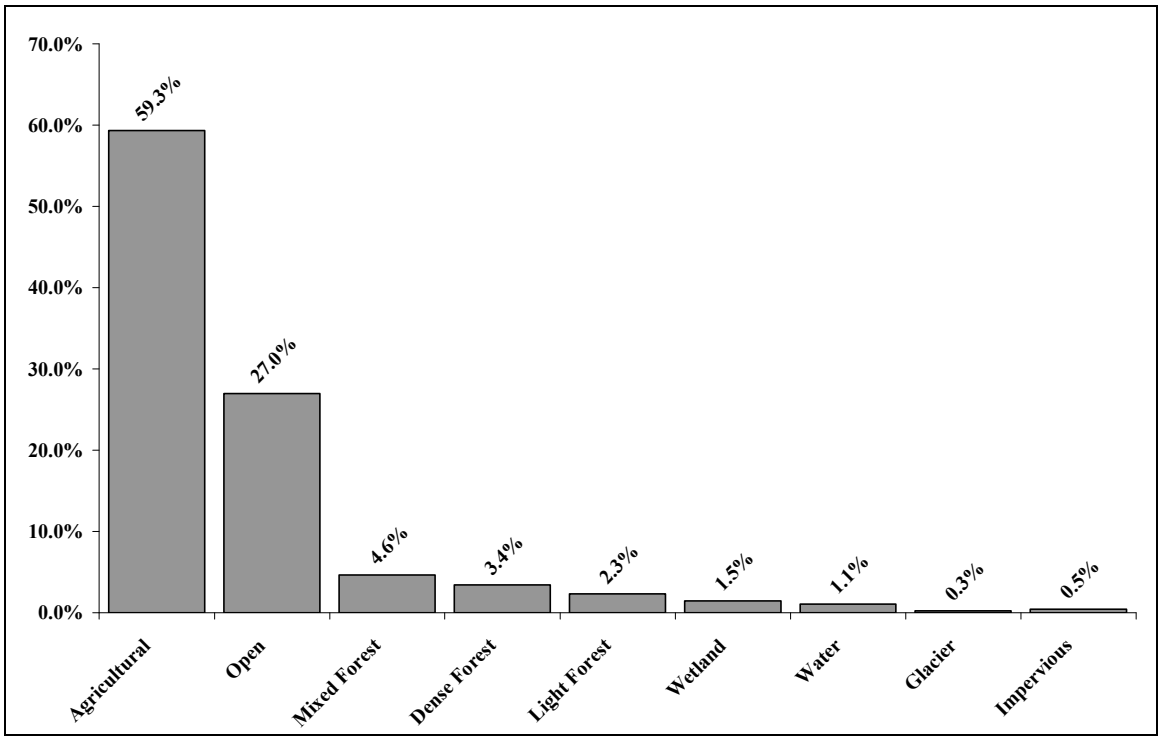

Figure 3.4: Land usage for the Upper South Saskatchewan River watershed

As shown, a majority of the land use (86%) in the watershed is characterized as agricultural or open land.

The model is set up to output streamflows at 30 grid cell outflow points in the model which roughly corresponds to the 30 sub-basin stream gauges that exist in the watershed and are shown on figure 3.5. The modeled (and measured) drainage areas and land use for each sub-basin is shown in table 3.1.

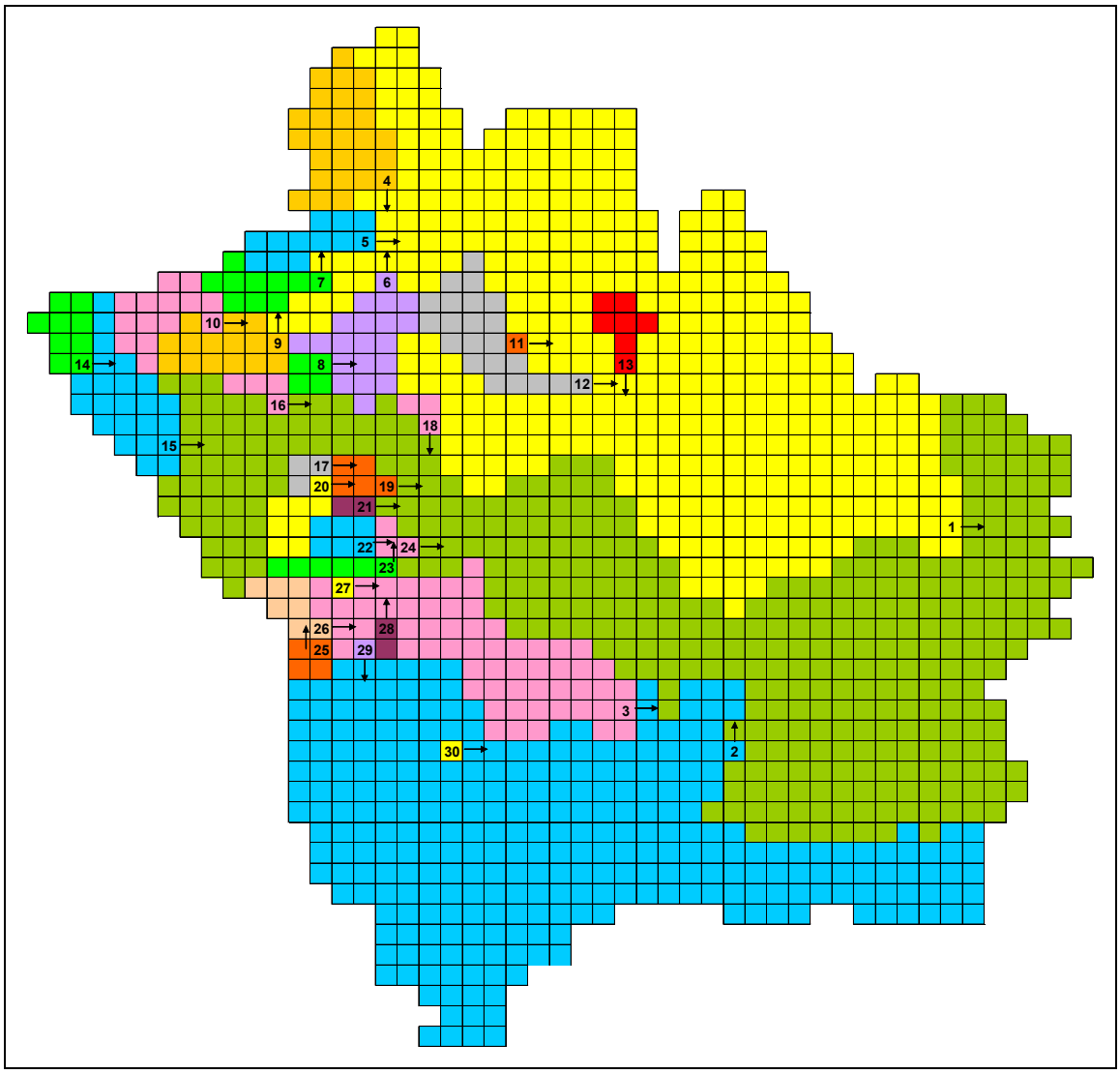

Figure 3.5: Sub-basins and stream gauge locations on the WATFLOOD model grid for the Upper South Saskatchewan River

Table 3.1: Land use for sub-basins in the Upper South Saskatchewan River watershed

Sub-basin #	Area (sq km)	Dense Forest %	Light Forest %	Mixed Forest %	Open %	Wetland %	Agricultural %	Glacier %	Water %	Impervious %
1	46250	2.6	1.6	3.3	28.6	0.8	61.8	0.2	1.2	0.0
2	32089	4.4	2.9	7.8	12.4	1.9	69.3	0.0	1.1	0.0
3	6827	2.7	2.1	6.1	7.3	2.4	78.6	0.0	0.8	0.1
4	1966	0.0	0.4	13.3	13.2	0.5	72.6	0.0	0.0	0.0
5	784	10.9	3.7	17.0	18.2	0.4	50.0	0.0	0.0	0.0
6	2612	0.2	4.3	16.2	10.5	5.2	63.7	0.0	0.0	0.0
7	760	28.4	21.9	33.9	8.2	1.1	6.1	0.0	0.0	0.0
8	506	0.3	11.1	51.1	18.0	17.7	2.2	0.0	0.0	0.0
9	2418	36.8	15.1	1.4	34.9	7.3	0.0	3.0	1.5	0.0
10	1012	21.4	13.6	0.1	44.5	10.3	0.0	7.0	3.0	0.0
11	68	0.0	0.0	0.0	0.0	0.0	100.0	0.0	0.0	0.0
12	2398	0.0	0.0	0.0	0.8	0.0	99.2	0.0	0.0	0.0
13	25189	5.1	3.1	6.6	14.9	1.5	67.4	0.3	1.1	0.1
14	413	18.6	8.3	0.0	45.4	7.9	0.0	15.8	3.9	0.0
15	3494	21.8	12.2	1.0	46.9	8.5	0.0	5.7	3.9	0.0
16	321	22.4	14.4	50.3	10.8	1.2	0.0	0.2	0.9	0.0
17	351	7.8	8.0	33.8	19.4	11.4	19.2	0.0	0.0	0.0
18	310	0.0	0.0	0.0	0.0	0.0	100.0	0.0	0.0	0.0
19	1528	8.4	15.1	22.3	25.8	4.6	21.7	0.2	0.1	1.6
20	777	13.1	26.1	21.6	35.4	3.1	0.0	0.4	0.1	0.0
21	240	0.0	1.4	54.4	19.6	5.7	18.9	0.0	0.0	0.0
22	537	6.2	6.9	47.4	17.6	1.3	20.6	0.0	0.0	0.0
23	630	13.1	7.8	31.3	19.7	2.4	23.5	1.1	1.3	0.0
24	1513	7.7	5.7	29.8	15.5	1.5	38.9	0.4	0.5	0.0
25	233	62.9	15.3	5.1	13.9	2.6	0.0	0.0	0.3	0.0
26	771	22.0	13.8	26.2	21.1	17.0	0.0	0.0	0.2	0.0
27	129	0.0	3.0	79.0	11.0	2.0	5.0	0.0	0.0	0.0
28	226	0.0	0.0	0.5	14.4	0.0	85.6	0.0	0.0	0.0
29	64	0.0	0.0	61.0	29.0	5.0	5.0	0.0	0.0	0.0
30	91	0.0	0.0	0.0	1.0	0.0	99.0	0.0	0.0	0.0

3.1.2 Gauge Locations & Available Data Sets

For this study, the hydrologic model has been set up to simulate continuously from January 1, 2002 to December 31, 2005. This study utilized historic data from 30 stream gauges (Environment Canada, 2007a) and 28 weather stations (Environment Canada, 2007b). Stream gauge data are in the form of average daily flow from each stream. Each stream gauge provides data for the corresponding sub-basin and is located at the outlet of a grid cell.

The available historic streamflow data from each stream gauge determine which sub-basins should be used for calibration. The available stream gauge data are shown in table 3.2.

Table 3.2: Available historic streamflow data for the Upper South Saskatchewan River watershed

STATION #	STATION NAME	DATA DAYS			
		2002	2003	2004	2005
1 - 05CK004	RED DEER RIVER NEAR BINDLOSS		********** COMPLETE **********		
2 - 05AG006	OLDMAN RIVER NEAR THE MOUTH		********** COMPLETE **********		
3 - 05AC023	LITTLE BOW RIVER NEAR THE MOUTH	May 1 - Oct 31	May 1 - Oct 31	May 1 - Oct 31	May 1 - Oct 31
4 - 05CC007	MEDICINE RIVER NEAR ECKVILLE		********** COMPLETE **********		
5 - 05CB004	RAVEN RIVER NEAR RAVEN		********** COMPLETE **********		
6 - 05CB001	LITTLE RED DEER RIVER NEAR THE MOUTH		********** COMPLETE **********		
7 - 05CA002	JAMES RIVER NEAR SUNDRE	Mar 1 - Oct 31	Mar 1 - Oct 31	Mar 1 - Oct 31	Mar 1 - Oct 31
8 - 05CA012	FALLENTIMBER CREEK NEAR SUNDRE	May 1 - Oct 31	May 1 - Oct 31	May 1 - Oct 31	May 1 - Oct 31
9 - 05CA009	RED DEER RIVER BELOW BURNT TIMBER CREEK		********** COMPLETE **********		
10 - 05CA004	RED DEER RIVER ABOVE PANTHER RIVER	Apr 1 - Oct 31	Apr 1 - Oct 31	Apr 1 - Oct 31	Apr 1 - Oct 31
11 - 05CE011	RENWICK CREEK NEAR THREE HILLS		********** COMPLETE **********		
12 - 05CE002	KNEEHILLS CREEK NEAR DRUMHELLER	Apr 11 - Oct 31	Mar 13 - Oct 31	Mar 10 - Oct 31	Mar 1 - Oct 31
13 - 05CE020	MICHICHI CREEK AT DRUMHELLER	Mar 23 - Oct 31	Mar 13 - Oct 31	NO DATA	Mar 1 - Oct 31
14 - 05BA001	BOW RIVER AT LAKE LOUISE	May 1 - Oct 31	May 1 - Oct 31	May 1 - Oct 31	May 1 - Oct 31
15 - 05BB001	BOW RIVER AT BANFF		********** COMPLETE **********		
16 - 05BG006	WAIPAROUS CREEK NEAR THE MOUTH		********** COMPLETE **********		
17 - 05BH009	JUMPINGPOUND CREEK NEAR THE MOUTH		********** COMPLETE **********		
18 - 05BH014	NOSE CREEK ABOVE AIRDIRE	NO DATA	NO DATA	NO DATA	May 1 - Oct 31
19 - 05BJ010	ELBOW RIVER AT SARCEE BRIDGE	Apr 16 - Oct 31	Apr 1 - Oct 31	Apr 14 - Oct 26	NO DATA
20 - 05BJ004	ELBOW RIVER AT BRAGG CREEK		********** COMPLETE **********		
21 - 05BK001	FISH CREEK NEAR PRIDDIS	Mar 1 - Oct 31	Mar 1 - Oct 31	Mar 1 - Oct 31	Mar 1 - Oct 31
22 - 05BL013	THREEPOINT CREEK NEAR MILLARVILLE	Mar 1 - Oct 31	Mar 1 - Oct 31	Mar 1 - Oct 31	Mar 1 - Oct 31
23 - 05BL014	SHEEP RIVER AT BLACK DIAMOND		********** COMPLETE **********		
24 - 05BL012	SHEEP RIVER AT OKOTOKS		********** NO DATA **********		
25 - 05BL022	CATARACT CREEK NEAR FORESTRY ROAD		********** COMPLETE **********		
26 - 05BL019	HIGHWOOD RIVER AT DIEBEL'S RANCH	Mar 1 - Oct 31	Mar 1 - Oct 31	Mar 1 - Oct 31	Mar 1 - Oct 31
27 - 05BL027	TRAP CREEK NEAR LONGVIEW	May 1 - Oct 31	May 1 - Oct 31	May 1 - Oct 31	May 1 - Oct 31
28 - 05BL023	PEKISKO CREEK NEAR LONGVIEW	Mar 1 - Oct 31	Mar 1 - Oct 31	Mar 1 - Oct 31	Mar 1 - Oct 31
29 - 05AB040	WILLOW CREEK AT SECONDARY 532	Mar 1 - Oct 31	Mar 1 - Oct 31	Mar 1 - Oct 31	Mar 1 - Oct 31
30 - 05AB029	MEADOW CREEK NEAR THE MOUTH	Apr 1 - Oct 31	Mar 1 - Oct 31	Mar 1 - Oct 31	Mar 1 - Oct 31

Weather stations provide temperature and precipitation data on a daily time scale. The locations of each station are displayed in figure 3.6.

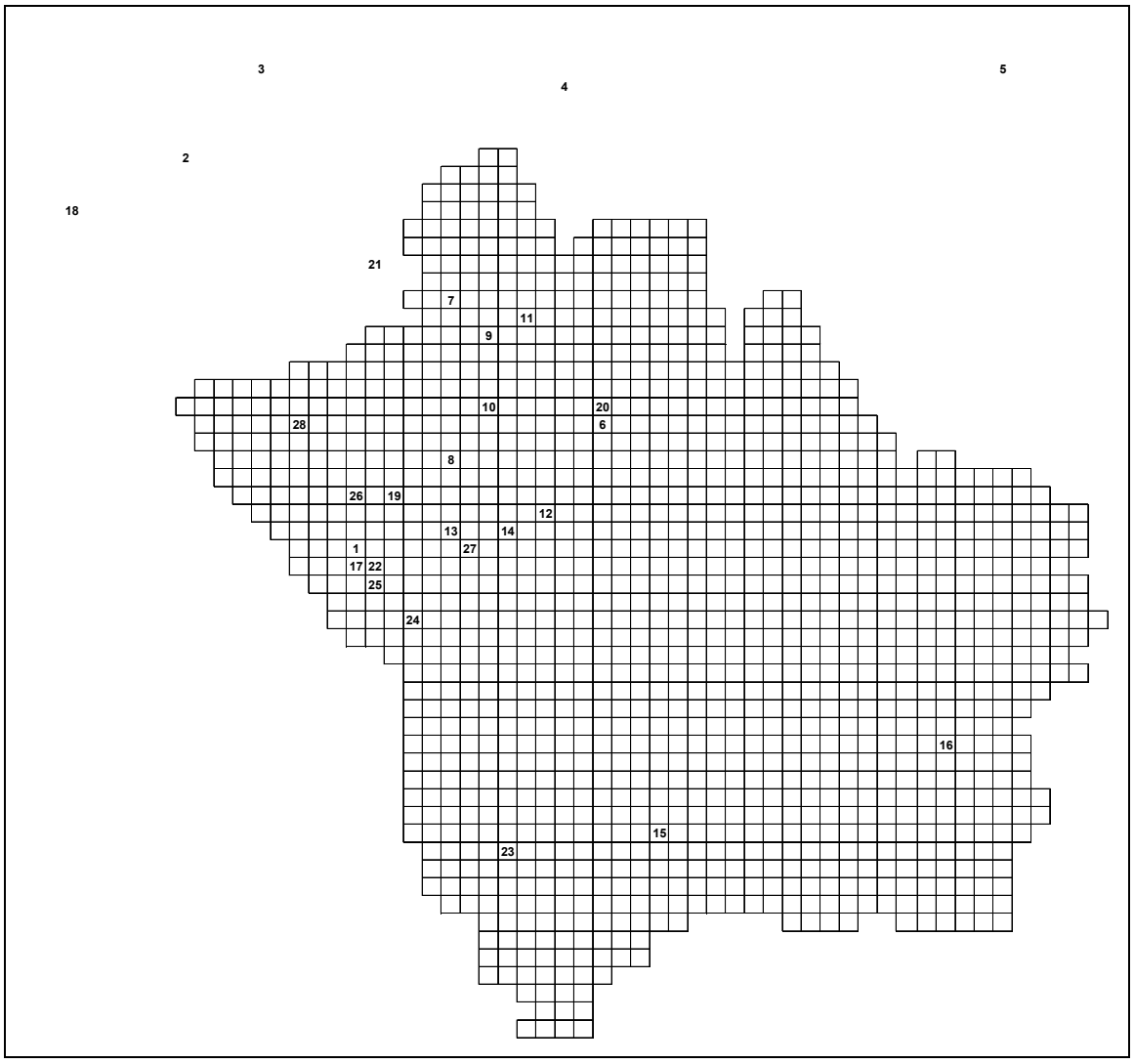

Figure 3.6: Weather station locations in the Upper South Saskatchewan River watershed

3.2 Manual Calibration

This section provides an outline of how manual calibration was performed on a WATFLOOD model of the Upper South Saskatchewan River watershed. The purpose of manual calibration is to determine a finite set of parameters that strongly influences modeling outputs. These parameters will be manually adjusted to values that result in significant improvements in model outputs. Selecting the influential parameter set and

determining an initial value for each parameter through manual adjustment reduces the parameter set and parameter space to be used for automated calibration and may produce more accurate results. Described here are the objective functions used during manual calibration, the method used for selecting sub-basins to calibrate, a description of the most relevant and sensitive parameters that control model outputs, sensitivity of calibrated parameters, and results obtained from manual calibration.

3.2.1 Objective Function

The objective function used for manual calibration (and later automated calibration) is the Nash-Sutcliffe model efficiency coefficient (Nash & Sutcliffe, 1970). The general form of this equation is:

$$E = 1 - \frac{\sum_{t=1}^{T} (Q_O^t - Q_m^t)^2}{\sum_{t=1}^{T} (Q_O^t - \overline{Q}_{Om})^2} \tag{3.1}$$

where Q_o^t is the observed discharge and Q_m^t is the modeled discharge for the time period t. Either daily flows or monthly average flows were used as a basis for model comparison. For the daily coefficient, the daily peak flows were used for Q_o and Q_m, and for the monthly coefficient, the average of the daily peak flows for each month were used for Q_o and Q_m.

In addition to the daily and monthly Nash-Sutcliffe model efficiency coefficients, visual hydrograph inspections were performed to determine the effect of each parameter on model outputs. Since the study does not aim to compare calibration results found using different objective functions, no other measures will be used.

3.2.2 Sub-basins Selected for Calibration

Each time a parameter was varied, the objective function was calculated for certain sub-basins and visual inspection of the hydrographs was performed. Prior to any parameter variation, the most appropriate sub-basins were selected for the purpose of learning the most from each parameter variation.

Throughout the calibration process, results from certain sub-basins are used to calibrate the model, while others are used for model validation. Validating the model is a process in which results from some sub-basins that were not used to measure model performance are compared to confirm model improvements. Limitations encountered in this study restricted the number of sub-basins that could be trusted for calibration or validation. Before sub-basin selection could take place, it was important to recognize and address the limitations this case study. Here, these limitations can be classified into three categories: data limitations, limitations caused by man-made hydraulic features, hydrologic modeling limitations.

Data Limitations

While the streamflow data set contains historic measurements from 30 stream gauges, it is clear from table 3.2 that the data set is not complete. Of the 30 stream gauge locations, only 13 contain daily data for the entire study period. One gauge has no data available for the study period, and several others are missing entire years of measurements. The remaining gauges have only summer data, which can still be useful for model validation purposes. The limited data set must be considered when selecting basins for calibration (section 3.2.2).

Man-made Hydraulic Features

One portion of the study area is heavily affected by man-made reservoirs and irrigation canals. Sub-basin three (see figure 3.5) is the watershed of the Little Bow River and has a drainage area of approximately 6,800 km^2. Of that area, drainage from the upper 4,230 km^2 is diverted into Travers Reservoir, and only 30 % of the annual

drainage is released back into the Little Bow River (Atlas of Alberta Lakes, 2005). The other 70% of the drainage is diverted into Little Bow River Lake which feeds irrigation canals for the region. Since the drainage released to the Little Bow River is controlled and depleted rather than naturally drained, the model output from this sub-basin, which only considers environmental influences, can not be used for calibration. Since this sub-basin makes up over 20% of the drainage area for Oldman River watershed (sub-basin 2), modeling results from the Oldman River are not useful for calibration.

Hydrologic Modeling Limitations

Hydrologic modeling limitations are the modeling software's inability to represent certain hydrologic processes. Here, the major hydrologic modeling limitation is the simplification of processes simulated on prairie agricultural land use. Fifty-nine percent of the entire watershed is allocated as agricultural use, most of which is located in the prairie region of the study area. Two aspects of prairie hydrology make hydrologic modeling on a regional scale extremely difficult. First, blowing snow can transport up to 75% of annual snow fall from open fields (Fang et al., 2007). This leads to varied snow melt patterns due to drifts, and lengthens spring runoff. This phenomenon is not simulated with WATFLOOD. Second, because much of the prairies contain glacially formed depressions many basins are internally drained. The runoff from internally drained basins contributes to pools that are formed in these glacial depressions. From there, water either infiltrates or evaporates. Only during the most extreme runoff events will these pools spill over and contribute to streamflow (Fang et al., 2007). The model could not be setup to simulate these hydrologic processes because of limitations with the WATFLOOD software. Because these two aspects of prairie hydrology are not simulated with WATFLOOD, calibration of sub-basins dominated by the agricultural land use is limited in this study. The agricultural land class parameters are not used during the initial manual calibration process; however, they are altered to improve modeling results once the other land class parameters have been estimated through manual calibration.

A second hydrologic modeling limitation in this study is the presence of glaciers in the mountains that lie along the western portion of the study area. Though they make up a very small percentage of any sub-basin (15% maximum), streamflow in watersheds that contain glaciers tends to be dominated by their summer melt cycles. WATFLOOD holds a limitation on initial snow depth at 8850 mm (8.85 m). This is not a high enough value for a glacier, as the snow cover should be effectively infinite for the purposes of modeling. If the glacier land class was assigned an initial snow depth of 8.85 m, the snow would melt off during the first spring, and the glaciers would no longer contribute to streamflow in the model as they would in reality. For this reason, several basins that contain significant glaciers (>5%) are not used in model calibration or validation.

The goal of initial sub-basin selection was to remove sub-basins with flawed or incomplete data sets. For the selection of sub-basins used during manual calibration, sub-basins with complete sets of streamflow data are desired. Additionally, sub-basins that are dominated by a certain land class are determined. When a sub-basin is dominated by a specific land class, the modeling results are heavily reliant on those land class parameters. For example, sub-basin 25 is the best candidate for calibrating the dense forest land class parameters (63% coverage – table 3.1). Starting with the default values, dense forest land class parameters could be calibrated using sub-basin 25, and then the parameter values would be applied basin-wide.

The land class parameters chosen for manual calibration were dense forest, light forest, mixed forest, and open land. These were selected because they represent the largest portion of the study area that is not dominated by different prairie drainage phenomenon. Agricultural land class parameters are calibrated as well, but because of unpredictable prairie hydrology, they were manually adjusted last and while considering the results from several sub-basins at a time. Considering the agricultural land class parameters last prevents the unpredictable behavior of prairie hydrology from producing parameter values that have poor accuracy throughout the entire watershed. Instead, knowing that the hydrology is unpredictable, the agricultural parameter values are adjusted last. These adjustments will be for the purpose of improving the objective function and not necessarily to represent the hydrology of a specific sub-basin's

agricultural land use (which is known to be unpredictable and geographically diverse). The sub-basins selected for manual calibration are shown in table 3.3.

Table 3.3: Sub-basins selected for manual calibration

Sub-basin #	Area (sq km)	Dense Forest %	Light Forest %	Mixed Forest %	Open %	Wetland %	Agricultural %	Glacier %	Water %	Impervious %
1	46250	2.6	1.6	3.3	28.6	0.8	61.8	0.2	1.2	0.0
4	1966	0.0	0.4	13.3	13.2	0.5	72.6	0.0	0.0	0.0
5	784	10.9	3.7	17.0	18.2	0.4	50.0	0.0	0.0	0.0
6	2612	0.2	4.3	16.2	10.5	5.2	63.7	0.0	0.0	0.0
9	2418	36.8	15.1	1.4	34.9	7.3	0.0	3.0	1.5	0.0
16	321	22.4	14.4	50.3	10.8	1.2	0.0	0.2	0.9	0.0
17	351	7.8	8.0	33.8	19.4	11.4	19.2	0.0	0.0	0.0
20	777	13.1	26.1	21.6	35.4	3.1	0.0	0.4	0.1	0.0
23	630	13.1	7.8	31.3	19.7	2.4	23.5	1.1	1.3	0.0
25	233	62.9	15.3	5.1	13.9	2.6	0.0	0.0	0.3	0.0

The shaded values in the above table indicate the land classes that were focused upon for each of the selected basins during manual calibration. Figure 3.7 shows the locations of the sub-basins listed in table 3.3.

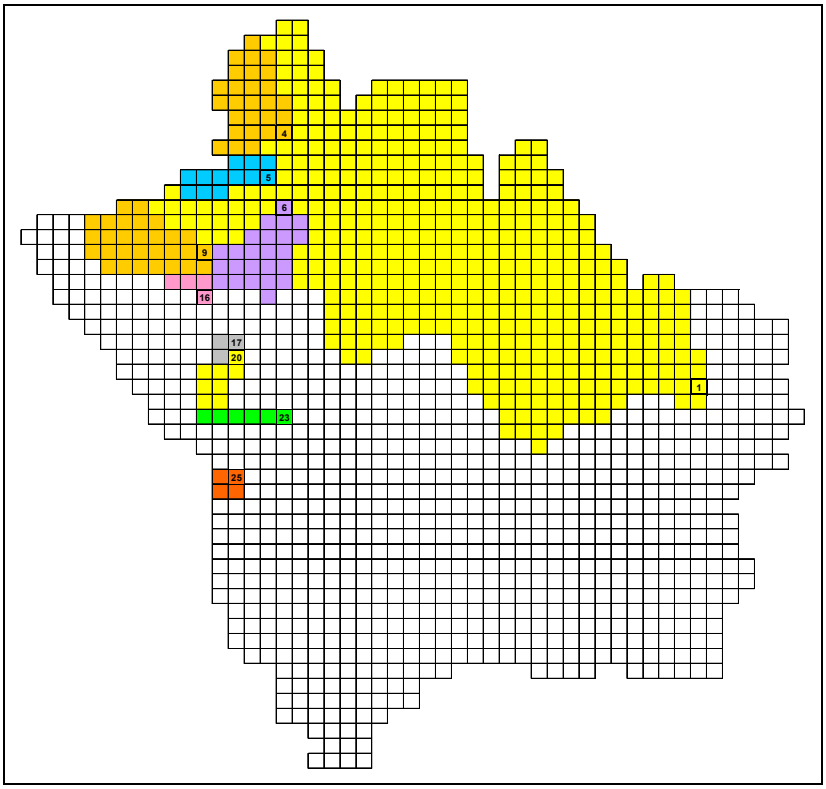

Figure 3.7: Sub-basins selected for manual calibration

As shown above, the sub-basins are diverse in drainage area, but not in geographic location as the southern portion is not well represented in manual calibration. The presence of Travers Reservoir in the southern portion of the study area controls and diverts too much water for model results to be considered relevant.

It is important to note that, while only the sub-basins shown above have been selected for manual calibration, results from other sub-basins are also compared to gauge data for validation purposes.

3.2.3 Calibrated Parameters

First, a sensitivity analysis was performed on all model parameters, and then only sensitive parameters were subjected to manual calibration. To determine which parameters should be calibrated, it is important to understand the function each parameter serves within the model. This section summarizes the parameters that were found through trial and error to have a significant effect on model outputs when altered.

River Class Parameters

Starting with the pre-calibrated model (all parameter values set to defaults as described in section 2.2.2) each parameter was varied one at a time (+ 25%) and the model was run. After each model run, the daily Nash-Sutcliffe coefficient was calculated and the hydrograph of a specific basin was visually analyzed. Visual analysis combined with parameter descriptions (Kouwen, 2007) helped determine how each parameter altered the modeling of each hydrologic process in WATFLOOD. Often, the visual analysis was challenging since changes in the hydrographs were small and difficult to decipher, which is why the objective function value was also as a primary tool during manual calibration. The sub-basin used for this initial sensitivity was sub-basin nine, and had an initial daily Nash-Sutcliffe coefficient of -0.096. Table 3.4 contains a list of river class parameters, the parameter variation for the sensitivity trial, the objective function changes that resulted from parameter variation, and how it influences the hydrologic

model. Each parameter was varied from their respective default values (described in section 2.2.2).

Table 3.4: River class parameter initial sensitivity and hydrograph impacts for sub-basin nine

Parameter	Parameter Variation	Change in Daily Nash-Sutcliffe	Impact on Hydrograph
LZF	+ 25%	0.028	shape of base flow depletion curve
PWR	+ 25%	0.012	shape of base flow depletion curve
R1	+ 25%	0.011	magnitude and timing of peak flow
R2	+ 25%	0.044	magnitude and timing of peak flow
MNDR	+ 25%	0.023	magnitude and timing of peak flow

The river class parameters all produced measurable differences in the daily Nash-Sutcliffe coefficients. Only one parameter was removed from the manual calibration as a result of the river class sensitivity analysis, and it was *R1*. Even though adjustments of *R1* produced measurable hydrograph changes, this process showed that both *R2* and *MNDR* influence the model in the same fashion as *R1* and thus it was eliminated as a calibration parameter.

Land Class Parameters

Land class parameters are analyzed in the same manner as river class parameters, but are considered separately for the purpose of selecting a parameter set that represents all of the significant hydrologic and hydraulic functions that influence the model. The land class parameters that were considered during the initial portion of manual calibration are described in section 2.2.2. Table 3.5 contains a list of land class parameters, the parameter variation for the sensitivity trial, the objective function changes that resulted from parameter variation, and how it influences the hydrologic model.

Table 3.5: Land class parameter initial sensitivity and hydrograph impacts for sub-basin nine

Parameter	Parameter Variation	Change in Daily Nash-Sutcliffe	Impact on Hydrograph
DS	+ 25%	0.000	no effect
DSFS	+ 25%	0.000	no effect
RE	+ 25%	0.020	magnitude of peak flow (interflow based)
AK	+ 25%	0.000	magnitude of peak flow (interflow based)
AKFS	+ 25%	0.000	magnitude of peak flow (interflow based)
RETN	+ 25%	0.002	magnitude of peak flow (evaporation based)
AK2	+ 25%	0.013	magnitude of peak flow (interflow based)
AK2FS	+ 25%	0.003	magnitude of peak flow (interflow based)
R3	+ 25%	0.000	no effect
R3FS	+ 25%	0.000	no effect
R4	+ 25%	0.000	no effect
CH	+ 25%	0.000	no effect
MF	+ 25%	0.009	magnitude peak flow (melt based)
BASE	+ 0.1	0.009	timing of peak flow (melt based)
RHO	+ 25%	0.000	total volume of flow (melt based)
FTAL	+ 0.01	0.006	magnitude of peak flow (evapotranspiration based)

There are several parameters that have little to no effect on the modeling results (*DS, DSFS, AK, AKFS, R3, R3FS, R4, CH, and RHO*) and were removed from the manual calibration process. Of the seven remaining land class parameters that had a higher impact on modeling results (*RE, RETN, AK2, AK2FS, MF, BASE, and FTAL*), the *RE, AK2*, and *AK2FS* parameters were observed to have the same effect on the output hydrographs. Since *RE* had a more significant effect on the daily Nash-Sutcliffe coefficient, it was retained for the manual calibration and *AK2* and *AK2FS* were removed from the list of parameters to be further calibrated.

The parameters that were considered for further calibration were: *LZF, PWR, R2, MNDR, MF, BASE, RE, RETN, FTAL.*

3.2.4 Manual Calibration Steps

This section outlines the method used during manual calibration. Using sub-basin nine as an example, the parameters selected for manual calibration in section 3.2.3 are varied in a specific order to improve the accuracy of the modeling results.

Starting with the pre-calibrated model the hydrograph and daily Nash-Sutcliffe coefficient were analyzed for a specific basin. One of the sub-basins used during manual calibration was sub-basin nine. A comparison of measured vs. modeled results with default parameter values for sub-basin nine is shown in figure 3.8.

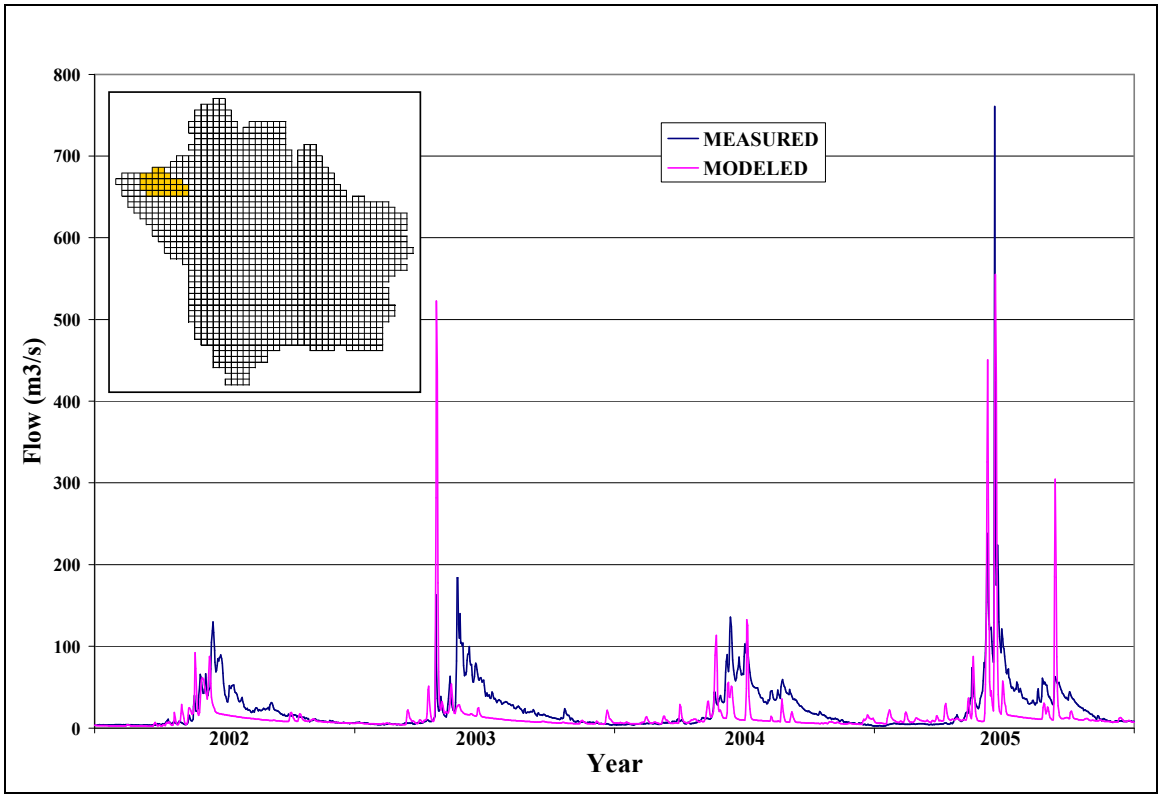

Figure 3.8: Measured streamflows vs. modeled streamflows from pre-calibrated model of Red Deer River below Burnt Timber Creek (sub-basin 9)

The modeled hydrograph consistently predicted flows that were less than the measured values. This was a result of both the magnitude of peak flows, and the shape of the base flow depletion curves. The Nash-Sutcliffe daily coefficient for the pre-calibrated sub-basin was -0.096. A general algorithm used to improve the hydrograph manually for each sub-basin is described as follows:

1. Set initial parameters (default values) for all calibrated parameters

2. Run model and identify visually analyze for strengths and weaknesses in the output hydrographs (magnitude of peak flows, etc)

3. Adjust base flow parameters (*LZF, PWR*) to improve the base flow depletion curve using both visual hydrograph analysis and the results of the objective function

4. Adjust streamflow parameters (*R2, MNDR*) to improve timing of peak flows using both visual hydrograph analysis and the results of the objective function

5. Focusing on the initial melt portions of the model outputs, adjust the snow melt parameters (*MF, BASE*) to improve the timing and magnitude of the peak flows resulting from snow melt using both visual hydrograph analysis and the results of the objective function

6. Adjust remaining parameters (*RE, RETN, FTAL*) to improve magnitude of all peak flows (those influenced by snow melt included) using primarily the results of the objective function

Steps 2 – 6 were performed iteratively using small parameter adjustments to ensure that certain land class parameters were not adjusted to hydrologically unrealistic values to compensate for inadequacies in the default parameter values of other land classes.

The purpose of visual hydrograph inspection was that particularly in the early stages of manual calibration, adjusting parameters that vary the timing of peak flows and base flow depletion (*LZF, PWR, R2, MNDR, MF, and BASE*) sometimes lead to an improved objective function, but a model that is further away from a reasonable representation of historic hydrographs when visually inspected. The objective function is not a perfect measure of model performance, and visual inspections help to ensure that modeling improvements occur when the objective function improves as sometimes the opposite can be the case. Since *RE, RETN*, and *FTAL* did not alter the timing of the hydrographs they were manually adjusted using objective function results only (though intermittent visual observations were still made to for validation). Adjusting only the parameters selected in section 3.2.3 the manually calibrated hydrograph for sub-basin 9

produced a daily Nash-Sutcliffe coefficient of 0.738. The hydrograph is shown in figure 3.9.

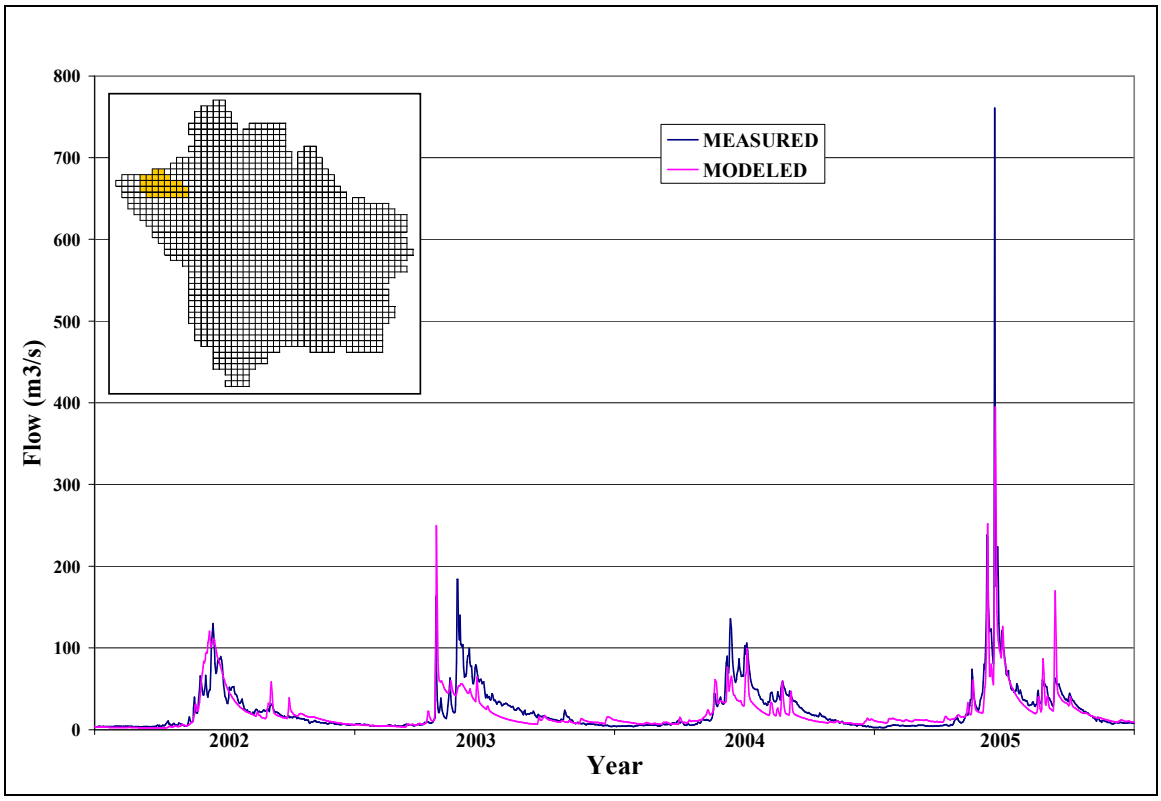

Figure 3.9: Measured streamflows vs. modeled streamflows from manual calibration of Red Deer River below Burnt Timber Creek (sub-basin 9)

While the monthly Nash-Sutcliffe coefficient was not considered during calibration, it was used as a form of validation for the calibrated model. The monthly Nash-Sutcliffe coefficient improved from -0.026 to 0.893.

The process of manual calibration was performed on each of the sub-basins shown in table 3.3, each time focusing on the land and river class parameters that dominate those basins respectively (shaded values). To complete the process of manually calibrating four river class parameters for three river types, and five land class parameters for five land types required approximately 2500 model runs.

3.2.5 Calibration Results

Manual calibration was performed on land class and river class parameters that had significant effects on the sub-basins listed in table 3.3. Outputs from several sub-basins with incomplete data sets were considered for the purpose of model validation. Additionally, while the performance metric of the Nash-Sutcliffe monthly coefficient was not used directly as a measure of accuracy, it was compared for the pre-calibrated and manually calibrated models to provide another measure of model accuracy. The parameter values found through manual calibration for each river class and land class parameter described in section 3.2.3 are shown in table 3.6 and 3.7 respectively.

Table 3.6: River class parameter values obtained through manual calibration

Parameter	River Class		
	1	2	3
LZF	0.100E-04	0.100E-04	0.700E-04
PWR	0.203E+01	0.100E+00	0.130E+00
R2	0.200E+00	0.300E+01	0.100E+00
MNDR	0.100E+01	0.900E+01	0.100E+01

Table 3.7: Land class parameter values obtained through manual calibration

Parameter	Land Class				
	1	2	3	4	6
RE	0.500E-01	0.200E-02	0.100E+00	0.200E+00	0.700E+00
RETN	0.200E+02	0.700E+02	0.800E+02	0.700E+02	0.700E+02
MF	0.100E+00	0.100E+00	0.100E+00	0.300E-01	0.100E+00
BASE	-0.200E+00	-0.100E+01	-0.100E+01	-0.300E+00	-0.100E+00
FTAL	0.20	0.30	0.20	0.20	0.6

To determine the success of manual calibration, results from sub-basins that were not used to manually calibrate the model (sub-basins not in table 3.3) were considered. Though these sub-basins did not have complete data sets, their Nash-Sutcliffe coefficients were calculated by comparing only the data available with modeling results. The pre-calibrated and manually calibrated values for the Nash-Sutcliffe daily and monthly coefficients are shown in table 3.8. Shaded rows indicate sub-basins used to manually calibrate the model.

Table 3.8: Pre-calibrated and manually calibrated Nash-Sutcliffe coefficients

Sub-basin #	Pre-Calibrated Nash Daily	Manually Calibrated Nash Daily	Improvement in Nash Daily?	Pre-calibrated Nash Monthly	Manually Calibrated Nash Monthly	Improvement in Nash Monthly?
1	-0.181	0.621	YES	-0.212	0.731	YES
4	0.031	0.169	YES	0.115	0.377	YES
5	-0.088	0.101	YES	0.234	0.605	YES
6	0.482	-0.001	NO	0.714	0.902	YES
7	0.094	0.425	YES	0.194	0.641	YES
8	0.483	0.545	YES	0.325	0.835	YES
9	-0.096	0.738	YES	-0.026	0.893	YES
16	0.410	0.619	YES	0.334	0.921	YES
17	0.700	0.492	NO	0.653	0.931	YES
19	-0.362	0.704	YES	-0.078	0.907	YES
20	0.265	0.779	YES	0.366	0.915	YES
21	0.606	0.405	NO	0.591	0.778	YES
22	0.468	0.503	YES	0.457	0.673	YES
23	0.307	0.621	YES	0.269	0.743	YES
25	-0.016	0.221	YES	0.244	0.329	YES
26	-0.080	0.419	YES	-0.028	0.552	YES
27	-0.055	0.365	YES	-0.146	0.470	YES
28	0.272	0.065	NO	0.357	0.470	YES
29	0.112	0.241	YES	0.118	0.534	YES
AVG/TOTAL	**0.177**	**0.423**	**15**	**0.236**	**0.695**	**19**

Though not all sub-basins were used during the manual calibration process, model accuracy was improved for almost all cases. Since the calibrated parameters influence modeling results watershed-wide, adjusting a parameter value to improve the results of one sub-basin can change (hopefully improve but possibly degrade) modeling results in other sub-basins. The model's accuracy was improved for 15 of 19 sub-basins (7 of 9 validation sub-basins) for the daily Nash-Sutcliffe coefficient, and for 19 of 19 sub-basins (9 of 9 validation basins) for the monthly Nash-Sutcliffe coefficient through automated calibration. The average of both the Nash-Sutcliffe daily and monthly values also increased significantly through manual calibration. Although the average values of the objective function may not be the best way to evaluate the success of all hydrologic calibrations it is effective in this case since each sub-basin (with the exception of sub-basin 1) is a head water basin and is considered independently of all others. Another option for comparing watershed-wide success would be a weighted average of the Nash-Sutcliffe coefficients using sub-basin area, rainfall, streamflow, or another measure as the weighting function. The objective function is weighted by average streamflow during the automated calibration in the following section.

3.3 Automated Calibration

The purpose of using an automated algorithm to calibrate the model was to refine some of the estimated parameter values found from manual calibration to improve model results. While manual calibration was used to identify important parameters, automated calibration searches the parameter space of some of those parameters to find the best solution within the given parameter ranges. This section provides an outline of how the manually calibrated model was improved using automated calibration. The method uses an objective function that is calculated using the results from multiple sub-basins in each trial. Described in this section is a brief description of the optimization algorithm selected for this study, an outline of the parameter ranges used, the objective function used, the selection of sub-basins, and results.

3.3.1 Optimization Algorithm (DDS)

The optimization algorithm chosen for this study is the dynamically dimensioned search (DDS) (Tolson & Shoemaker, 2007). For DDS to function with WATFLOOD, it requires a model parameter set, and the corresponding parameter ranges in terms of maximum and minimum values. The DDS manual (Tolson & Seglenieks, 2007) recommends that for optimization problems involving 10 or more parameters that 1000 function evaluations can typically generate reasonable results, so that will be the value used for this study. Details on the specifics of the DDS algorithm can be found in (Tolson & Shoemaker, 2007).

3.3.2 Parameter Selection & Parameter Ranges

The parameters selected for automated calibration are chosen with a goal of representing the major hydrologic processes that heavily influence modeling results. Through the manual calibration the dominant processes were found to be: snow melt, base flow

depletion, evapotranspiration, streamflow rates, evaporation, and interflow. The parameters selected to represent each process are shown in table 3.9:

Table 3.9: Automated calibration parameters selected by hydrologic process

Hydrologic Process	**Parameters**
Snow Melt	MF, BASE
Baseflow Depletion	LZF
Evapotranspiration	RETN
Stream Flow Rates	R2
Evaporation	FTAL
Interflow	RE

Each process was assigned one parameter for automated calibration except for snow melt. For snow melt, two parameters were selected since both *MF* and *BASE* have significantly different effects on the output hydrographs. Both *PWR* and *MNDR* were not included in the automated calibration process because they influence the output hydrographs in a very similar manner to *LZF* and *R2* respectively, but less significantly (table 3.4).

Initially, the range of each parameter was chosen as approximately +/- 50% of the value obtained from manual calibration as long as that range does not exceed the reasonable boundaries for the parameter which are governed by hydrologic and physical limitations (i.e. *MNDR* cannot be less than 1). For *BASE* an initial range was selected as +/- 1.5 degrees, and for *FTAL*, initial ranges were selected as +/- 0.2 (minimum of 0.01, and maximum of 1.0).

Following each automatic calibration trial, the ranges for each parameter were reset according to the results of the trial. Figure 3.10 depicts a decision diagram outlining how parameters were adjusted after each trial.

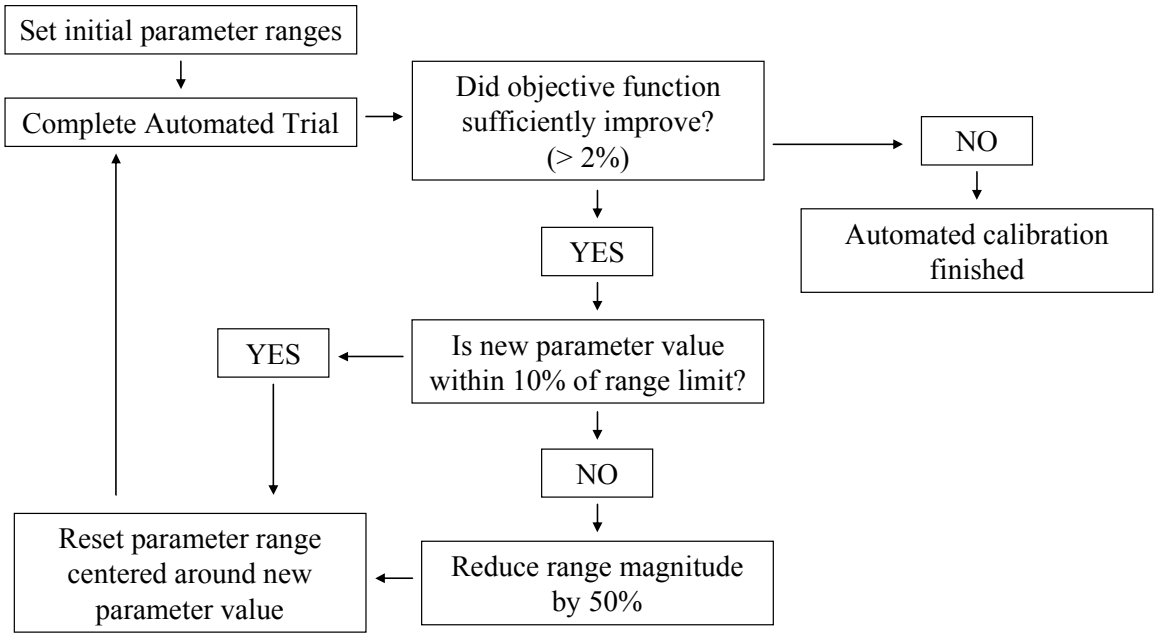

Figure 3.10: Automated calibration parameter adjustment flow chart

As shown above, trials will continue until the model does not show sufficient improvement.

3.3.3 Objective Function Weighting Method

The objective function used for automated trials is a weighted sum of the Nash-Sutcliffe daily coefficients based on the average flow from each sub-basin. The weighting function is as follows:

$$N_d = \frac{\sum_{b=1}^{n} N_b * Q_b}{\sum_{b=1}^{3} Q_b} \tag{3.2}$$

where N_d is the weighted Nash-Sutcliffe daily value used to evaluate the model, N_b is the Nash-Sutcliffe daily value from each sub-basin involved in the calculation, and Q_b is the average measured flow for the calibration period from each sub-basin involved in the calculation.

3.3.4 Sub-basin Selection

The sub-basins selected for automatic calibration were not the same set selected for manual calibration. The purpose of this was to increase the number of sub-basins that could be used as validation sub-basins to gain more information about the success of the weighted objective function. The sub-basins used for the automated calibration objective function calculation are selected from the sub-basins listed in table 3.3. The sub-basins were chosen to represent all major land classes, and represent a variety of geographic areas so that the automated algorithm calibrates to an objective function that represents historic data from a variety of regions within the watershed. The sub-basins were also chosen to have a full historic streamflow data set for the simulation period (January 1, 2002 to December 31, 2005). The sub-basins used in automated calibration are shown in table 3.10 and figure 3.11.

Table 3.10: Sub-basins used for automated calibration

Sub-basin #	Area (sq km)	Dense Forest %	Light Forest %	Mixed Forest %	Open %	Wetland %	Agricultural %	Glacier %	Water %	Impervious %
5	784	10.9	3.7	17.0	18.2	0.4	50.0	0.0	0.0	0.0
9	2418	36.8	15.1	1.4	34.9	7.3	0.0	3.0	1.5	0.0
16	321	22.4	14.4	50.3	10.8	1.2	0.0	0.2	0.9	0.0
20	777	13.1	26.1	21.6	35.4	3.1	0.0	0.4	0.1	0.0
23	630	13.1	7.8	31.3	19.7	2.4	23.5	1.1	1.3	0.0
25	233	62.9	15.3	5.1	13.9	2.6	0.0	0.0	0.3	0.0

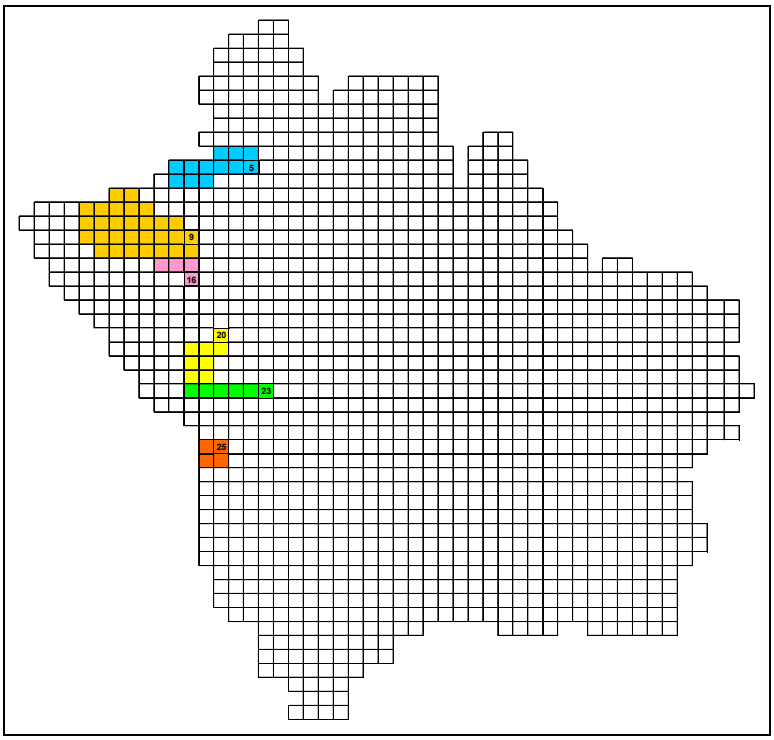

Figure 3.11: Sub-basins used for automated calibration

The simulation outputs (streamflow) from the six selected sub-basins are subjected to the daily Nash-Sutcliffe coefficient, and then incorporated into the weighted objective function (equation 3.2) using a script called "MultiNash" (Appendix B). Although a small portion of the watershed is represented during automated calibration, results from several other basins will be considered for validation purposes once the calibration process is complete.

3.3.5 Automated Calibration Results

Automated calibration was performed using the iterative process described in figure 3.10. Although the model is calibrated using the results from the six sub-basins listed in table 3.10, model validation is considered for all sub-basins with acceptable data (table 3.8). The manually calibrated model had a weighted (using sub-basins in table 3.10) Nash-Sutcliffe daily coefficient of 0.669. This weighted Nash-Sutcliffe daily coefficient was improved through the automated process to 0.743. The parameter values found through

the automated calibration process for each river class and land class parameter described in section 3.2.3 are shown in table 3.11 and 3.12 respectively.

Table 3.11: River class parameter values obtained through automated calibration

Parameter	River Class		
	1	2	3
LZF	0.110E-04	0.112E-04	0.706E-04
R2	0.670E+00	0.329E+01	0.140E+00

Table 3.12: Land class parameter values obtained through automated calibration

Parameter	Land Class				
	1	2	3	4	6
RE	0.520E-01	0.200E-02	0.820E-01	0.167E+00	0.728E+00
RETN	0.166E+02	0.644E+02	0.830E+02	0.631E+02	0.755E+02
MF	0.976E-01	0.128E+00	0.129E+00	0.316E-01	0.102E+00
BASE	-0.197E+00	-0.113E+01	-0.102E+01	-0.314E+00	-0.115E+00
FTAL	0.22	0.32	0.25	0.12	0.72

The automatic calibration was done using the weighted objective function as a measure of model accuracy, and the parameter values found were applied across the entire basin. Although the weighed objective function improved through automated calibration, the success of the method is measured by considering modeling improvements from the individual sub-basins in the model. Additionally, the Nash-Sutcliffe monthly coefficients are used as performance metric since the automated process measures considered only the daily measurements. The Nash-Sutcliffe daily and monthly coefficients resulting from automated calibration are compared to the manually calibrated values for all acceptable basins in table 3.13. Shaded rows indicate sub-basins that were automatically calibrated.

Table 3.13: Nash-Sutcliffe coefficients from manual and automated calibrations

Sub-basin #	Manually Calibrated Nash Daily	Automated Nash Daily	Improvement in Nash Daily?	Manually Calibrated Nash Monthly	Automated Nash Monthly	Improvement in Nash Monthly?
1	0.621	0.673	YES	0.731	0.768	YES
4	0.169	0.293	YES	0.377	0.316	NO
5	0.101	0.426	YES	0.605	0.782	YES
6	-0.001	0.763	YES	0.902	0.911	YES
7	0.425	0.422	NO	0.641	0.640	NO
8	0.545	0.677	YES	0.835	0.830	NO
9	0.738	0.768	YES	0.893	0.958	YES
16	0.619	0.753	YES	0.921	0.968	YES
17	0.492	0.559	YES	0.931	0.955	YES
19	0.704	0.689	NO	0.907	0.878	NO
20	0.779	0.814	YES	0.915	0.920	YES
21	0.405	0.612	YES	0.778	0.841	YES
22	0.503	0.618	YES	0.673	0.728	YES
23	0.621	0.679	YES	0.743	0.777	YES
25	0.221	0.653	YES	0.329	0.787	YES
26	0.419	0.541	YES	0.552	0.708	YES
27	0.365	0.286	NO	0.470	0.479	YES
28	0.065	0.195	YES	0.470	0.447	NO
29	0.241	0.228	NO	0.534	0.561	YES
AVG	**0.423**	**0.560**	**15**	**0.695**	**0.750**	**14**

Although only six sub-basins were automatically calibrated, improvements were made in the Nash-Sutcliffe daily and monthly coefficients in most cases. Automated calibration improved the model accuracy for 15 of 19 sub-basins (9 of 13 validation sub-basins) for the daily Nash-Sutcliffe coefficient, and for 14 of 19 sub-basins (8 of 13 validation sub-basins) for the monthly Nash-Sutcliffe coefficient. Although the weighted average showed improvement, the method is validated by the improvement of the basins that were not considered during the automated calibration.

Finally, the pre-calibrated model results were compared to the fully calibrated (automated) results. The Nash-Sutcliffe daily and monthly coefficients resulting from automated calibration were compared to the pre-calibrated model for all acceptable basins in table 3.14. Shaded rows indicate sub-basins that were automatically calibrated.

Table 3.14: Nash-Sutcliffe coefficients from pre-calibrated and automatically calibrated model

Sub-basin #	Pre-Calibrated Nash Daily	Automated Nash Daily	Improvement in Nash Daily?	Pre-calibrated Nash Monthly	Automated Nash Monthly	Improvement in Nash Monthly?
1	-0.181	0.673	YES	-0.212	0.768	YES
4	0.031	0.293	YES	0.115	0.316	YES
5	-0.088	0.426	YES	0.234	0.782	YES
6	0.482	0.763	YES	0.714	0.911	YES
7	0.094	0.422	YES	0.194	0.640	YES
8	0.483	0.677	YES	0.325	0.830	YES
9	-0.096	0.768	YES	-0.026	0.958	YES
16	0.410	0.753	YES	0.334	0.968	YES
17	0.700	0.559	NO	0.653	0.955	YES
19	-0.362	0.689	YES	-0.078	0.878	YES
20	0.265	0.814	YES	0.366	0.920	YES
21	0.606	0.612	YES	0.591	0.841	YES
22	0.468	0.618	YES	0.457	0.728	YES
23	0.307	0.679	YES	0.269	0.777	YES
25	-0.016	0.653	YES	0.244	0.787	YES
26	-0.080	0.541	YES	-0.028	0.708	YES
27	-0.055	0.286	YES	-0.146	0.479	YES
28	0.272	0.195	NO	0.357	0.447	YES
29	0.112	0.228	YES	0.118	0.561	YES
AVG	**0.177**	**0.560**	**17**	**0.236**	**0.750**	**19**

The automated calibration using a multi-basin approach produced improved modeling results relative to pre-calibrated results in 17 of 19 sub-basins for the daily Nash-Sutcliffe coefficient and 19 of 19 sub-basins for the monthly Nash-Sutcliffe coefficient.

3.4 Summary

The Upper South Saskatchewan River watershed was modeled in WATFLOOD and calibrated to a daily Nash-Sutcliffe coefficient using both manual and automated calibration. Figure 3.12, 3.13, and 3.14 display hydrographs from the pre-calibrated model and those produced by manual and automated calibration respectively for sub-basin 9.

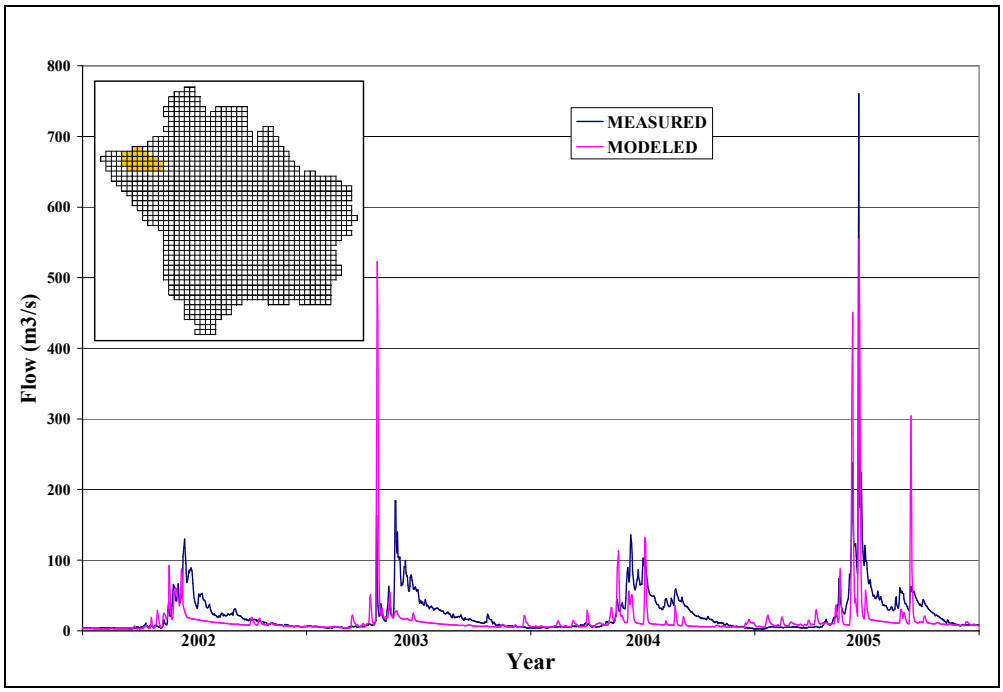

Figure 3.12: Measured streamflows vs. modeled streamflows from pre-calibrated model of Red Deer River below Burnt Timber Creek (sub-basin 9)

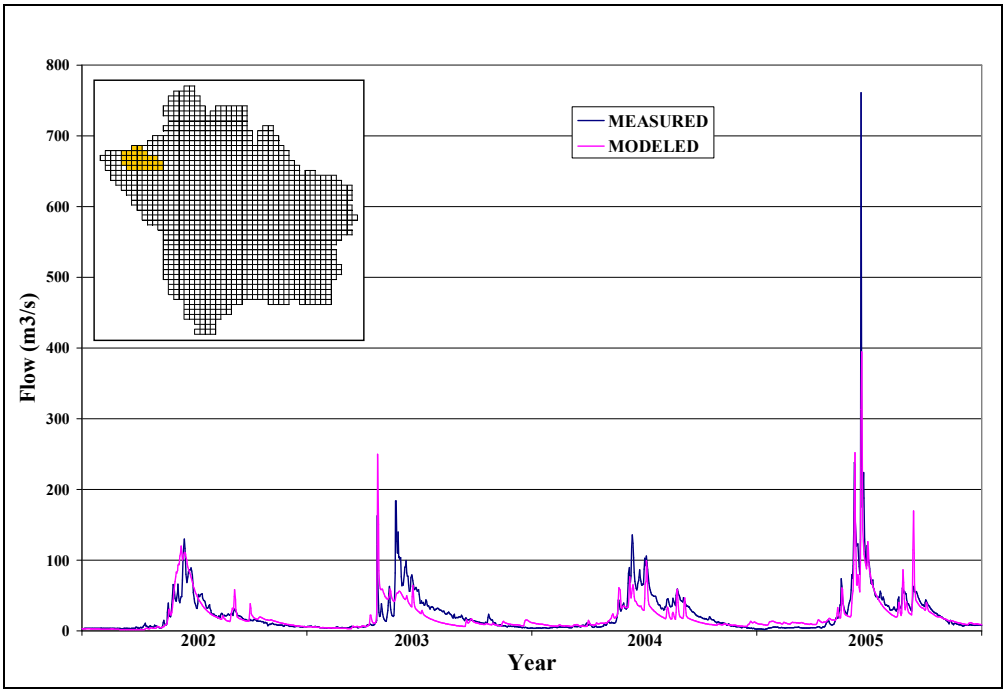

Figure 3.13: Measured streamflows vs. modeled streamflows from manually calibrated model of Red Deer River below Burnt Timber Creek (sub-basin 9)

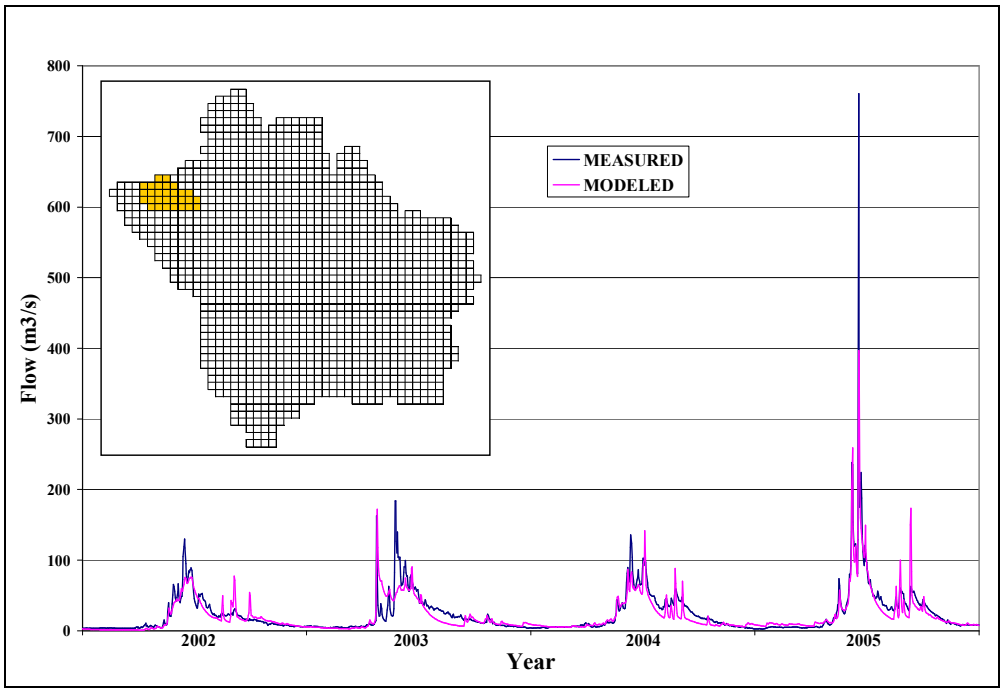

Figure 3.14: Measured streamflows vs. modeled streamflows from automated calibration of Red Deer River below Burnt Timber Creek (sub-basin 9)

Calibration was successful in that manual calibration produced improved modeling results in 15 of 19 sub-basins for the daily Nash-Sutcliffe coefficient and 19 of 19 sub-basins for the monthly Nash-Sutcliffe coefficient. Automated calibration using a multi-basin approach produced improved modeling results relative to manually calibrated results in 15 of 19 sub-basins for the daily Nash-Sutcliffe coefficient and 14 of 19 sub-basins for the monthly Nash-Sutcliffe coefficient. The automated calibration using a multi-basin approach produced improved modeling results relative to pre-calibrated results in 17 of 19 sub-basins for the daily Nash-Sutcliffe coefficient and 19 of 19 sub-basins for the monthly Nash-Sutcliffe coefficient.

The approach was very effective in improving modeling results over the entire watershed, producing consistent improvements in almost all of the sub-basins used for validation. There are several potential improvements that could be made to improve the calibration. First, more parameters could be included in the automatic calibration process. Although this would provide the opportunity for a more accurate model, but it

might come at the cost of increased computational time as more model evaluations might be required to ensure a sufficient solution has been found.

A second possible way to improve the calibration of this model would be to alter the weighting function used for the automated calibration or to change the sub-basins used in the calculation of "MultiNash." Though this would not guarantee improved modeling results, it would give insight into how the weighting function and sub-basin selection can impact automatic calibration.

Chapter 4

Impacts of Precipitation De-clustering

The first portion of this thesis dealt with hydrologic model calibration using both manual and automated calibration methods. This chapter applies the automatic calibration methodology to four models, each with a precipitation data set that has been reduced from the original set used in chapter 3. The first goal of this chapter is to determine how removing specific rain gauges from the precipitation data set affected the calibration potential of hydrologic models on both the local (sub-basin) and global (regional scale watershed). The results of this study will not only provide information on the effects of removing precipitation data, it is intended to provide insight into the potential to improve hydrologic models by increasing the number and/or density of available meteorological stations. Results from areas of the watershed with different spatial distributions of precipitation gauges are also analyzed in an attempt to determine a relationship between rain-gauge density and calibrated Nash-Sutcliffe coefficients.

The second goal of this portion of the study was to observe how parameter values vary from the "optimum" values found from calibrating the model described in chapter 3. Comparing how each parameter varies when the precipitation inputs are changed will reveal how uncertainty in precipitation translates to potential uncertainty in different parameter values.

The rain gauge data set that was used to produce the input precipitation data for the model was reduced several times through a de-clustering method. Each time the rain gauge set was reduced, a new input data set was interpolated (using equation 2.2 and 2.3) and the model was re-calibrated using the method outlined in Chapter 3.

The results of this study will help to determine how removing precipitation data points impacts hydrologic modeling calibrations. It will help to determine areas of regional scale hydrologic models that require more precipitation gauges and areas that

can have use a reduced data set without significantly decreasing the accuracy of modeling results.

4.1 De-clustering Method

De-clustering is the process of removing data points in an effort to improve the spatial distribution of the data. De-clustering of the precipitation data reduces rain gauge density and provides a rain gauge set that is used to create a new interpolation to be used as an input data set.

4.1.1 Rain Gauge Removal Order

Starting with a set of rain gauges that included all 28 gauges in the study area, a clustering index was calculated using a variation on the nearest neighbour removal order (Ahrens, 2005) according to:

$$CI = \sum_{i=1}^{N} d_i^2 \tag{4.1}$$

where CI is the clustering index, d_i is the distance between the selected rain gauge and the closest neighboring rain gauge and N is the number of neighboring rain gauges used to calculate CI. For each rain gauge, d_i is calculated for the closest N (4 for this study) neighboring rain gauges and the gauge with lowest CI is removed and the process is repeated. An example of how CI values would be calculated is shown in section 2.1.4.

The order of removal of the 28 rain gauges according to equation 4.1 is shown in table 4.1.

Table 4.1 – Rain gauge removal order

Gauge	CI
17	1.36E+03
1	2.14E+03
22	3.91E+03
14	4.09E+03
13	5.62E+03
9	6.50E+03
19	6.55E+03
27	9.68E+03
10	1.02E+04
6	1.34E+04
26	1.35E+04
11	1.76E+04
8	2.36E+04
7	3.82E+04
12	4.21E+04
28	5.80E+04
24	8.07E+04
21	9.68E+04
15	1.35E+05
3	1.78E+05
20	1.98E+05
25	3.06E+05
4	4.71E+05
23	9.06E+05
2	N/A
16	N/A
5	N/A
18	N/A

The final four gauges (2, 16, 5, and 18) listed above do not have a clustering index because at least four other gauges are required for this calculation.

4.1.2 De-clustering Trials

De-clustering of the initial rain gauge set was done four times. Each trial removed five rain gauges (including those removed in previous trials). Table 4.2 shows summarizes the gauges removed each step.

Table 4.2: Rain gauges removed for each de-clustering trial

Trial	Gauges Removed
23 Gauges	17, 1, 22, 14, 13
18 Gauges	9, 19, 27, 10, 6
13 Gauges	26, 11, 8, 7, 12
8 Gaugues	28, 24, 21, 15, 3

The rain gauge sets were interpolated to generate precipitation data for each grid cell according to the IDW interpolation method outlined in section 2.1.3 (equation 2.2 and 2.3), with a maximum search radius implemented according to Shepard's method (Yoeli, 1975). The search radius selected for this interpolation was 100 km, and the minimum number of points required for the interpolation was 1.

The locations of the rain gauges used in the complete set (used for calibration in chapter 3) are compared to the rain gauge sets used in the de-clustering trials in figure 4.1 (a – e).

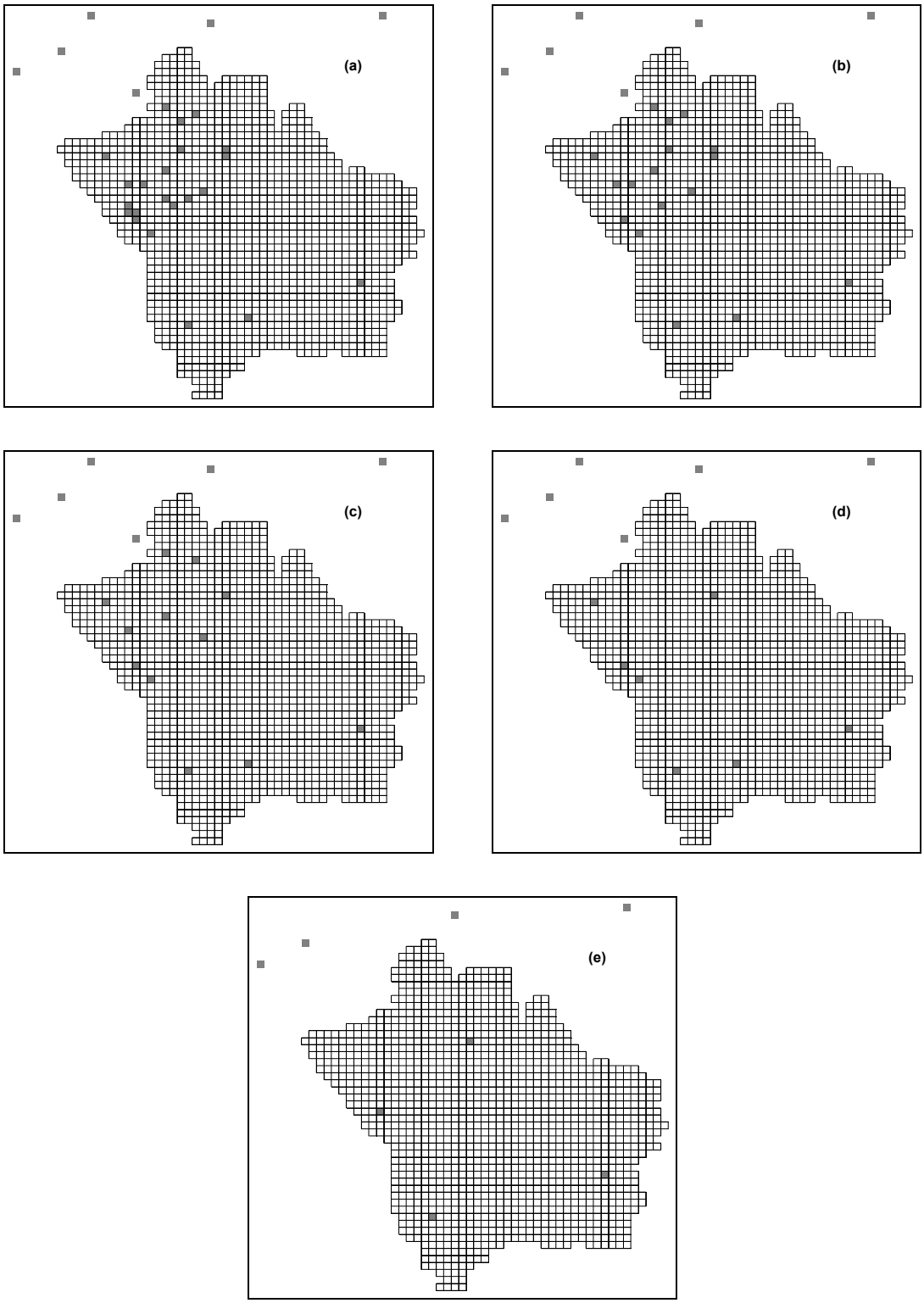

Figure 4.1: Rain gauges used for de-clustering trials (a) Complete rain gauge set; (b) Trial 1 rain gauge set; (c) Trial 2 rain gauge set; (d) Trial 3 rain gauge set; (e) Trial 5 rain gauge set

4.2 Calibration Results

Once the interpolation for the rain gauge set was complete, the model was run with the new precipitation interpolations used as the input data set. The parameter values for this first model run were the final parameter values from the automated calibration (Table 3.11 and 3.12).

The initial Nash-Sutcliffe daily and monthly coefficients for each de-clustering trial are shown in table 4.3 and 4.4 respectively.

Table 4.3: Initial daily Nash-Sutcliffe coefficients for de-clustering models

Sub-basin #	Full Set Calibrated Nash Daily	Trial 1 Pre-calibrated Nash Daily	Trial 2 Pre-calibrated Nash Daily	Trial 3 Pre-calibrated Nash Daily	Trial 4 Pre-calibrated Nash Daily
1	0.673	0.598	0.653	0.276	0.033
4	0.293	0.320	0.295	0.290	0.103
5	0.426	0.342	0.526	0.168	-0.154
6	0.763	0.550	0.736	0.236	-0.231
7	0.422	0.427	0.368	0.400	0.005
8	0.677	0.665	0.596	0.629	-0.364
9	0.768	0.763	0.757	0.757	0.147
16	0.753	0.737	0.658	0.633	-0.467
17	0.559	0.445	0.355	0.321	-0.353
19	0.689	-0.569	0.502	0.183	-0.612
20	0.814	0.748	0.650	0.658	0.278
21	0.612	0.475	0.420	0.402	-0.329
22	0.618	0.543	0.530	0.517	0.274
23	0.679	0.608	0.605	0.605	0.399
25	0.653	0.628	0.637	0.637	0.418
26	0.541	0.502	0.498	0.502	0.142
27	0.286	0.228	0.228	0.221	-0.214
28	0.195	0.189	0.313	0.313	0.000
29	0.228	0.224	0.308	0.308	0.265
AVG	**0.560**	**0.443**	**0.507**	**0.424**	**-0.035**

Table 4.4: Initial monthly Nash-Sutcliffe coefficients for de-clustering models

Sub-basin #	Full Set Calibrated Nash Monthly	Trial 1 Pre-calibrated Nash Monthly	Trial 2 Pre-calibrated Nash Monthly	Trial 3 Pre-calibrated Nash Monthly	Trial 4 Pre-calibrated Nash Monthly
1	0.768	0.655	0.754	0.317	0.227
4	0.316	0.398	0.354	0.437	0.292
5	0.782	0.661	0.845	0.572	0.027
6	0.911	0.811	0.844	0.435	-0.151
7	0.640	0.648	0.545	0.604	-0.087
8	0.830	0.860	0.676	0.766	-0.223
9	0.958	0.953	0.945	0.948	0.145
16	0.968	0.960	0.825	0.796	-0.499
17	0.955	0.915	0.657	0.716	-0.108
19	0.878	0.381	0.682	0.515	0.596
20	0.920	0.829	0.783	0.818	0.657
21	0.841	0.726	0.754	0.744	-0.304
22	0.728	0.693	0.684	0.673	0.574
23	0.777	0.726	0.719	0.721	0.719
25	0.787	0.766	0.774	0.774	0.606
26	0.708	0.679	0.678	0.680	0.608
27	0.479	0.448	0.446	0.444	0.533
28	0.447	0.447	0.507	0.507	0.662
29	0.561	0.556	0.600	0.600	0.661
AVG	**0.750**	**0.690**	**0.688**	**0.635**	**0.260**

As may be expected, the general trend of the pre-calibrated models was a decreased Nash-Sutcliffe coefficient as the number of rain gauges used to interpolate the input data was reduced. Starting from each pre-calibrated model, each of the models was calibrated using automated calibration as described in section 3.3.

Automated calibration identified unique parameter sets for each model with de-clustered input data sets. Parameter variation was tracked for each river and land class parameter to determine how they varied from the "optimal" values that were found from calibration of the complete data set. Figure 4.2 shows the parameter variation of the river class parameters (*LZF* and *R2*) from the de-clustering trials.

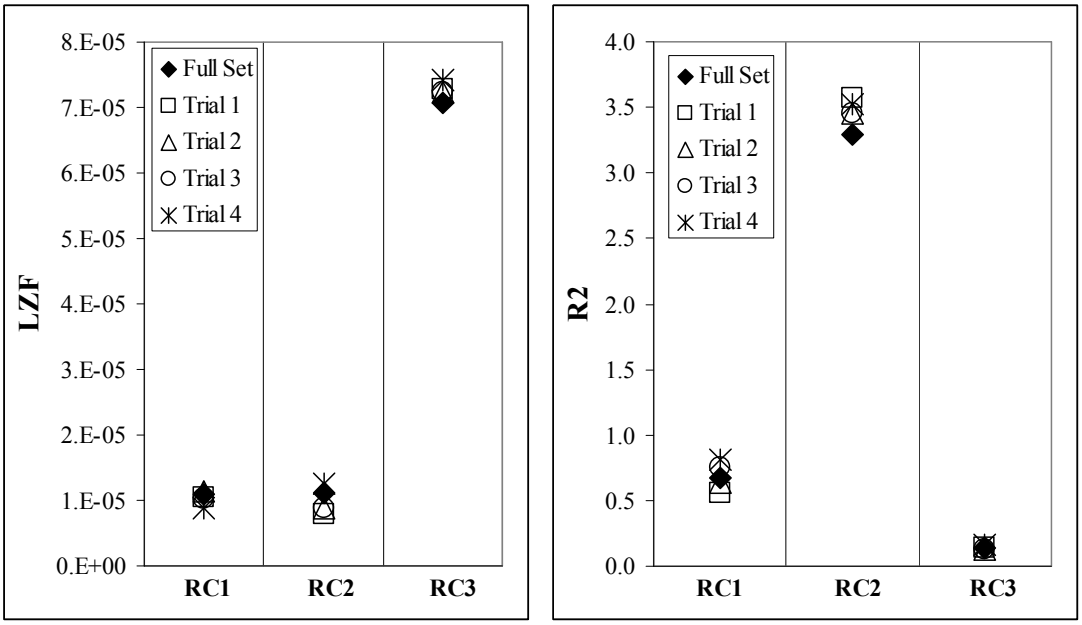

Figure 4.2: River class parameter variation resulting from de-clustering trials

The values of *LZF* and *R2* found through automated calibration of the de-clustered models were all very similar. The river class parameters *LZF* and *R2* control the base flow depletion curve and the timing of the peak flows. It was expected that these values would not vary significantly when a de-clustered precipitation set was used as the model input since they have already been calibrated to match the shape of the base flow depletion curve (*LZF*), and the timing of the peak flows (*R2*) of the historic data set. They have very little to do with modeled runoff volume which is where most of the uncertainty in the de-clustered models comes from.

Land class parameters control the magnitude of the peak flows and the volume of runoff simulated by WATFLOOD. Different interpolations would likely lead to different volumes of input precipitation, and thus, variation of the land class parameters optimize the Nash-Sutcliffe coefficients was expected. Figure 4.3 shows the parameter variation of the land class parameters (*RE, RETN, MF, BASE,* and *FTAL*) from the de-clustering trials.

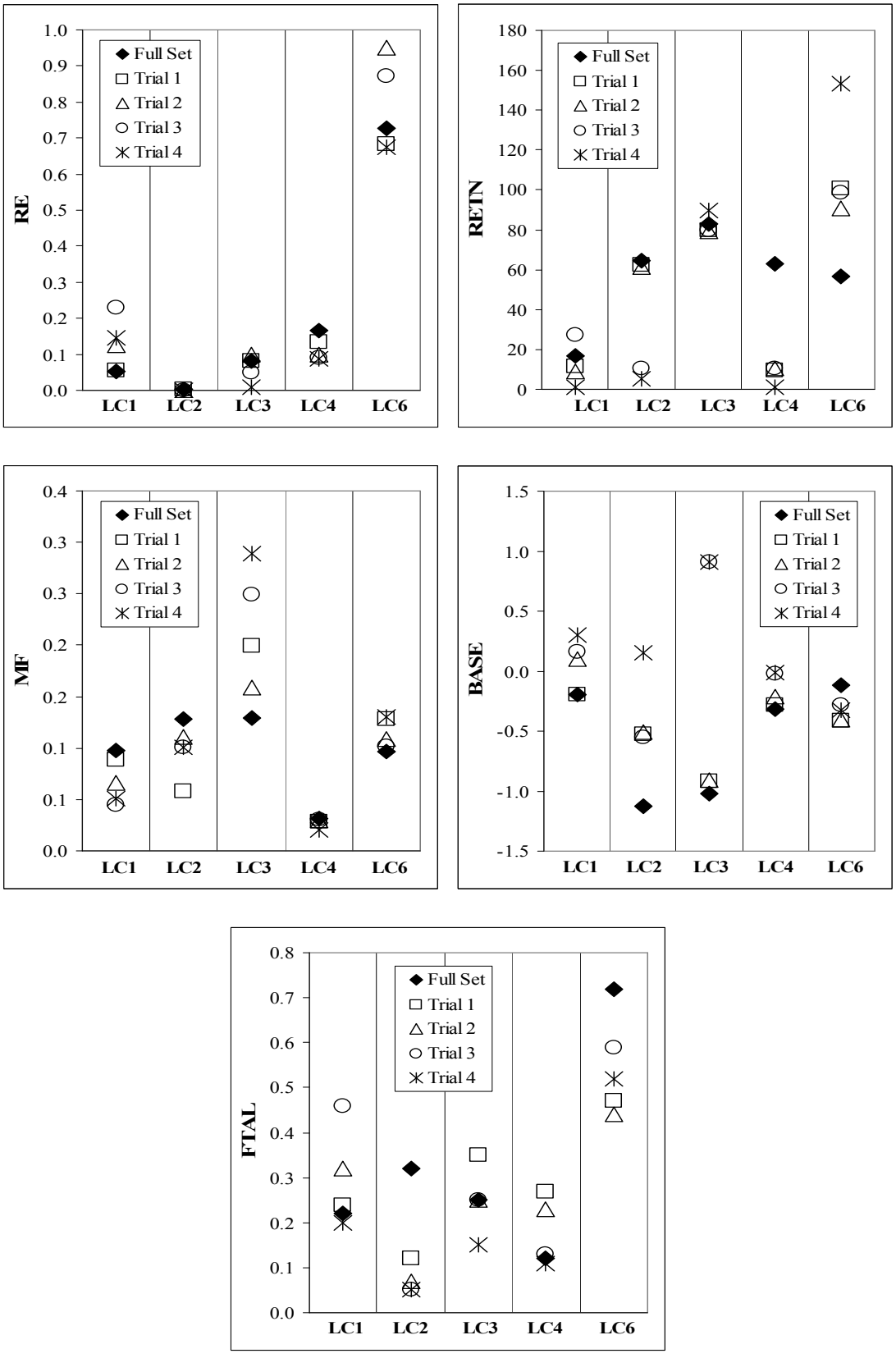

Figure 4.3: Land class parameter variation resulting from de-clustering trials

Compared to the river class parameters, the de-clustered models produced more variation in the land class parameter values. The variation of the land class parameters was within a reasonable range, with all parameters having variation less than one order of magnitude, and with *BASE* having no variation more than two degrees Celsius.

The initial and calibrated weighted daily Nash-Sutcliffe coefficients for each trial are shown in table 4.5.

Table 4.5: Initial and calibrated weighted daily Nash-Sutcliffe coefficients for de-clustering trials

Trial	Full Set Calibrated	Trial 1	Trial 2	Trial 3	Trial 4
Numer of Gauges	28	23	18	13	8
Initial Weighted Daily Nash	0.669	0.711	0.693	0.676	0.174
Calibrated Weighted Daily Nash	0.743	0.732	0.721	0.714	0.315

Although the weighted daily Nash-Sutcliffe coefficients were improved for each trial through automated calibration, analysis of the results for each sub-basin was required to determine how precipitation de-clustering impacts modeling results on a local and global scale. Table 4.6 and 4.7 show the daily and monthly Nash-Sutcliffe coefficients respectively for each trial for each sub-basin. The shaded values indicate the best result for each sub-basin.

Table 4.6: Calibrated daily Nash-Sutcliffe coefficients for each de-clustering trial

Sub-basin #	**Full Set Calibrated Nash Daily**	**Trial 1 Calibrated Nash Daily**	**Trial 2 Calibrated Nash Daily**	**Trial 3 Calibrated Nash Daily**	**Trial 4 Calibrated Nash Daily**
1	0.673	0.616	0.670	0.400	0.128
4	0.293	0.237	0.298	0.222	0.001
5	0.426	0.409	0.596	0.384	0.113
6	0.763	0.481	0.732	0.380	0.006
7	0.422	0.438	0.415	0.373	0.066
8	0.677	0.633	0.610	0.633	-0.079
9	0.768	0.783	0.778	0.791	0.277
16	0.753	0.720	0.665	0.610	-0.255
17	0.559	0.420	0.364	0.366	-0.056
19	0.689	-0.465	0.542	0.279	0.152
20	0.814	0.785	0.704	0.719	0.453
21	0.612	0.428	0.410	0.423	-0.072
22	0.618	0.523	0.542	0.513	0.402
23	0.679	0.616	0.637	0.616	0.540
25	0.653	0.617	0.613	0.565	0.326
26	0.541	0.538	0.541	0.564	0.438
27	0.286	0.209	0.217	0.329	0.422
28	0.195	0.188	0.296	0.337	0.192
29	0.228	0.221	0.318	0.338	0.423
AVG	**0.560**	**0.442**	**0.524**	**0.466**	**0.183**

Table 4.7: Calibrated monthly Nash-Sutcliffe coefficients for each de-clustering trial

Sub-basin #	Full Set Calibrated Nash Monthly	Trial 1 Calibrated Nash Monthly	Trial 2 Calibrated Nash Monthly	Trial 3 Calibrated Nash Monthly	Trial 4 Calibrated Nash Monthly
1	0.768	0.658	0.731	0.394	0.276
4	0.316	0.263	0.337	0.267	-0.011
5	0.782	0.690	0.833	0.513	0.256
6	0.911	0.837	0.898	0.428	-0.085
7	0.640	0.638	0.594	0.582	0.078
8	0.830	0.818	0.723	0.710	-0.248
9	0.958	0.962	0.957	0.959	0.361
16	0.968	0.948	0.858	0.780	-0.487
17	0.955	0.908	0.687	0.703	-0.091
19	0.878	0.481	0.732	0.482	0.501
20	0.920	0.869	0.847	0.868	0.661
21	0.841	0.686	0.762	0.696	-0.306
22	0.728	0.666	0.707	0.642	0.465
23	0.777	0.734	0.770	0.736	0.676
25	0.787	0.747	0.734	0.685	0.440
26	0.708	0.709	0.725	0.714	0.600
27	0.479	0.385	0.474	0.463	0.518
28	0.447	0.525	0.626	0.502	0.524
29	0.561	0.522	0.615	0.594	0.633
AVG	**0.750**	**0.687**	**0.716**	**0.617**	**0.251**

Two things to consider are that the results from sub-basins 16-25 had consistently better daily and monthly Nash-Sutcliffe coefficients with the full precipitation data set used as a model input. Additionally, the best daily and monthly Nash-Sutcliffe coefficients for sub-basins 26-29 resulted from models that used de-clustered precipitation data sets. Figures 4.4 and 4.5 show the average daily and monthly Nash-Sutcliffe values for each de-clustering trial. Three values are shown: the total average for each trial, the average value for basin 16-25, and the average value for basins 26-29.

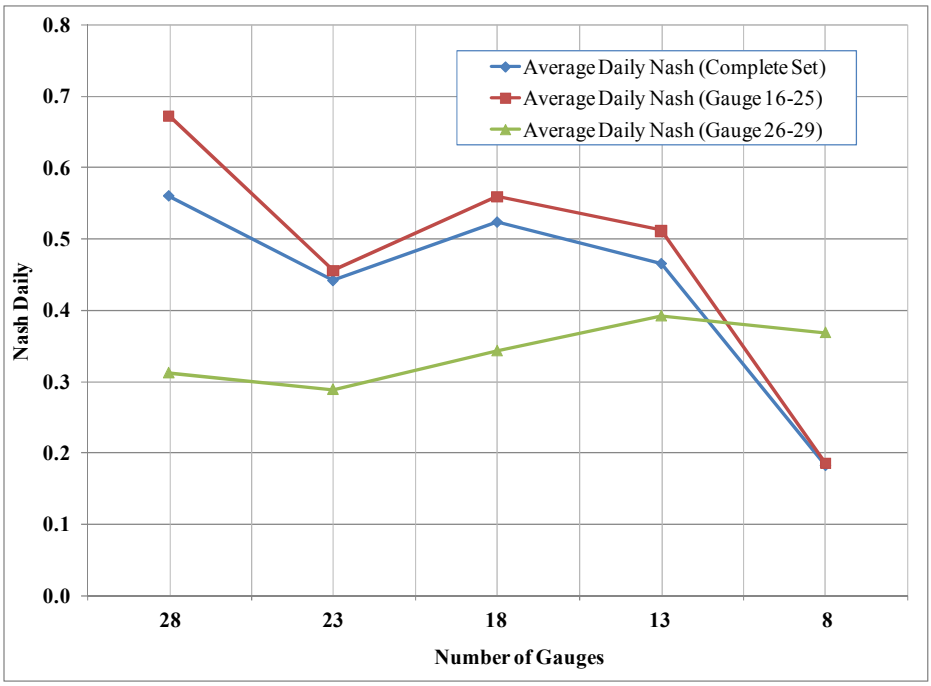

Figure 4.4: Daily Nash-Sutcliffe values from de-clustering trials

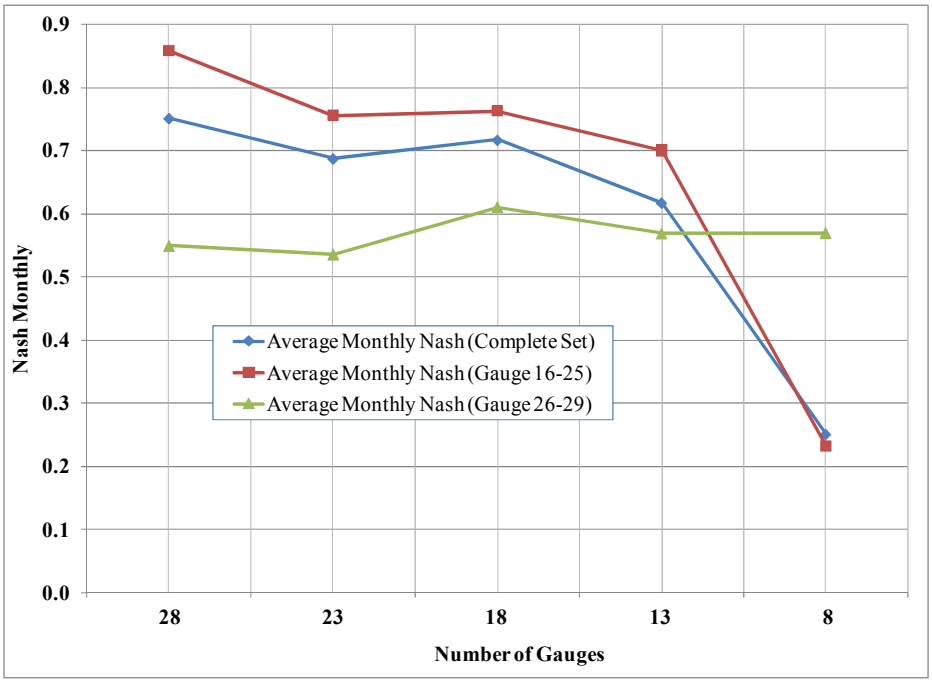

Figure 4.5: Monthly Nash-Sutcliffe values from de-clustering trials

Figures 4.6 and 4.7 show the locations of sub-basins 16-25, and 26-29 respectively with and overlay of the locations of the full rain gauge set.

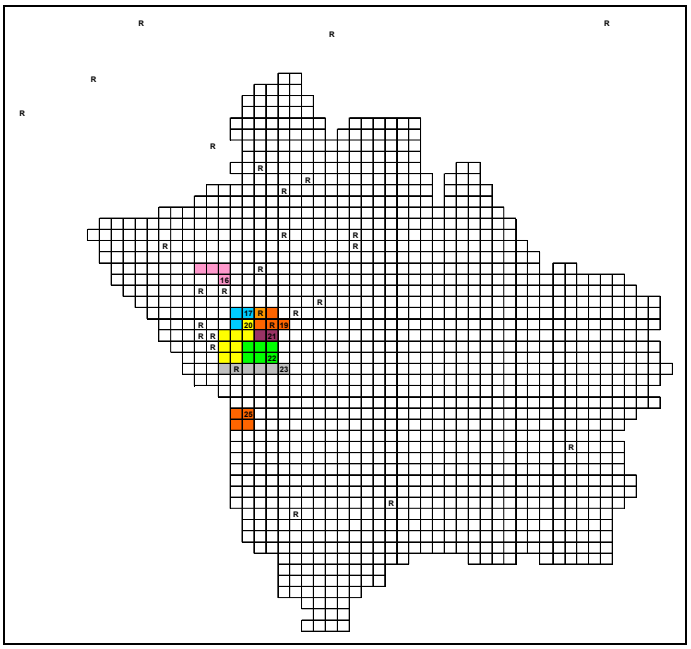

Figure 4.6: Sub-basin 16-25 shown with full precipitation set locations

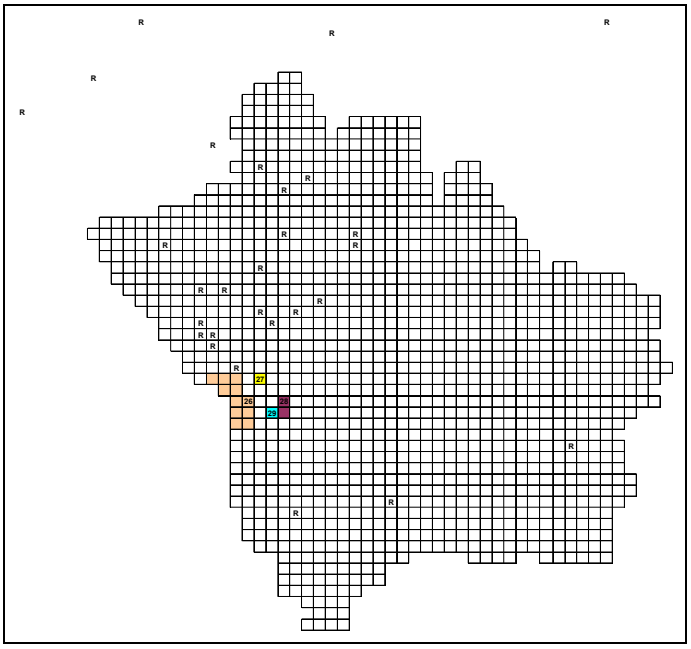

Figure 4.7: Sub-basin 26-29 shown with full precipitation set locations

Sub-basins 16-25 (with the exception of 25) are all located in a region of the watershed that has a very high density of rain gauges, while sub-basins 26-29 are located just outside of the same dense region. The sub-basins located within the dense rain gauge

region (sub-basins 16-23) produced better modeling results when the entire rain gauge set was used, and thus, benefited from the proximity of the gauges. The sub-basins located just outside of the dense region (sub-basins 26-29) were heavily influenced by the clustered points. When some of those points were removed, the precipitation interpolations that influence these sub-basins were more balanced and the Nash-Sutcliffe coefficients were improved.

It is apparent that some of the de-clustering trials produced certain sub-basins where the best daily and monthly Nash-Sutcliffe values did not correspond to the model with the most complete input data set; however, a majority of sub-basins were best represented by the model developed with a full precipitation data set. On a global scale, the full precipitation set produced a model with the highest average daily and monthly Nash-Sutcliffe values.

4.3 Discussion

The primary findings resulting from the work outlined in this chapter is the relationship between rain gauge density and calibrated model results on a local and global scale. It was found that watershed-wide (globally), modeling results were more accurate when more rain gauges were used for the model input. There were, however, geographic areas of the model (local) that had improved modeling results when a de-clustered data set was used as the input. This section discusses potential interpretations and implications of results of the calibrations described in this chapter.

On a global scale, the results are quite straight forward to interpret. The average Nash-Sutcliffe values of each de-clustering trial show that models with more input data produced more accurate modeling results upon calibration. This supports the theory that more input data will produce regional scale models with stronger predictive abilities over the entire watershed.

On a local scale, the results shown in this chapter are more complex. Since some sub-basins had the best Nash-Sutcliffe coefficients from de-clustered models, the results require more interpretation. It should be noted that some of the more complex results might be due to poor optimizer performance as the calibration method used is not perfect (nor is any). Additional optimization trials might lead to significantly better results. The sub-basins previously shown in figure 4.7 are all located in a geographic region with a low local rain gauge density and no rain gauges actually lie within the sub-basin boundaries. The best modeling results were produced by using a de-clustered data set. If this study was done in reverse (i.e. starting with 8 rain gauges and increasing to 28), no rain gauges are added within the sub-basin limits, and thus, there is no guarantee that more data would improve modeling results.

The sub-basins previously shown in figure 4.6, which are located in a region with a higher local rain gauge density, suffered from de-clustering. Again, if the study was performed in reverse, several rain gauges would have been added within the limits of the displayed sub-basins, and improved modeling results would have been expected.

The local rain gauge density in this study was found to be very important to modeling results when the rain gauges were within the limits of the sub-basin being modeled. When rain gauges are added outside the limits of a sub-basin, it is very difficult to predict the effect it will have on modeling results.

This case study shows that portions of the model (sub-basins 26-29) with low local rain gauge density can still produce reasonably accurate results (0.33 to 0.56 daily Nash-Sutcliffe coefficients for this study as shown in table 4.6); however, sub-basins located within geographic regions of higher rain gauge density (sub-basins 16-25) produced significantly better and more consistent results (0.56 to 0.81 daily Nash-Sutcliffe coefficients as shown in table 4.6). For a regional scale model it would be very difficult to trust modeling results fuelled by a scarce data set regardless of the quality of the model's predictive power. With good values determined for the river class parameters, the uncertainty in precipitation mainly translates to uncertainty in the land class

parameter values and can offset inaccurate precipitation input data produced by poor local rain gauge density.

The results presented in this chapter are difficult to generalize to hydrologic models in general, as the site was quite data poor with respect to available rain gauge data. Without using an initial data set that contains consistently spaced rain gauges, the importance of the rain gauge density for each trial can be very difficult to interpret. The ideal scenario to test the effects of de-clustering would involve having a rain gauge located in every grid cell in the study area. Gauges would then be removed according to equation 4.1, and the model would be re-calibrated. Starting off the scenario with equally spaced rain gauges would give more importance to the rain gauge density values when compared to the resulting Nash-Sutcliffe coefficients of each de-clustered model.

A limitation that is always present in hydrologic modeling is the error in the recorded historic precipitation data at each individual rain gauge, and this error can be compounded when less data is available. While each rain gauge is likely to have some error in each recorded precipitation event, the errors in models with a high density of data points can even each other out when spatially interpolated. With a low density model that essentially becomes subjected to a nearest neighbour interpolation, huge portions of the model are fuelled by an input that is based on only one rain gauge that may have significant error. The potential for this compounded error is another reason why models with low rain gauge density are very difficult to trust.

The value of an added data point is only as good as the proximity it has to the sub-basin being studied. In a regional scale model, with many sub-basins there are bound to be geographic locations of the watershed that are relatively data-poor with regards to rain gauge availability. To trust the results of a regional scale model that has parameter flexibility similar to the WATFLOOD model used in this case study, the local rain gauge density must be sufficient and at least partially within the boundaries of the sub-basins considered. Though there is evidence that some data points can be removed without significantly decreasing modeling accuracy in geographic locations with high rain gauge

density, the results of this chapter show that the best results for a regional scale model will come from using all available precipitation inputs.

Chapter 5

Summary

This primary purpose of this thesis was to present a general approach to calibrating a regional scale hydrologic model using a WATFLOOD model of the upper South Saskatchewan River watershed as a case study. Initially, manual calibration was described and performed on several sub-basins within the watershed. Using the manual calibration results as a basis for automated calibration, a multi-basin automated calibration approach was developed and applied to the model. The results demonstrated that both methods were effective tools for improving modeling results. Not only were the daily Nash-Sutcliffe coefficients of the sub-basins subjected to calibration all improved, the results from x of y sub-basins used for validation were also improved. Additionally, improvement in the monthly Nash-Sutcliffe coefficient was observed for every sub-basin in the calibrated model relative to the pre-calibrated model. Overall, the average daily Nash-Sutcliffe coefficient of the 19 calibration and validation sub-basins improved from an initial value of 0.17 before calibration to 0.43 after manual calibration and then to 0.56 after refinements with automatic calibration.

The calibration method was applied to four models that used de-clustered precipitation data as their input with the purpose of determining the effects of rain gauge density on modeling results. The results of the four calibrations, based on the daily and monthly Nash-Sutcliffe coefficients of all 19 sub-basins, were compared to the initial calibrated model that used the entire precipitation data set. Of the 19 sub-basins considered, 11 of had the best daily Nash-Sutcliffe coefficients in the model that used the entire precipitation data set, and the best values for the remaining 8 sub-basins were produced from a de-clustered model.

Calibration of the de-clustered models produced almost no variation in the river class parameters from the values found during the calibration of the initial model. Variation was found in the land class parameter values, but it was within a reasonable

range, with optimal parameters being modified less than one order of magnitude from their original values. Because the variation in the river class parameters was so low compared to the land class parameters, future de-clustering studies should consider placing a priority on re-calibrating land class parameters and not river class parameters. De-clustered models create uncertainty in precipitation volume which translates to uncertainty in land class parameter values since they have a much higher influence on runoff volumes than river class parameters.

In general, models that used more input data produced better modeling results than de-clustered models; however, de-clustered models did produce better results in some cases. Because the variation of the parameter values was within reasonable ranges for each of these improved cases, extended study into the effects of precipitation gauge density on modeling accuracy may provide stronger conclusions on how input precipitation data can be modified or supplemented to improve modeling results.

References

Ahrens, B. (2005). Distance in spatial interpolation of daily rain gauge data. *Hydrology and Earth System Sciences Discussions*, 2, 1893-1923.

Allen, R. J. & DeGaetano, A. T. (2005). Areal Reduction Factors for Two Eastern United States Regions with High Rain-Gauge Density. *Journal of Hydrologic Engineering*, 10:4, 327-335.

ArcInfo. (1991). *Cell-based modelling with GRID*. Environmental Systems Research Institute, Inc., Redlands, USA.

Bedient, P. & Huber, W. (2002). *Hydrology and Floodplain Analysis*. New Jersey: Prentice Hall.

Beven, K. J. & Hornberger, G. M. (1982). Assessing the effect of spatial pattern of precipitation in modelling streamflow hydrograph. *Water Resources Bulletin*, 18, 823-829.

Beven, K. (2000). Uniqueness of place and process representations in hydrological modeling. *Hydrology and Earth System Sciences*, 4(2), 203-213.

Boyle, P. D., Gupta, V. H. & Sorooshian, S. (2000). Toward improved calibration of hydrologic models: Combining the strengths of manual and automatic method. *Water Resources Research*, Vol. 36, No. 12, 3663-3674

Clark, I. (1979). *Practical Geostatistics*. London: Applied Science Publishers.

Cooper, V. A., Nguyen, V. T. V. & Nicell, J. A. (1997). Evaluation of global optimization methods for conceptual rainfall-runoff model calibration. *Water Science and Technology*, 36 (5), 53-60.

Crawford, N. H. & Burges, S. J. (2004). *History of the Stanford Watershed Model*. Water Resources Impact, Volume 6, Number 2, 3-5.

Crawford, N. H. & Linsley, R. K. (1966). *Digital Simulation in Hydrology: Stanford Watershed Model IV*. *Technical Report No. 39*, Department of Civil Engineering, Stanford University, p. 210.

Debo, T. N. & Reese, A. J. (2002). *Municipal Stormwater Management, 2nd edition*. Lewis Publishers.

Dent, M. C., Lynch, S. D. & Schulze, R. E. (1988). *Mapping mean annual and other rainfall statisitics over Southern Africa*. University of Natal, Department of Agricultural Engineering.

Donald, J.R. (1992). *Snowcover depletion curves and satellite snowcover estimates for snowmelt runoff modelling*. Ph.D. Thesis, University of Waterloo, ON, Canada, 232 p.

Dorninger, M. Schneider, S. & Steinacker, R. (2008). On the interpolation of precipitation data over complex terrain. *Meteorology and Atmospheric Physics*, 101, 175-189.

Duan, Q., Gupta, V., & Sorooshian, S. (1993). A shuffled complex evolution approach for effective and efficient optimization. *Journal of Optimization Theory and Applications*, 76, 501-521.

Environment Canada. (2007a). *Real-Time Hydrometric Data*. http://scitech.pyr.ec.gc.ca/waterweb/formNav.asp (retrieved May, 2007).

Environment Canada. (2007b). *Hourly Observation Data*. http://www.climate.weatheroffice.ec.gc.ca/climateData/canada_e.html (retrieved May, 2007).

Fang, X., Minke, A., Pomeroy, J., Brown, T., Westbrook, C., Guo, X. & Guangul, S. (2007). *A Review of Canadian Prairie Hydrology: Principles, Modeling and Response to Land Use and Drainage Change*. Centre for Hydrology Report, University of Saskatchewan.

Fenicia, F., Solomatine, D. P., Savenije, H. H. G. & Matgen, P. (2007). Soft combination of local models in a multi-objective framework. *Hydrology and Earth System Sciences*, 11, 1797-1809.

Franchini, M., Galeati, G. & Berra, S. (1998). Global optimization techniques for the calibration of conceptual rainfall-runoff models. *Hydrological Sciences Journal*, 43 (3), 443-458.

Gan, T. Y., & Biftu, G. F. (1996). Automatic calibration of conceptual rainfall-runoff models: optimization algorithms, catchment conditions, and model structure. *Water Resources Research*, 32 (12), 3513-3524.

Government of Alberta Environment. (2009). *Environment: South Saskatchewan River Basin Water Information Portal*. http://ssrb.environment.alberta.ca (retrieved May, 2009).

Jain, K. S. & Sudheer, K. P. (2008). Fitting of Hydrologic Models: A Close Look at the Nash-Sutcliffe Index. *Journal of Hydrologic Engineering*, 10, 981-986.

Johnson, R. (2000). *Miller & Freund's Probability and Statistics for Engineers*. New Jersey: Prentice Hall.

Kouwen, N. (2007). *WATFLOOD/WATROUTE Hydrologic Model Routing & Flow Forecasting System*. University of Waterloo, Department of Civil Engineering.

Kuczera, G. (1997). Efficient subspace probabilistic parameter optimization for catchment models. *Water Resources Research*, 33 (1), 177-185.

Lynch, S. D. & Schulze, R. E. (1995). *Techniques for Estimating Areal Daily Rainfall*. University of Natal, Department of Agricultural Engineering.

MacFarlane, A. & Tuson, A. (2008). Local search: A guide for the information retrieval practitioner. *Information and Processing Management*, 45, 159-174.

Madsen, H. (2000). Automatic calibration of a conceptual rainfall-runoff model using multiple objectives. *Journal of Hydrology*, 235, 276-288.

Madsen, H. (2003). Parameter estimation in distributed hydrological catchment modeling using automatic calibration with multiple objectives. *Advances in Water Resources*, 26, 205-216.

Madsen, H. & Wilson, G., Ammentorp, H. C., (2002). Comparison of different automated strategies for calibration of rainfall-runoff models. *Journal of Hydrology*, 261, 48-59.

Nash, J. E., & Sutcliffe, J. V. (1970). River flow forecasting through conceptual models part I - A discussion of principles. *Journal of Hydrology*, 10 (3), 282-290.

Ruelland, D., Ardoin-Bardin, S., Billen, G. & Servat, E. (2008). *Journal of Hydrology*, 361, 96-117.

SCALANT (NATO) ASW Research Centre, 1979. Spezia, Italy.

Schafer, N. W. (1991). *Modelling the areal distribution of daily rainfall*. Unpublished. M. Sc. Eng. Thesis, University of Natal, Department of Agricultural Engineering.

Seth, S. M., (2004). *Physically based hydrological modelling*. National Institute of Hydrology, India.

Shepard, D. (1968). *A two dimensional interpolation function for irregularly spaced data*. Proceedings of 23rd Naional Conference of the Association for Computing Machinery, Princeton, NJ, ACM, 517-524.

Smith, M. J., Goodchild, M. F. & Longley, P. A. (2006). *Geospatial Analysis – a comprehensive guide. 3rd edition*. Troubador Publishing Ltd.

Thyer, M., Kuczera, G. & Bates, B. C. (1999). Probabilistic optimization for conceptual rainfall-runoff models: a comparison of the shuffled complex evolution and simulated annealing algorithms. *Water Resources Research*, 35 (3), 767-773.

Tolson, B. A. & Shoemaker, C. A. (2007). Dynamically dimensioned search algorithm for computationally efficient watershed model calibration. *Water Resources Research*, 43, W01413.

Tolson, B. & Seglenieks, F. (2007). *DDS_MESH1 Program (Windows) Basic User Instructions – DRAFT VERSION*. University of Waterloo, Department of Civil and Environmental Engineering.

University of Alberta Press. (1990). *Atlas of Alberta Lakes*. http://sunsite.ualberta.ca/Projects/Alberta-Lakes/view/?region=South%20Saskatchewan%20Region&basin=Oldman%20River%20Basin&lake=Travers%20Reservoir&number=123 (retrieved September, 2008).

Wang, Q. J. (1991). The genetic algorithm and its application to calibrating conceptual rainfall-runoff models. *Water Resources Research*, 27 (9), 2467-2471.

Yoeli, P. (1975). *Compilation of data for computer-assisted relief cartography*. Pg 352-367, Davis, JC and McCullagh, MJ (Eds): Display and Analysis of Spatial Data (NATO Advanced Study Institute). John Wiley & Sons, London.

Yoo, C (2002). Basin average rainfall and its sampling error. *Water Resources Research*, Vol. 38, No. 11, 1259.

Zabinsky, Z. (1998). Stochastic Methods for Practical Global Optimization. *Journal of Global Optimization*, 13, 433-444.

APPENDICES

APPENDIX A

Gridded Model Set-up Data

This appendix contains essential data required for replication of this study. Figures in this appendix show for each cell: cell number (A.1), element area (A.2), flow direction (A.3), elevation (A.4), contour (A.5), number of channels (A.6), and land allocation for eight land classes plus impervious land class (A.7 – A.15). How each of these values is used in WATFLOOD can be found in the WATFLOOD manual (Kouwen, 2007).

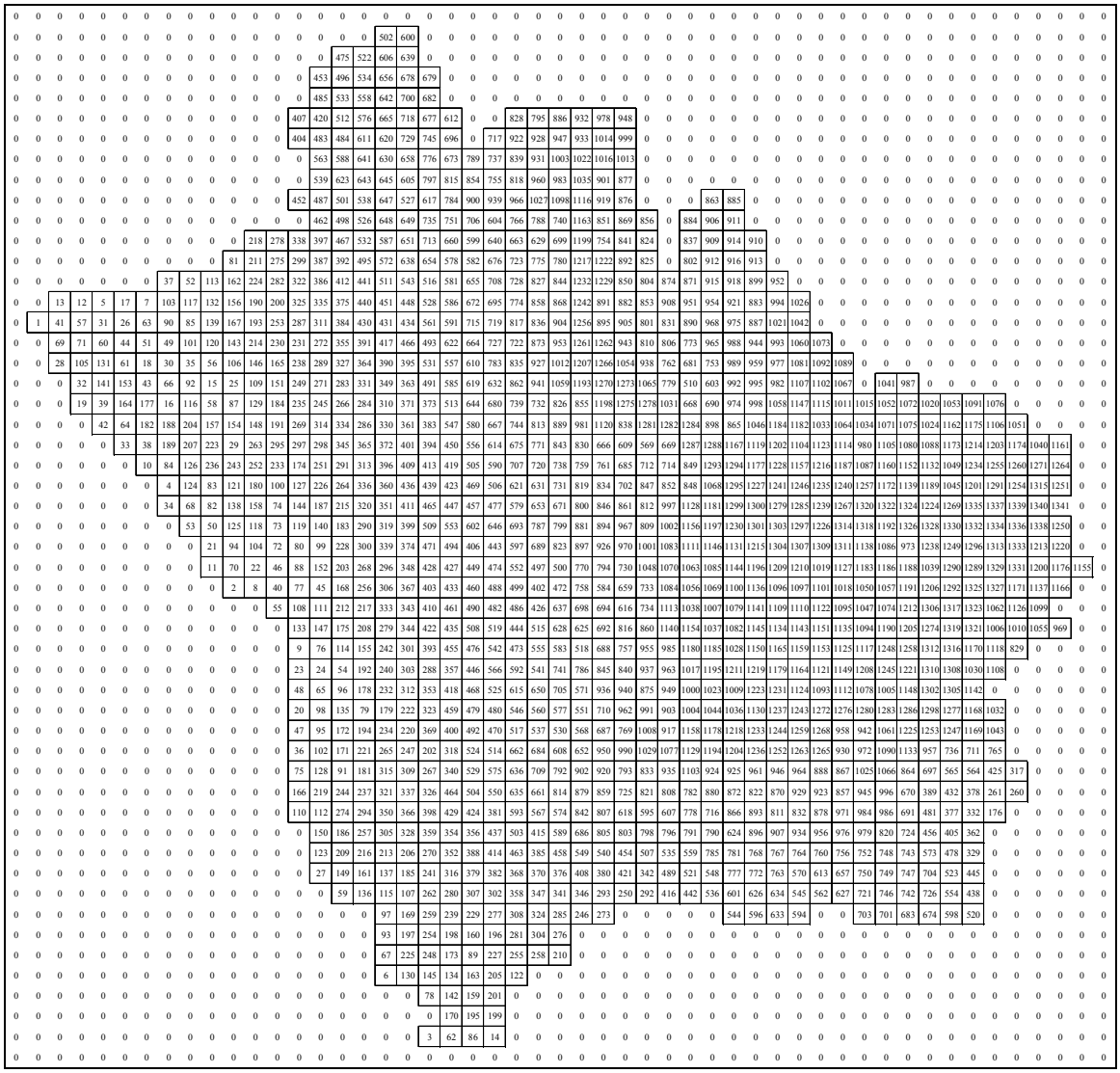

Figure A.1: Grid cell numbers

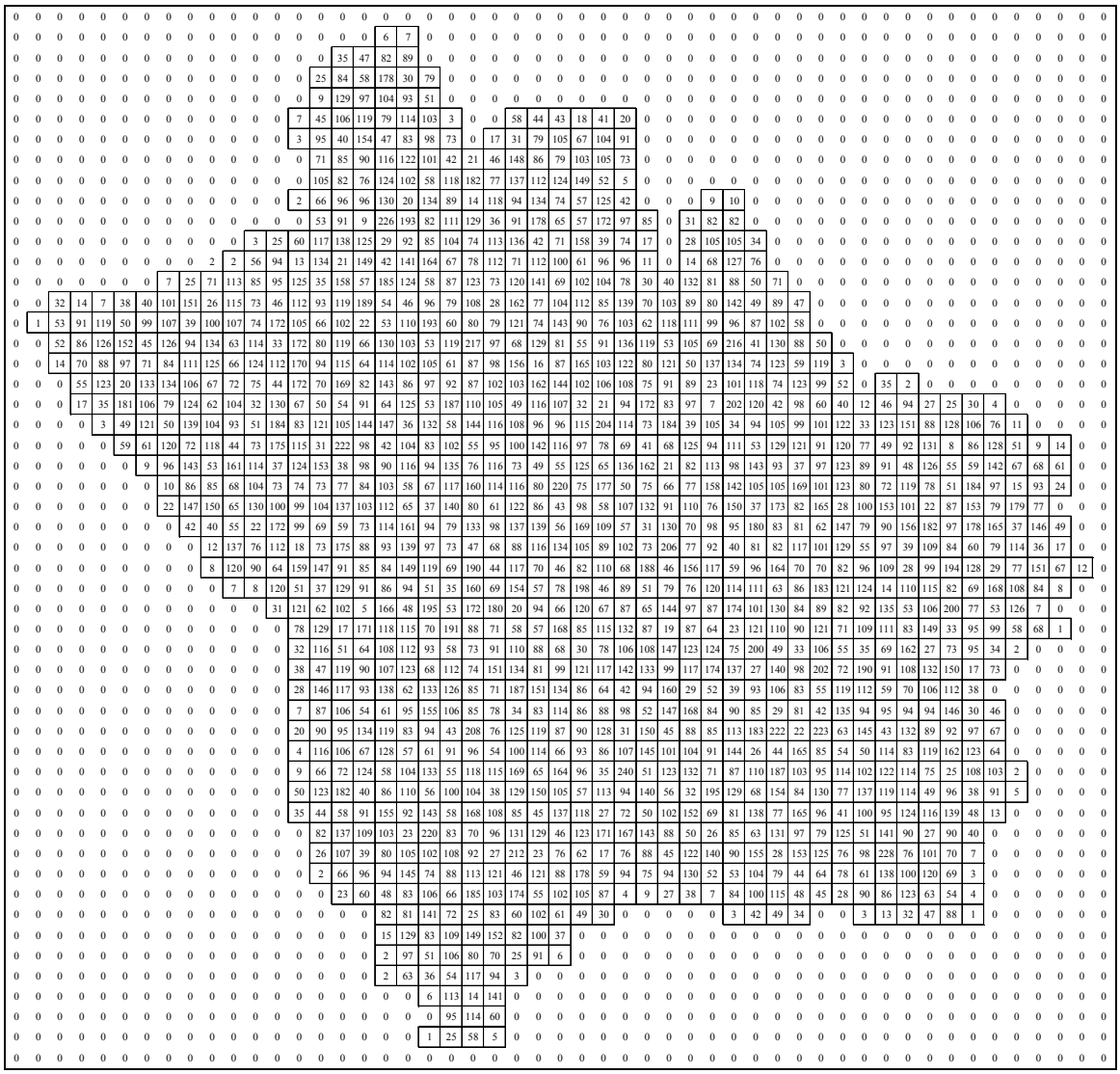

Figure A.2: Grid cell areas

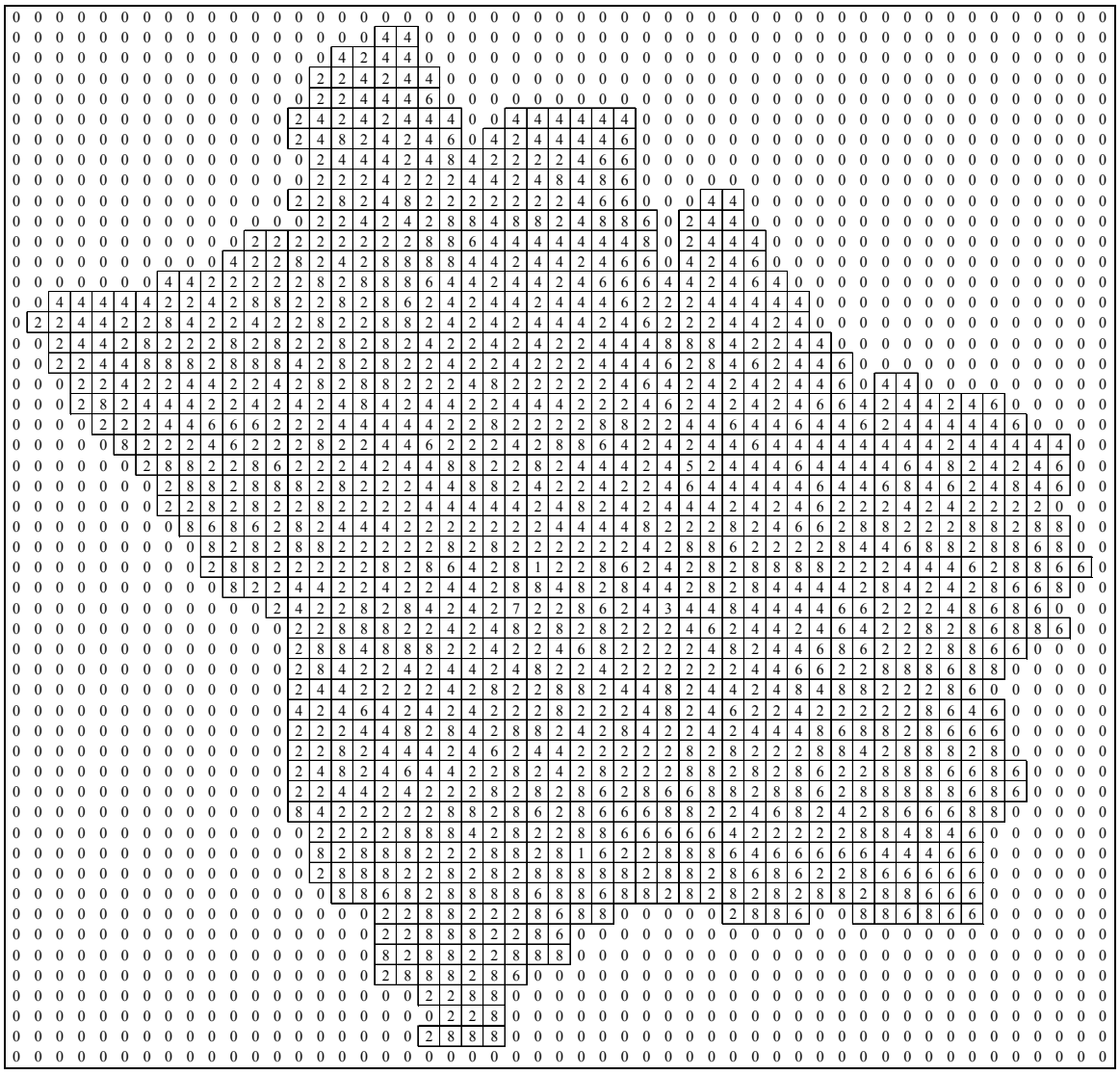

Figure A.3: Flow direction for each grid cell

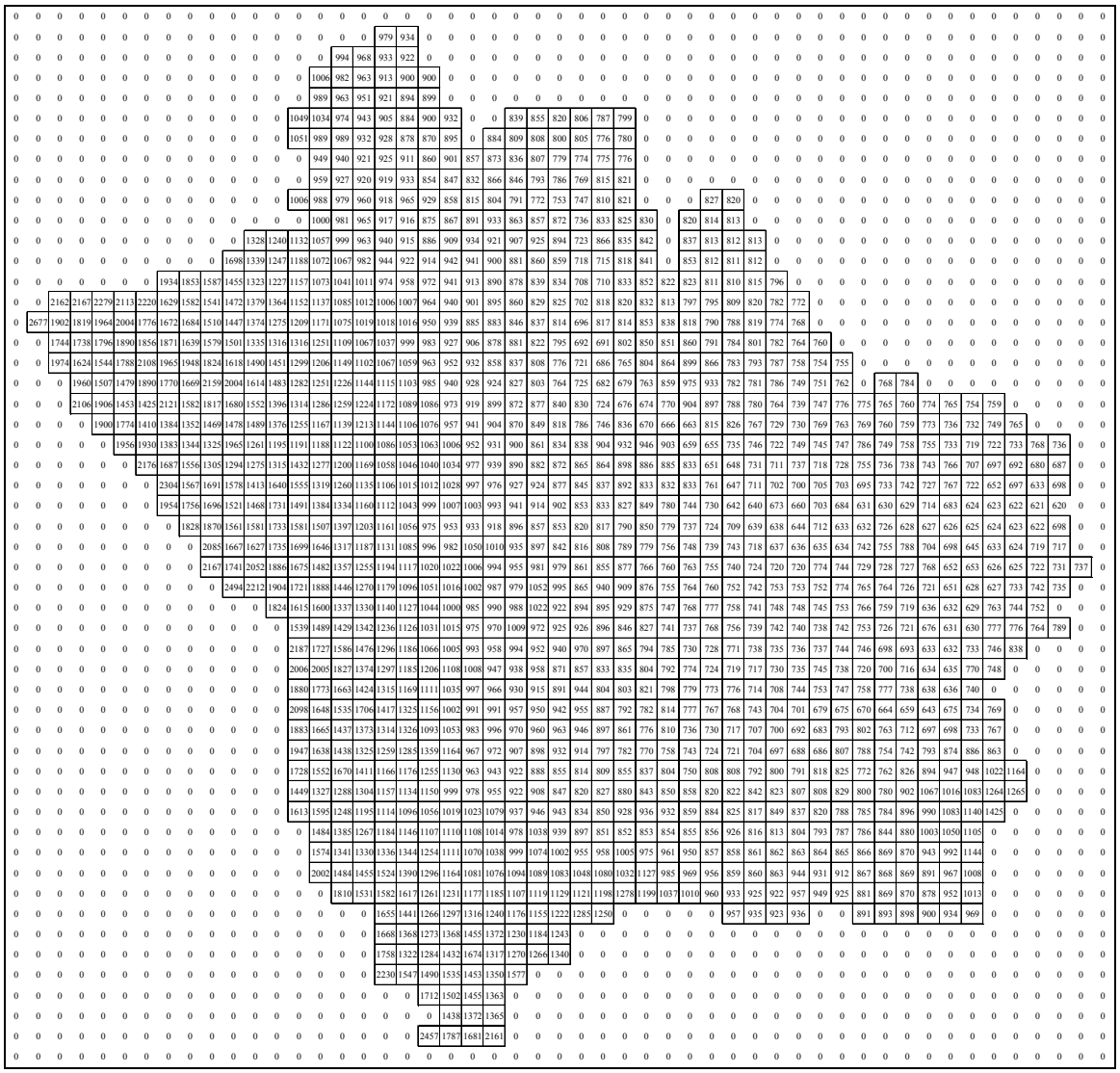

Figure A.4: Grid cell elevations

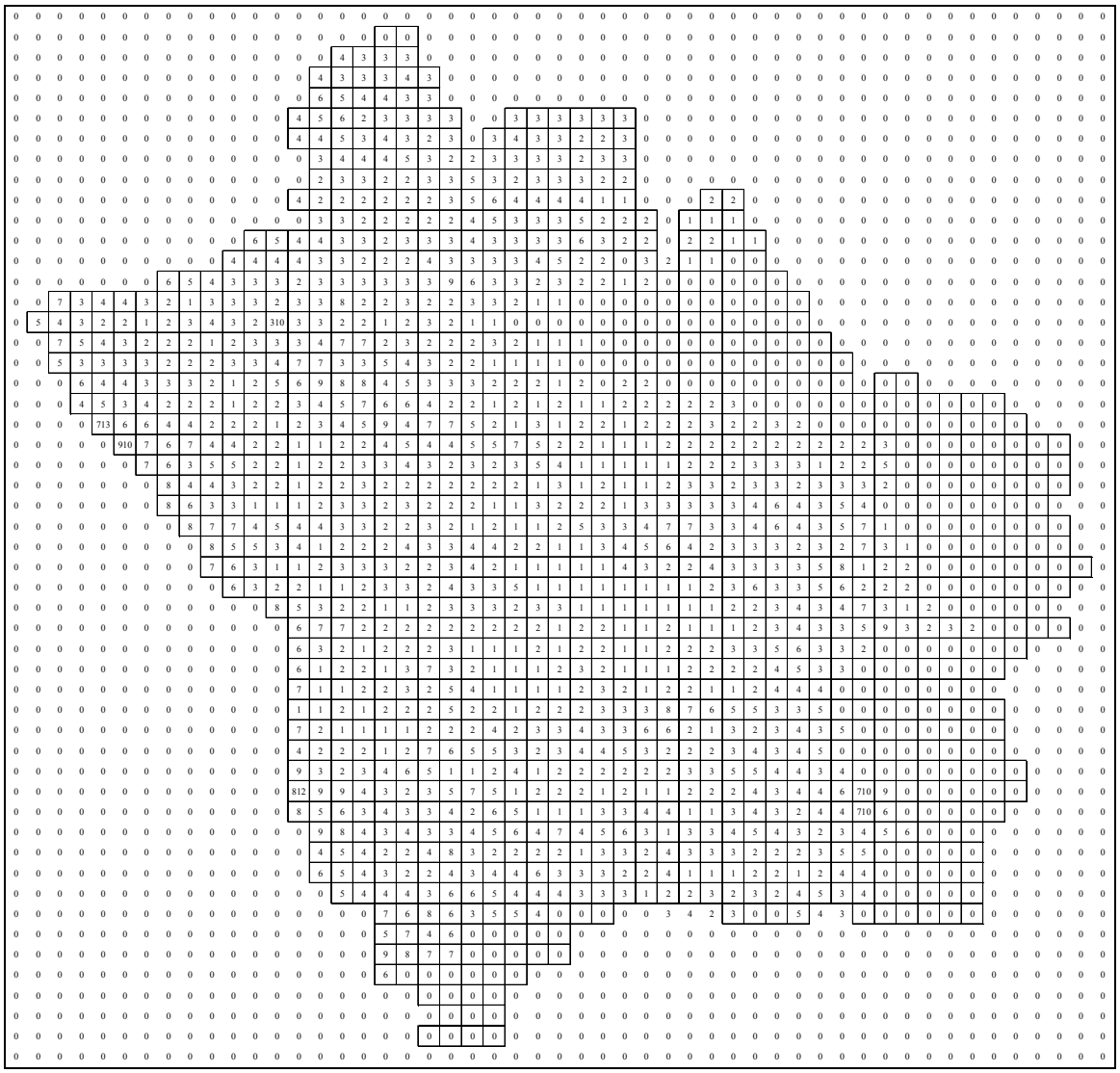

Figure A.5: Grid cell contours

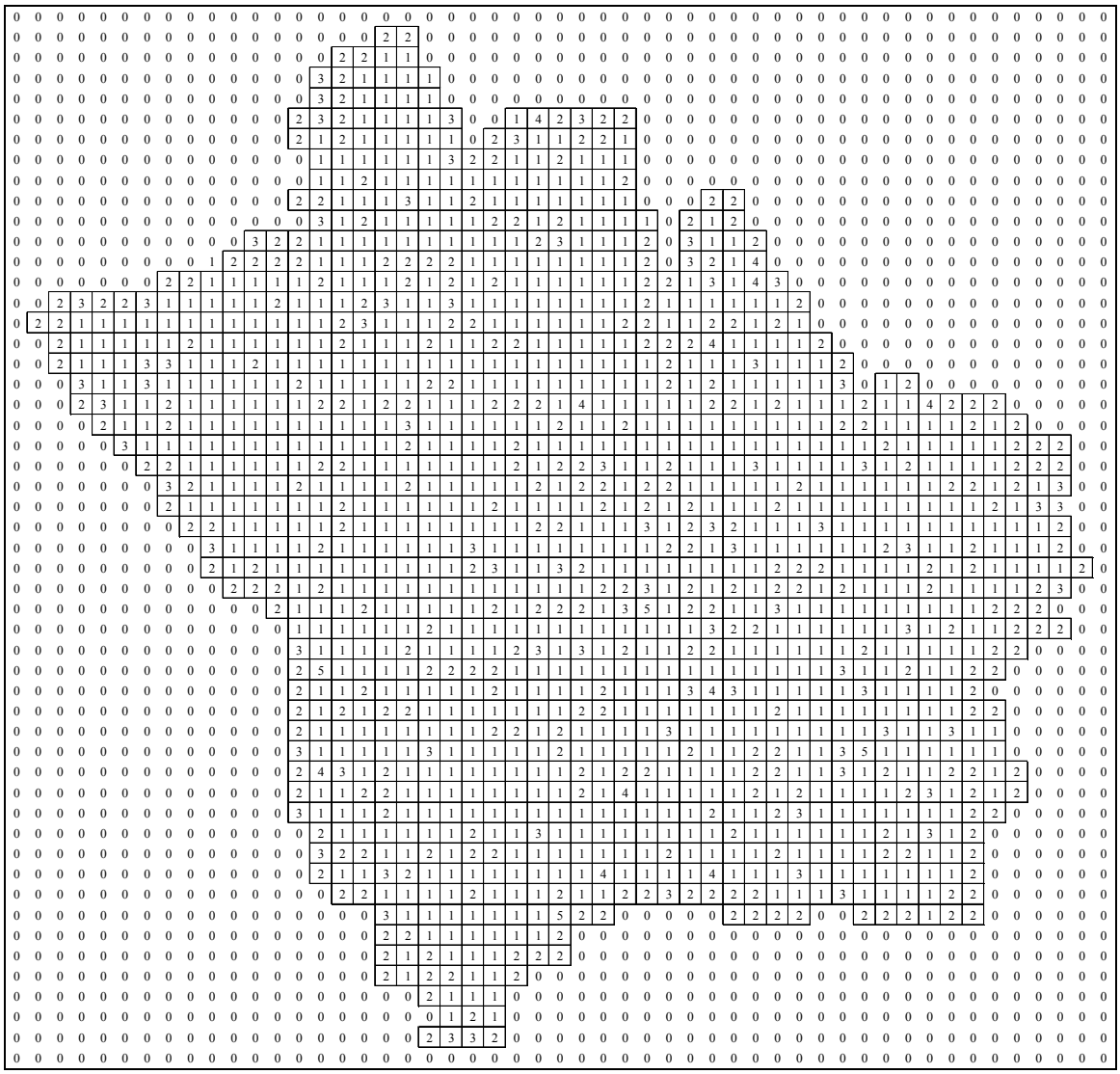

Figure A.6: Number of channels in each grid cell

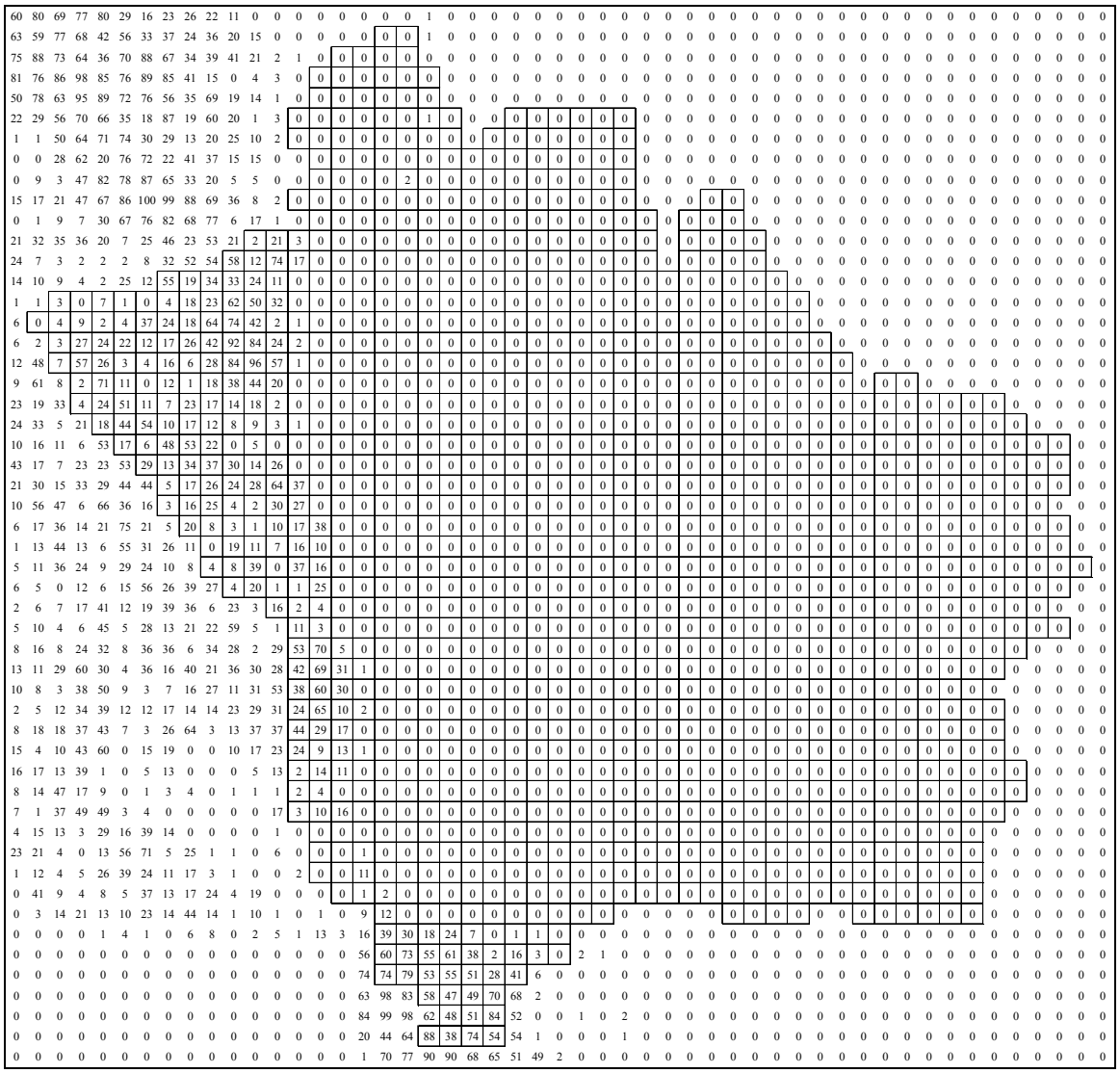

Figure A.7: Land class 1 (dense forest) allocation for each grid cell

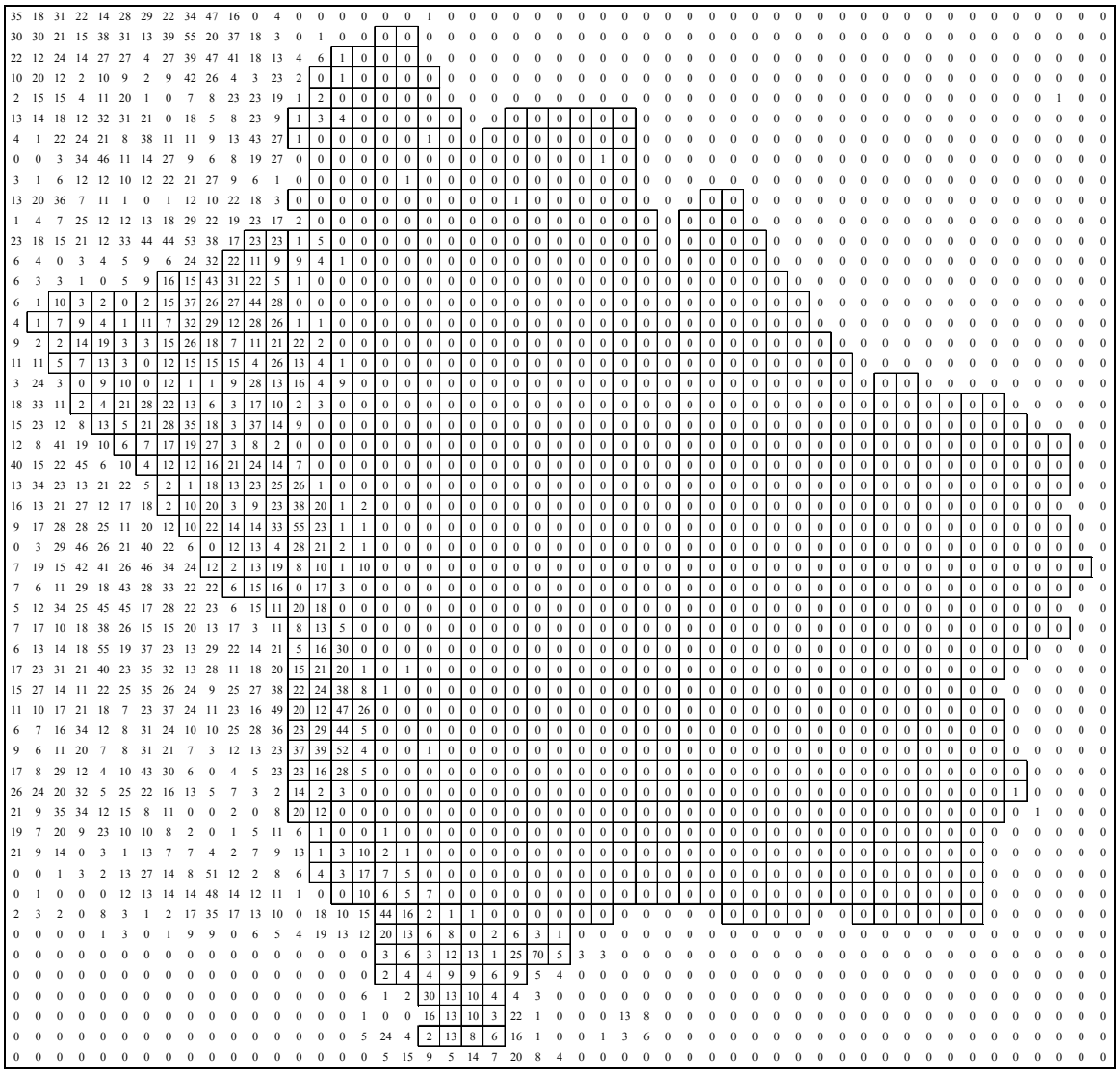

Figure A.8: Land class 2 (light forest) allocation for each grid cell

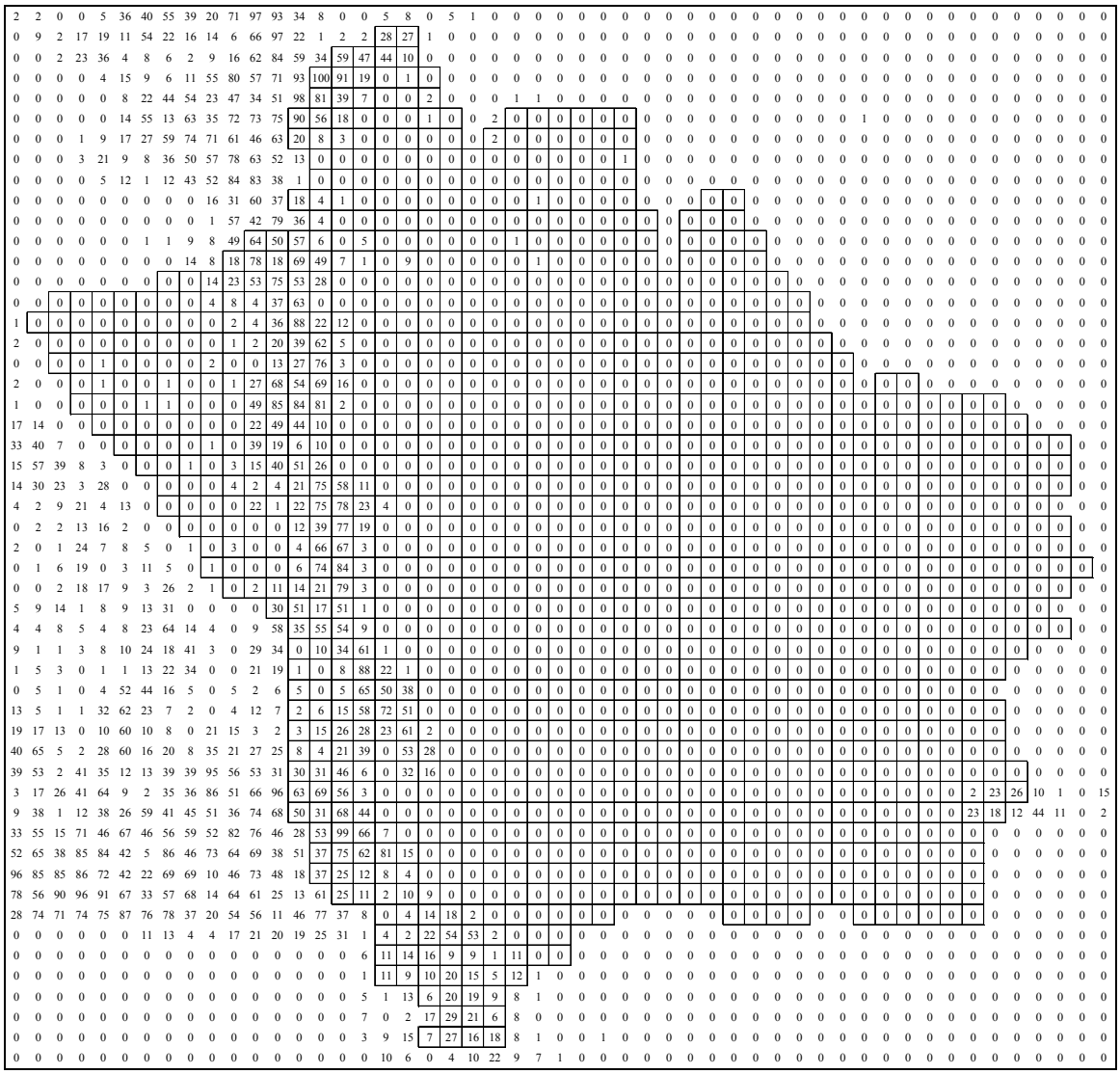

Figure A.9: Land class 3 (mixed forest) allocation for each grid cell

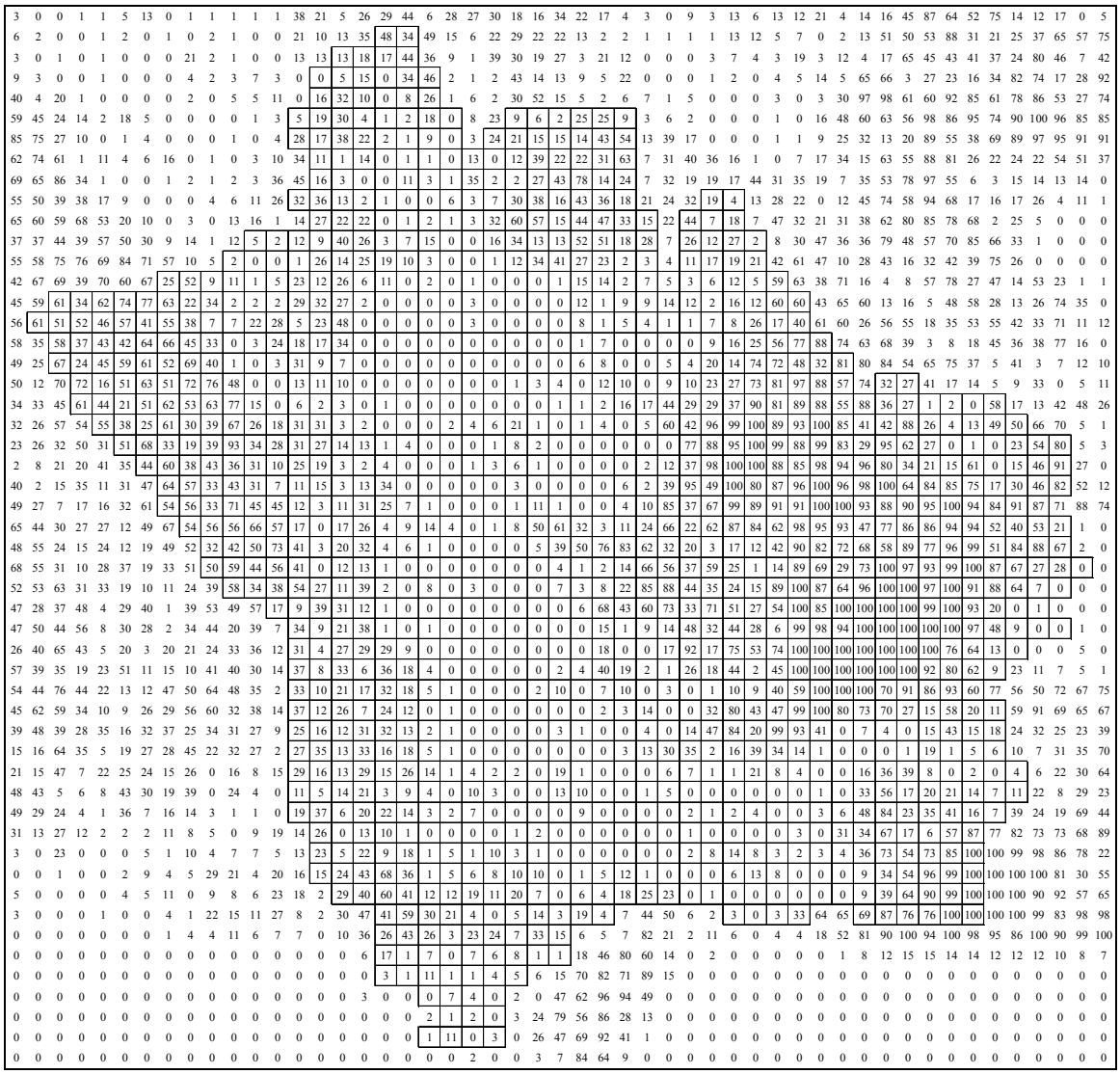

Figure A.10: Land class 4 (open) allocation for each grid cell

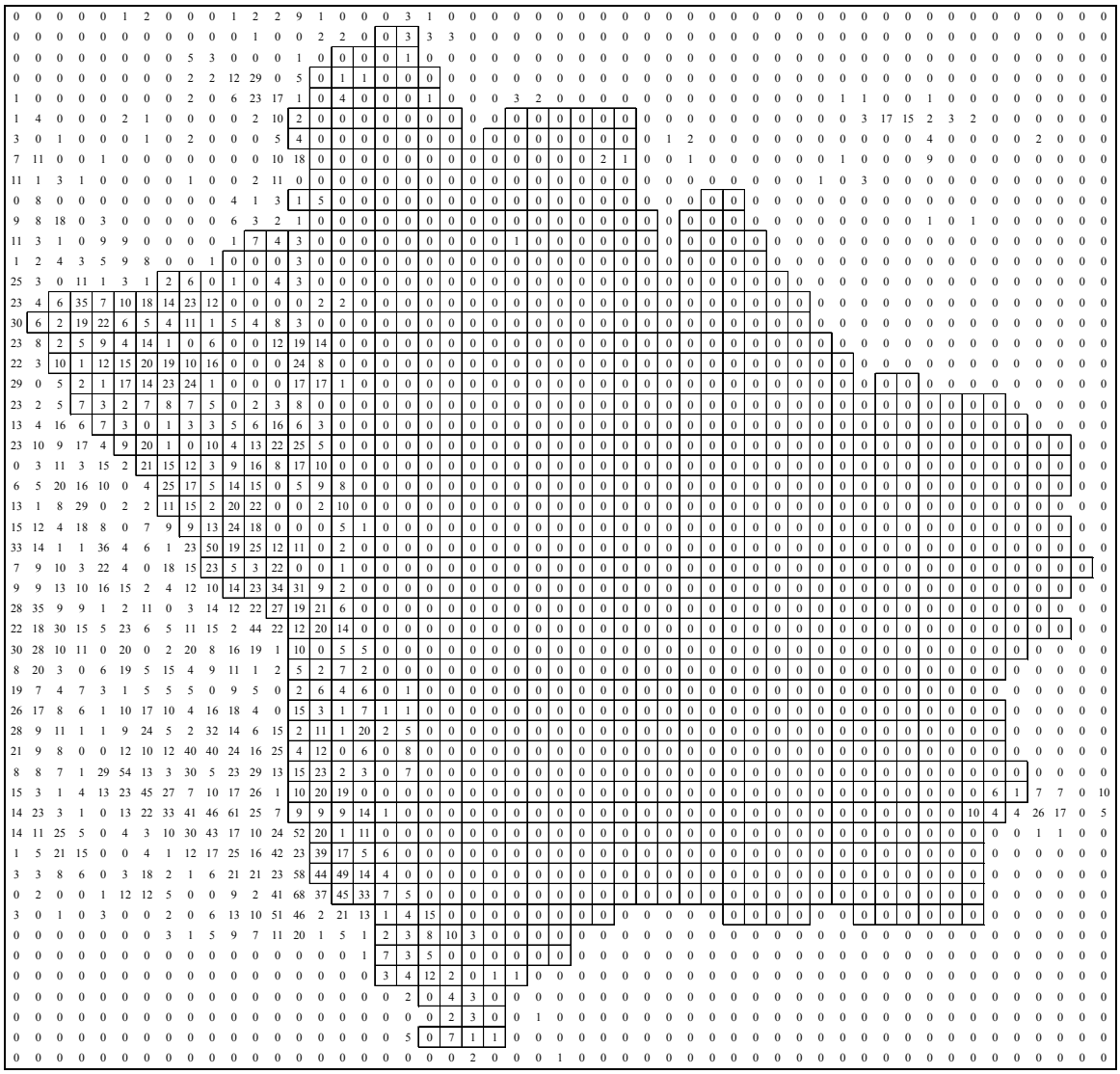

Figure A.11: Land class 5 (wetland) allocation for each grid cell

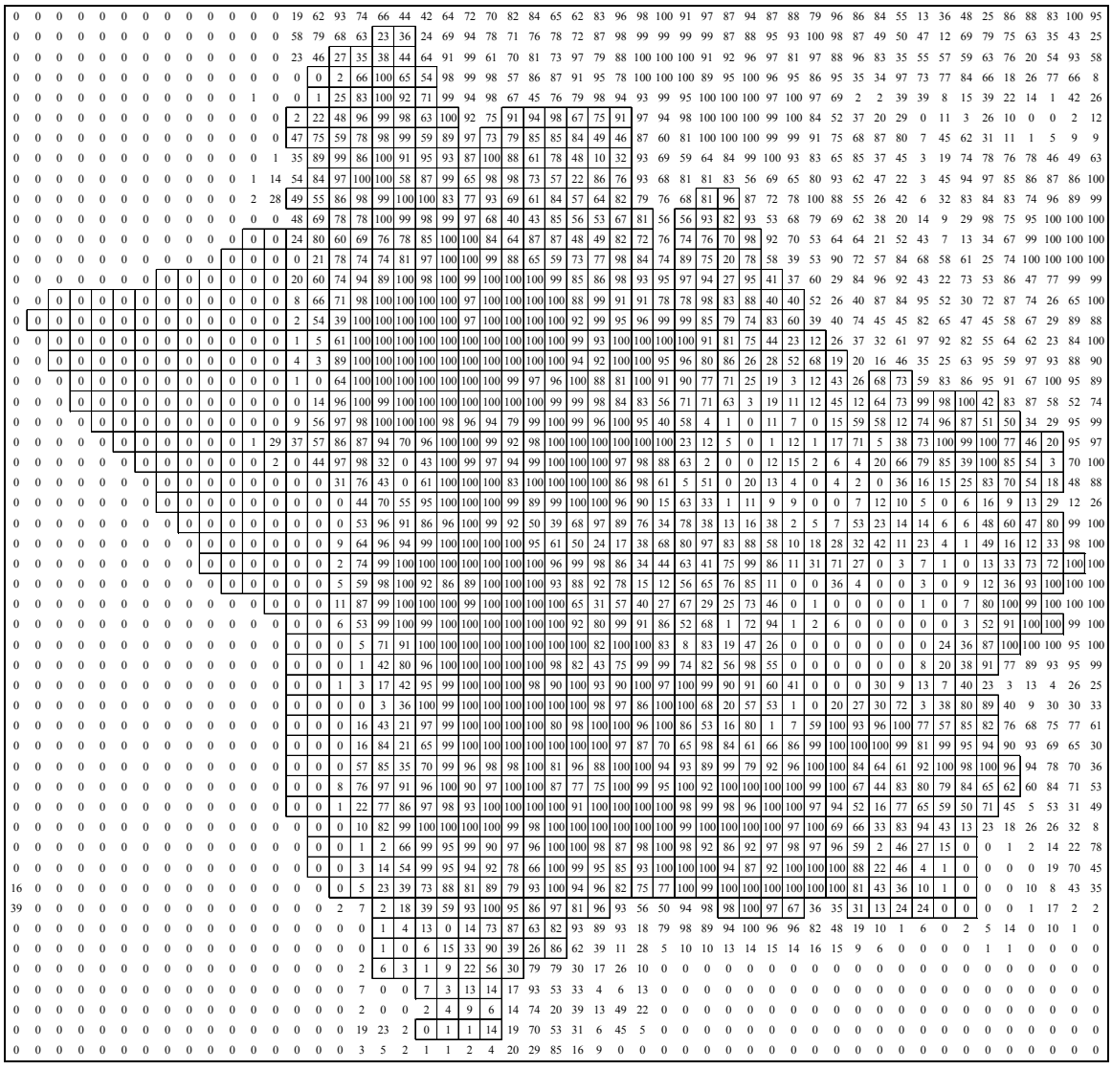

Figure A.12: Land class 6 (agricultural) allocation for each grid cell

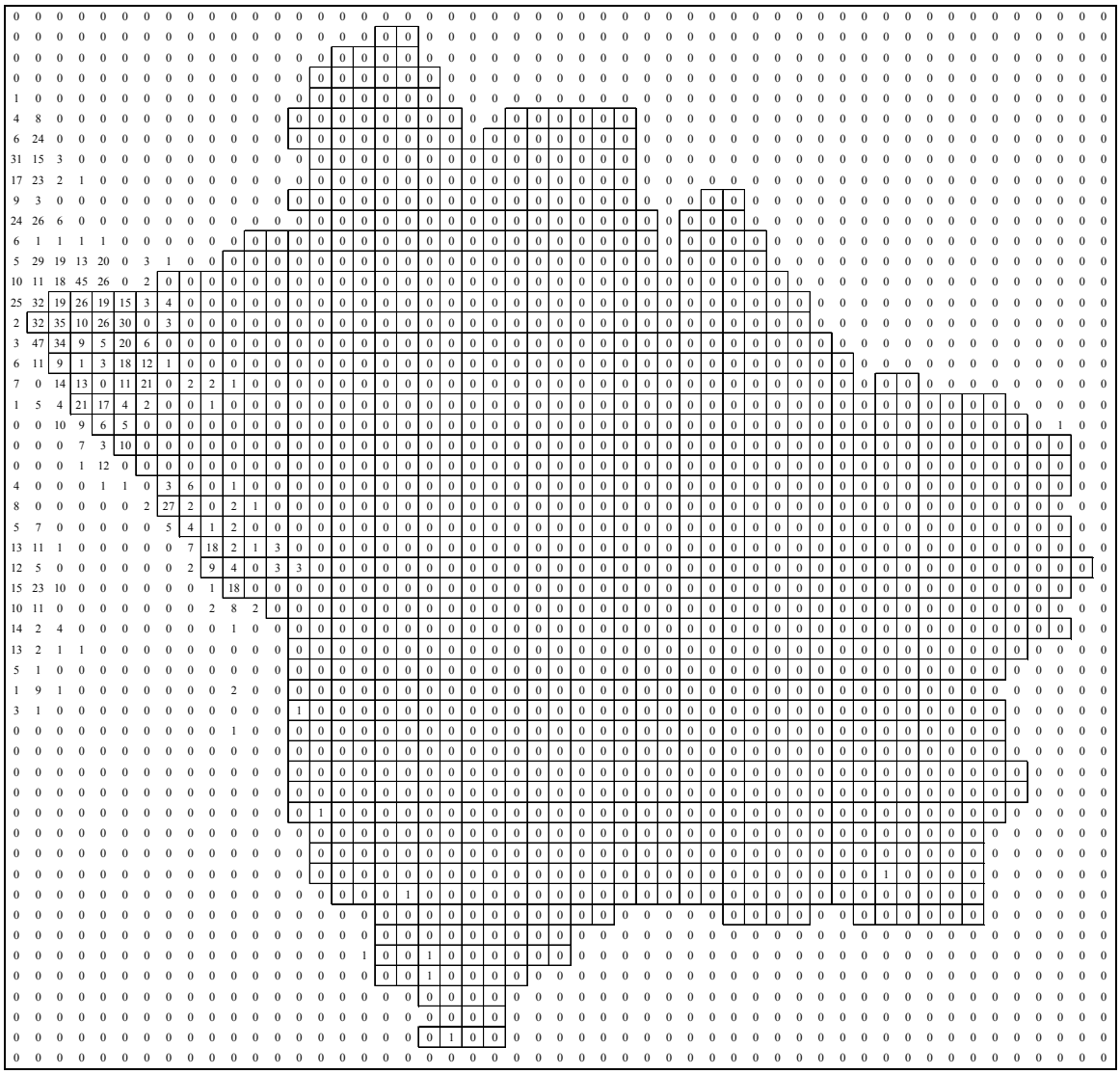

Figure A.13: Land class 7 (glacier) allocation for each grid cell

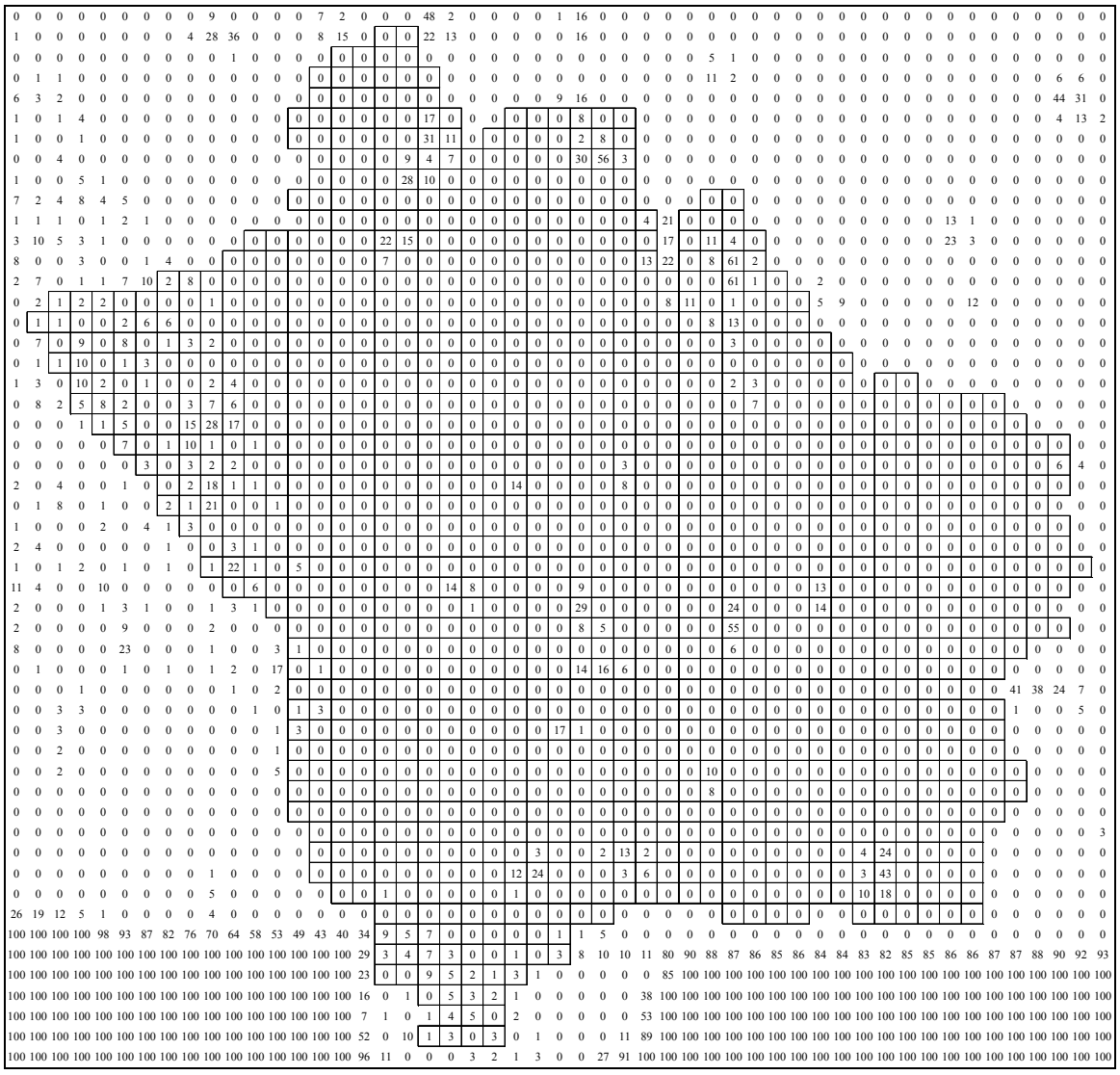

Figure A.14: Land class 8 (water) allocation for each grid cell

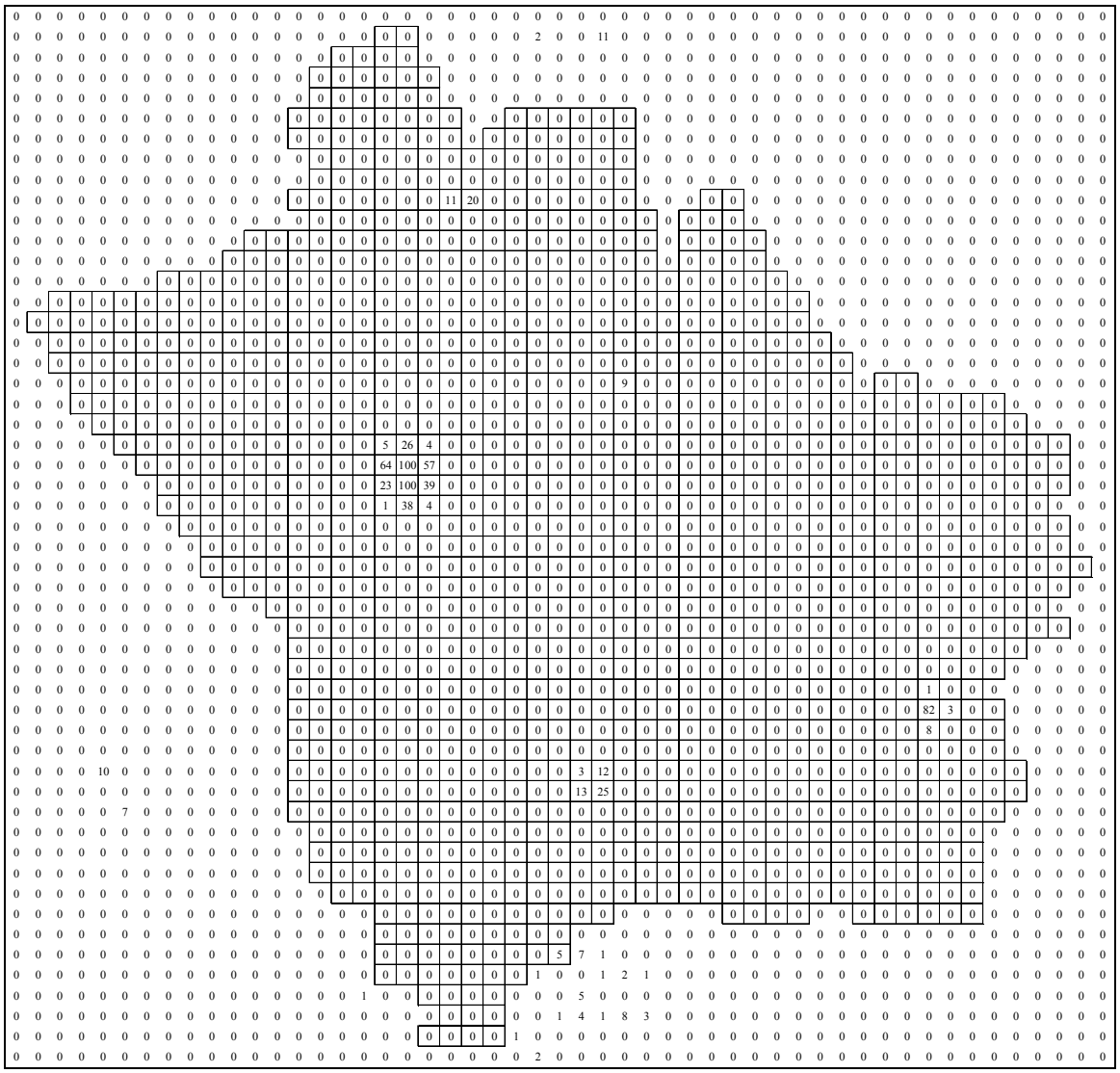

Figure A.15: Land class 9 (impervious) allocation for each grid cell

APPENDIX B

"MultiNash" Script

This appendix contains the Visual Basin code for the multi-basin weighting script "MultiNash".

```
Private Sub MultiNash()

Dim dbTemp As Double                ‘Temp double
Dim dbNash(1 To 30) As Double       ‘Holds all 30 Nash daily values
Dim dbFactor(1 To 30) As Double     ‘Weighting factor for each stream gauge
Dim dbSum As Double                 ‘Sum of streamflows from gauges in calc
Dim dbSums(1 To 30) As Double       ‘Sum (average) of each gauge’s streamflow
Dim dbNewNash As Double             ‘Holds weighted Nash daily value

Open App.Path & "\nash_daily.csv" For Input As #1

        Input #1, dbTemp                ‘input blank line
        Input #1, dbTemp                ‘input blank line
        Input #1, dbTemp                ‘input blank line

        For I = 1 To 30
           Input #1, dbNash(I)          ‘input all 30 Nash daily values
           Input #1, dbTemp
           dbFactor(I) = 0              ‘set all factors to 0
        Next I

        Close #1

‘   Set average streamflow for Basins used in Calibration
‘   Activate desired gauges, others are commented out

‘    dbSums(1) = 79106
‘    dbSums(4) = 5662
dbSums(5) = 3229
‘    dbSums(6) = 6753
‘    dbSums(7) = 7568
dbSums(9) = 34972
dbSums(16) = 3533
‘    dbSums(17) = 3301
```

```
‘    dbSums(19) = 7737
‘    dbSums(20) = 13876
‘    dbSums(21) = 1555
‘    dbSums(22) = 4222
dbSums(23) = 9113
dbSums(25) = 3278
‘    dbSums(26) = 12826
‘    dbSums(27) = 2086
‘    dbSums(28) = 1956

dbSum = 0

For I = 1 To 30
   dbSum = dbSum + dbSums(I)              ‘Add up streamflows from selected basins
Next I

For I = 1 To 30
   dbFactor(I) = dbSums(I) / dbSum        ‘Calculated weighting for each basin
Next I


dbNewNash = 0

For I = 1 To 30
   dbNewNash = dbNewNash + dbNash(I) * dbFactor(I)     ‘Calculates weighted Nash
Next I

Open App.Path & "\sum_nash.txt" For Output As #2
   Print #2, dbNewNash                                 ‘Prints weighted Nash
Close #2

Unload MultiNash

End Sub
```